Investigations of the Characteristics, Origin, and Residence Time of the Upland Residual Mantle of the Piedmont of Fairfax County, Virginia

U.S. GEOLOGICAL SURVEY PROFESSIONAL PAPER 1352

Investigations of the Characteristics, Origin, and Residence Time of the Upland Residual Mantle of the Piedmont of Fairfax County, Virginia

By M.J. PAVICH, G.W. LEO, S.F. OBERMEIER, *and* J.R. ESTABROOK

U.S. GEOLOGICAL SURVEY PROFESSIONAL PAPER 1352

Residual soil and saprolite developed from metasediments, metagranite, diabase, and serpentinite have been analyzed petrographically, texturally, mineralogically, and chemically. These analyses are used to interpret the chemical mechanisms of alteration of Piedmont crystalline rock to saprolite and the mechanical and chemical alteration of saprolite to soil

UNITED STATES GOVERNMENT PRINTING OFFICE, WASHINGTON: 1989

DEPARTMENT OF THE INTERIOR

MANUEL LUJAN, Jr., *Secretary*

U.S. GEOLOGICAL SURVEY

Dallas L. Peck, *Director*

Library of Congress Cataloging in Publication Data

Investigations of the characteristics, origin, and residence time of the Upland residual mantle of the Piedmont of Fairfax County, Virginia.
(U.S. Geological Survey professional paper ; 1352)
Bibliography: p.
Supt. of Docs. no.: I 19.16:1352
1. Weathering—Virginia—Fairfax County. 2. Saprolites—Virginia—Fairfax County. 3. Soils—Virginia—Fairfax County. I. Pavich, M.J. II. Series.
QE570.I58 1989 551.3'02'09755291 86-607938

For sale by the Books and Open-File Reports Section, U.S. Geological Survey, Federal Center, Box 25425, Denver, CO 80225

CONTENTS

ILLUSTRATIONS

[Plates are in pocket]

TABLES

INVESTIGATIONS OF THE CHARACTERISTICS, ORIGIN, AND RESIDENCE TIME OF THE UPLAND RESIDUAL MANTLE OF THE PIEDMONT OF FAIRFAX COUNTY, VIRGINIA

By M.J. PAVICH, G.W. LEO, S.F. OBERMEIER, and J.R. ESTABROOK

ABSTRACT

Undisturbed cores of upland regolith developed from a variety of crystalline rocks of the Piedmont province in Fairfax County, Va., have been obtained by using a combination of Shelby tubes, Denison sampler, and modified diamond core drilling. The core study correlated variations in chemistry, mineralogy, and texture with engineering properties throughout individual weathering profiles and contrasted these parameters among weathering profiles developed from various parent rocks. Coring sites were chosen to obtain a maximum depth of weathering on diverse lithologies. The rocks that were investigated included metapelite, metagraywacke, granite, diabase, and serpentinite. Four to twelve samples per core were selected for analysis of petrography, texture, clay mineralogy, and major-element chemistry. The number of samples was determined on the basis of (1) the thickness of the weathering profile (from about 1 m in serpentinite to more than 30 m in pelitic schist) and (2) megascopic changes in the weathering profile. Shear strength and compressibility were determined on corresponding segments of core. Standard penetration tests were performed adjacent to coring sites to evaluate in-place engineering properties.

The regolith profiles on all rocks can be subdivided into soil, massive subsoil, saprolite, and weathered rock zones. Major differences in thicknesses of these zones are related to parent rock. Total regolith thickness is related to saprolite thickness. Saprolite is thickest on quartzofeldspathic metapelite, metagraywacke, and granite; thinner on diabase; and thinnest on serpentinite. Thickness of saprolite is related to rock structure and mineralogy.

Geochemical changes of saprolite developed from each rock type follow predictable trends from fresh rock to soil profile, with increases in Ti, Al, Fe^{3+}, and H_2O^+relative to absolute losses of Si, Fe^{2+}, Mg, Ca, and Na. These variations are more pronounced in the weathering profiles above mafic and ultramafic rocks than in those above metagraywacke. Clay minerals in granite, schist, and metagraywacke saprolites are kaolinite, dioctahedral vermiculite, interlayered mica-vermiculite, and minor illite. Gibbsite is developed in near-surface samples of schist.

Standard penetration test data for the upper 7 m of saprolite above schist, metagraywacke, and granite suggest alternations between stronger and weaker horizons that correlate with megascopically identified zones: soil, massive subsoil, and saprolite. The data correlate with density. Shear strength increases fairly regularly downward in the weathering profile. The engineering behavior of diabase saprolite is controlled by a dense, plastic, near-surface clay layer (montmorillonite and kaolinite) overlying rock that is weathered to a granular state (grus); the engineering properties of serpentinite are controlled by a very thin weathering profile.

Similarities in regolith thickness, zonation, mineralogy, and chemistry of quartzofeldspathic rocks indicate the existence of fundamental geochemical and geomechanical controls on regolith evolution on the Piedmont upland. Data from the profiles of quartzofeldspathic regolith are used to construct a model suggesting the principal rate-control steps in the development and downwasting of the upland regolith. This model is consistent with available information about Piedmont hydrology and tectonic uplift.

INTRODUCTION

A thick mantle of residual regolith covers the bedrock in upland areas of Virginia's outer Piedmont. The regolith mantle exhibits a weathering profile that is typically composed of progressively more weathered material upward from fresh bedrock to the land surface. The weathering profile is divided into the following zones, from bottom to top: weathered rock (firm, but more or less brittle, and distinctly altered), saprolite (typically so weak it can be excavated easily with a shovel but retains the structures and textures of the bedrock), a structureless massive subsoil zone, and a distinctly layered soil zone.

Detailed surficial mapping of the Piedmont of Northern Virginia (Froelich and Heironimus, 1977) has revealed that most upland areas underlain by crystalline bedrock have thick weathering profiles averaging 15 m but locally as much as 50 m thick. These weathering profiles constitute a predominantly in-place regolith that displays a systematic zonation of physical and chemical properties (Leo and others, 1977). The thickness and zonation of the regolith profiles vary predictably with bedrock type and with topographic position. The regolith is thickest beneath upland areas overlying foliated quartzofeldspathic rocks and thinnest over ultramafic rocks and on steep side slopes.

The precise age and rate of regolith production in the Piedmont remain unresolved. Because of a lack of suitable radiometric dating techniques, models that subdivide the residual weathering profiles into surficial

lithostratigraphic units must be constructed. The erosional history of these lithostratigraphic units must be interpreted from the inferred residence times of the units.

This study provides a preliminary interpretation of the petrographic, mineralogic, geochemical, and geotechnical properties of the upland mantle. Comprehensive data were obtained from continuous cores of the regolith on selected quartzofeldspathic, mafic, and ultramafic rock types of Fairfax County in Northern Virginia. This study proposes elements of a testable model that relates the genesis of these surficial units to the downwasting of the Piedmont upland. The model is based on evidence that Piedmont upland soils are developed in place by mechanical and chemical alteration of saprolite and that rock structure plays a fundamental role in determining the rate of rock weathering and of saprolite development. The model is used to interpret near-surface weathering processes, the geologic history of the mantle, and the evolution of the geomorphic surface of this area of the Piedmont. The model also provides ideas about the maximum residence time of regolith on the Piedmont upland and about the relation of regolith residence time to regional uplift.

PREVIOUS WORK

Theories about the origin, age, and geologic history of the regolith as related to the geologic history of the Piedmont have long been discussed. In 1899, William Morris Davis proposed that the thick regolith of the Virginia Piedmont upland had formed on a tectonically stable peneplain. He further postulated that the steep valleys of the Piedmont, which expose fresh bedrock, resulted from regional uplift that postdated the erosional beveling and formation of regolith on the upland. Davis (1899, p. 358) stated,

> the uplands of the Piedmont belt, with their deep soils, are of an essentially different cycle of development from the narrow valleys, with their bare ledges. The two elements of form remain mutually inconsistent until reconciled by the postulate of an uplift of the region between their developments. But if this postulate is accepted, the plain is shown to have been a lowland of faint relief before the existing narrow valleys were cut in it.

Hack (1960) developed a different model for the Appalachian region for the late Tertiary and Quaternary. Simply stated, Hack argued for continuity of landforms, including thickness of upland regolith on the Piedmont, and for maintenance of relative relief between more resistant and less resistant rock types during a long period of continuous downwasting. He called this geomorphic continuity during erosion "dynamic equilibrium."

Cleaves (1973, 1974) and Froelich and Heironimus (1977) demonstrated that the thickness of the upland mantle and the landforms of the Piedmont are clearly related to bedrock type, and Cleaves (1973) suggested that resistance to weathering and erosion is related to bedrock properties such as mineralogy and structure. Cleaves and Costa (1979) discussed bedrock control on the landforms and on the upland mantle in Baltimore County, Md. They concluded that the upland interfluves have been virtually unaffected by erosion since the Miocene. They cited evidence that saprolitization has been active since the Miocene, and they implied that much of the present upland saprolite is as old as Miocene.

Despite its ubiquitous distribution over the Piedmont of Virginia and the other southeastern States, only a few recent studies discuss the basic textural, chemical, mineralogical, and physical properties of the upland mantle. Studies of chemical weathering processes have been made in the Maryland-Virginia Piedmont by Plaster and Sherwood (1971), Cleaves (1968, 1973), Cleaves and others (1970, 1974), and Leo and others (1977); in the North Carolina Piedmont by Cady (1950); and in the South Carolina Piedmont by Gardner and others (1978) and Gardner (1980). Experience with engineering properties of saprolite has been summarized by Sowers (1954, 1963), Deere and Patton (1971), and Obermeier (1979).

PHYSIOGRAPHY, BEDROCK GEOLOGY, AND CLIMATIC HISTORY OF THE NORTHERN VIRGINIA PIEDMONT

Fairfax County, Va., lies in the central part of the mid-Atlantic geographic region and includes part of the suburban development that fringes Washington, D.C. The Piedmont physiographic section of Fairfax County lies between the early Mesozoic basins (underlain by sedimentary and igneous rocks) to the west and the Coastal Plain (underlain by unconsolidated sediments) to the east (fig. 1). The Piedmont is a broad, moderately dissected upland having accordant interfluves at altitudes of 110–140 m. Relief along principal drainages is 30 m. The Piedmont upland of Fairfax County is underlain by a variety of folded, faulted, and commonly foliated metasedimentary rocks and igneous rocks (pl. 1). It is thus representative of the outer Piedmont Crystalline Province (Thornbury, 1965, p. 88–99) of Virginia and Maryland. In addition to thick weathering profiles, the Piedmont upland area exhibits the following characteristics:

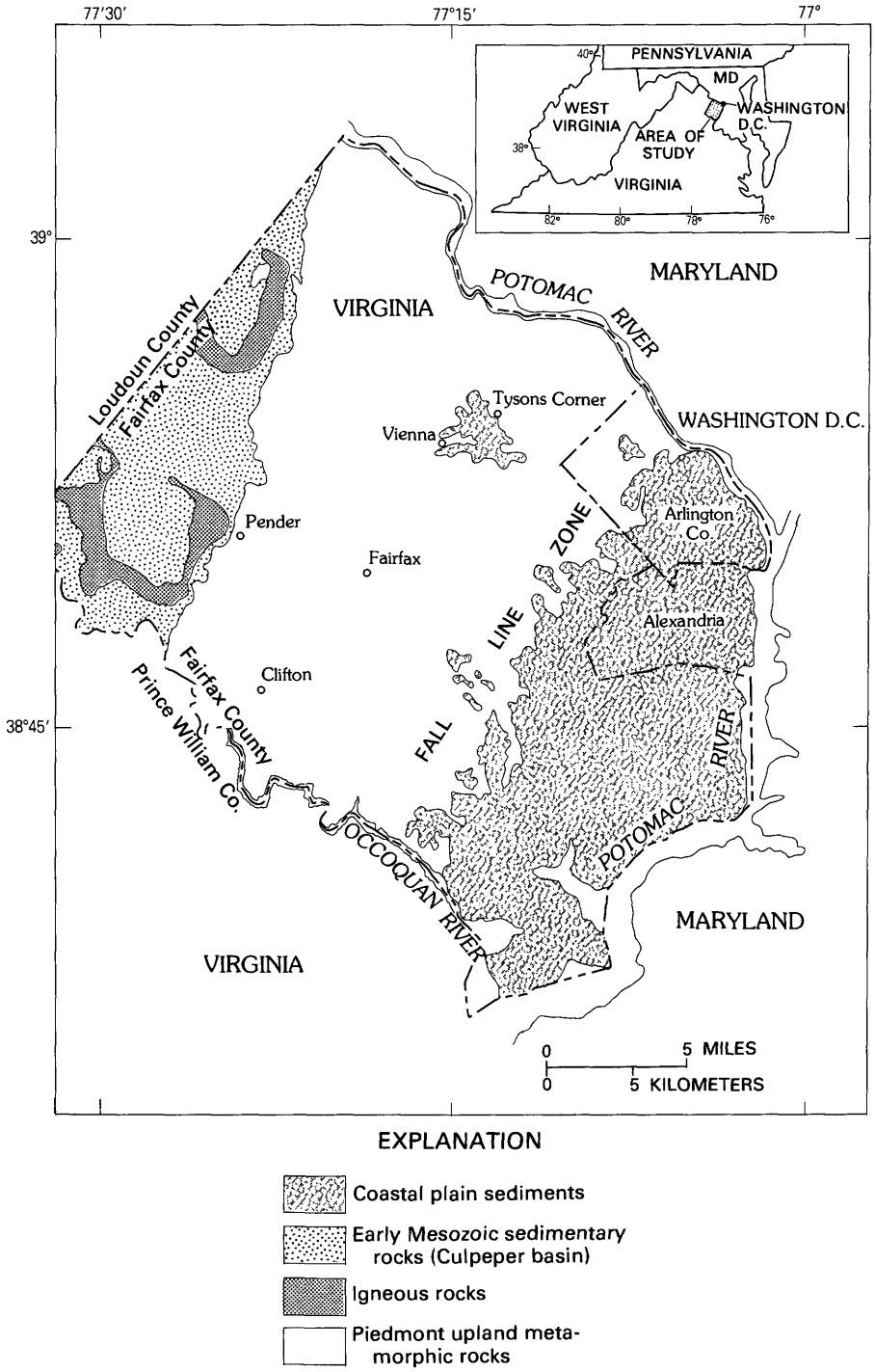

FIGURE 1.—Physiographic divisions of Fairfax County, Va.

(1) It forms a topographically high area relative to the early Mesozoic basins to the west, the Coastal Plain to the east, and two major river valleys (the Potomac and Occoquan) to the north and south.
(2) It exhibits high drainage density. Most of its perennial streams are incised into unweathered bedrock. Stream courses commonly follow prominent rock structures such as foliations or joints.
(3) It is underlain by intensely folded, faulted, and foliated rocks ranging in metamorphic grade from chlorite zone to first sillimanite zone having diverse lithologies.

The most common crystalline rock types of the Fairfax County Piedmont are metasedimentary rocks that have compositions varying between arenaceous and argillaceous. The major quartzofeldspathic metasedimentary rocks (shown in pl. 1) are pelitic schist, metagraywacke, phyllite, gneiss, and hornfels. Next in abundance are granitoid rocks, predominantly the foliated Occoquan Granite in the southern part of the county. Rocks of mafic to ultramafic composition crop out in a broad, generally northeast-trending belt west and southwest of the city of Fairfax. Narrow, north-trending belts of serpentinite are common in the north-central part of Fairfax County. Tabular diabase bodies intrude sandstone and siltstone in the early Mesozoic Culpeper basin and intrude schist in the western part of the county.

The Piedmont crystalline rocks other than the diabase are structurally complex. During regional metamorphism they were isoclinally folded and refolded (Drake and Froelich, 1977). A steeply dipping multiple foliation, which strikes north-northeast, and the predominant joint set, which strikes east-west, are the principal structural features that control local topographic grain.

The eastern third of the county is covered by Cretaceous and younger sands and clays of the Coastal Plain, which are capped locally by upland gravel.

The climate of Fairfax County is typical of the mid-Atlantic region. The summers are warm and humid, and the winters are mild. The average temperature is 10 °C. The highest summer temperature is approximately 38 °C, and the minimum winter temperature is rarely below −20 °C. Extended periods of subzero weather are rare, and the depth of frosts rarely exceeds a few decimeters. Average rainfall is 104 cm/yr and is evenly distributed throughout the year. Maximum rainfall intensity is usually in the summer; longest drought periods generally occur in the fall.

The climatic history of the mid-Atlantic region during the Pleistocene is inferred from the pollen record in sediments that record glacial and interglacial oscillations of climate. Sirkin and others (1977) concluded that interglacial climates of this region were similar to the present climate. Glacial climates were probably cooler and drier than the present climate (Denny and others, 1979). The Pliocene climate of the region, inferred from pollen spectra in the Walston Silt (Owens and Denny, 1979), was warm and humid.

GENERAL PROPERTIES OF WEATHERING PROFILES

REGOLITH ZONATION

The upland regolith on igneous and metasedimentary rocks in Fairfax County originates from in-place chemical weathering of bedrock. A systematic vertical zonation of weathered products overlies the bedrock; different physical and engineering properties characterize each zone. Generalized relations among the weathering zones and some physical and engineering properties for regolith in Fairfax County are shown in table 1, and generalized weathering profiles for quartzofeldspathic and mafic rocks are depicted in figure 2. The regolith is commonly divided from bottom to top into four major zones: weathered rock, saprolite, massive subsoil, and soil. Massive subsoil is not always present, as shown in figure 2*B*.

Unweathered rock has no visible alteration of minerals, although joints may be iron stained. Contacts between unweathered and weathered rock vary from abrupt to gradational. Weathered rock characteristically has 10 percent or more core-stones, stones that are so fresh and hard that they ring when struck with a hammer. Core-stones generally are discoid or plate shaped in foliated, micaceous metamorphic rocks (fig. 2*A*) and are nearly spheroidal in massive igneous and metamorphic rocks (fig. 2*B*). Joints are slightly cemented or stained, and the minerals most susceptible to weathering, generally the feldspars and biotite, have been somewhat altered.

Saprolite is the untransported, isovolumetric weathering product of crystalline rocks (Becker, 1895). Saprolite constitutes the bulk of the weathering profile over quartzofeldspathic rocks of the Piedmont (fig. 2). Saprolite sometimes is referred to as the pedologic C horizon but is here considered to be the weathering product of the underlying crystalline bedrock that has decomposed in place. Saprolite retains the original rock structure, foliation, and jointing, but the bulk density can be as low as half that of the original rock. Saprolite is soft enough to be dug or chopped with a hand shovel. It has properties of both soil and rock; that is, it has the strength and compressibility of soil and the structure and fractures of rock. Joints in saprolite commonly are

TABLE 1.—*Description of weathering profile for igneous and metasedimentary rocks in Fairfax County, Va. (modified from Deere and Patton, 1971)*

Zone		Description[1]	RQD[2] (NX core percent)	Percent core recovery (NX core)	Relative permeability	Relative strength	Common thickness (meters)
Soil	A Horizon	Top soil, roots, organic material. Zone of leaching and eluviation. Generally porous and sandy.	Not applicable.	0	Medium to high	Very low	0.1–0.2
	B Horizon	Characterically clay enriched, also accumulations of Fe and Al. No relict structures present.	Not applicable.	0	Low	Commonly low, medium if very dry.	0.3–1.0
Massive subsoil		No relict rock structure. Less dense than soil B horizon. Less clay than soil B horizon. Depleted in cations and silica relative to Fe and Al. May contain clasts of saprolite.	Not applicable.	0	Medium	Low	0.5–1.0
Saprolite		Relict rock structures retained. Clay-bearing silt or clay-bearing sand grading to sand at depth. Commonly micaceous; feldspars and mafic minerals altered to clays. Less than 10 percent core stones. Joints strongly cemented with oxides at many places.	0 or not applicable.	Generally 0–10 percent.	Medium	Low to medium (relict structures very significant.	1–15
Weathered rock	Transition (from saprolite to partly weathered rock).	Highly variable, saprolitelike to rocklike. Fines commonly fine to coarse sand (grus). 10–95 percent core stones. Feldspars and mafic minerals altered in part.	Variable, generally 0–50 percent.	Variable, generally 10–90 percent.	High (water losses common during drilling).	Medium to low where weak structures and relict structures are present.	0.3–3
	Partly weathered rock.	Rocklike, soft to hard rock. Joints stained to altered. Slight alteration of feldspars and mafic minerals.	Generally 50–75 percent.	Generally 90 percent.	Medium to high	Medium to high[3].	0.3–3
Unweathered rock		No iron stains to trace along joints. No weathering of feldspars and micas. No sheared zones.	>75 percent (generally >90 percent.	Generally 100 percent.	Low to medium	Very high[3].	—

[1]The descriptions provide the only reliable means of distinguishing the zones.
[2]RQD stands for Rock Quality Designation, described in Deere and others (1967). RQD in percent equals length of core pieces 4 in. (10.3 cm) and longer divided by length of run times 100. NX core diameter in 1.75 in. (4.5 cm).
[3]Considering only intact rock with no adversely oriented geologic structures.

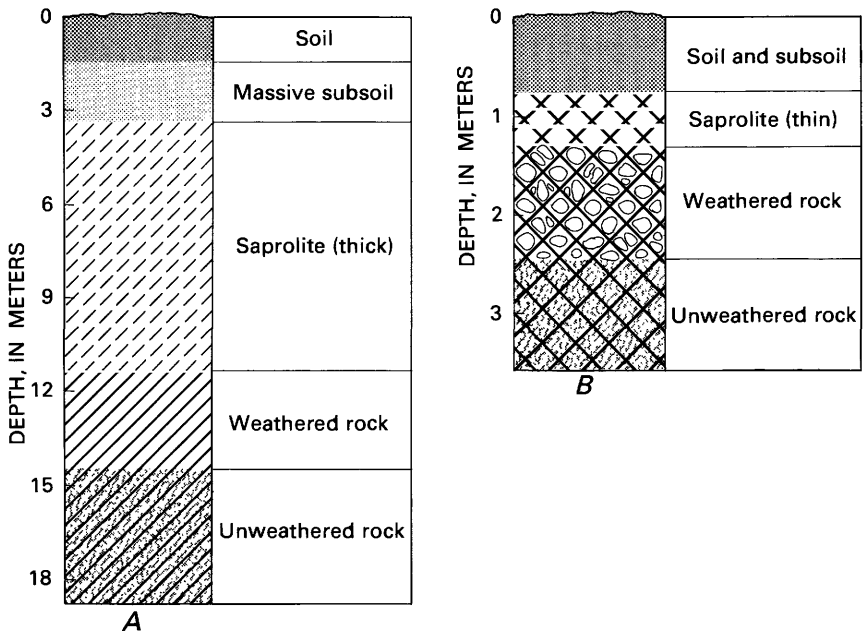

FIGURE 2.—**Generalized weathering profiles developed on crystalline rocks of the Piedmont in Fairfax County, Va. (modified from Langer, 1978). *A*, Foliated metasedimentary and granitic rocks. *B*, Massive igneous rocks (such as diabase).**

cemented by iron and manganese in the upper few meters.

The massive subsoil is transitional between the clay-rich B horizon of the soil and the top of the saprolite. The subsoil contains significantly less clay (commonly less than 20 percent) and has a lower specific gravity than the B horizon has. The subsoil contains no parent rock structure such as joints and fractures. It is commonly less than 0.6 m thick and grades downward into saprolite. The massive subsoil is commonly developed beneath the flat upland interfluves.

The soil includes the pedologic A and B horizons. The B horizon, between the subsoil and the A horizon, is compact, dense, and clay rich; it usually contains at least 40 percent clay. The B horizon is typically about 0.6 m thick. It is the zone of clay accumulation. Relative to the overlying A horizon and the underlying horizons, the B horizon is enriched in aluminum and iron. Over most of the area underlain by metasedimentary rocks, the A horizon of the soil is a thin (0.1 m) layer of silty sand that contains less than 20 percent clay and that commonly contains angular quartz gravel. The quartzose sand and gravel are derived from local weathering products in the subsoil. The gravel is a lag deposit that has been concentrated at the surface by the erosion of sand and finer particles.

REGOLITH HYDROLOGY

Reactions between ground water and the mineral constituents of the weathering profile constitute the chemical weathering process (Bricker and others, 1968). Thus, hydrologic properties of the regolith are critically important to the processes and rates of chemical weathering.

Water infiltrates the soil and subsoil and moves along foliation planes and joints in the saprolite and along joints and fractures in weathered and fresh bedrock. The rate of movement is controlled by the permeability of these zones and by local hydraulic gradients. Water movement through the regolith is a major control on the hydrologic mass balance (Johnston, 1962).

Precipitation, surface runoff, ground-water flow, and evapotranspiration are parts of a continuous hydrologic cycle involving the atmosphere, the lithosphere, and the biosphere. The hydrologic mass balance for a single drainage basin is based on the formula:

$$P = R+E \pm S$$

where
P=precipitation,
R=runoff (direct and baseflow),
E=evapotranspiration, and
S=ground-water storage.

In this region, these parameters average P=104 cm/yr, R=38 cm/yr, and E=71 cm/yr. Although precipitation in the mid-Atlantic region usually is distributed evenly throughout the year, runoff and evapotranspiration vary significantly over time. Storage may change markedly from year to year, but over several years the net storage change is zero (Richardson, 1976).

Runoff is divided into direct runoff, which occurs within a few hours or days after a storm, and baseflow, which occurs continuously and which is sustained by discharge of water stored in the ground-water reservoir. On the average, baseflow constitutes 60 percent of stream discharge (R.H. Johnston, U.S. Geological Survey, oral commun., 1978).

Evapotranspiration follows a seasonal cycle of plant respiration. During fall and winter, respiration is generally low, but it rises abruptly during spring and summer. Crooks and others (1967) obtained a figure of 65 percent loss of total precipitation by evapotranspiration in the Patuxent River basin in the Maryland Piedmont. A graphical summary of the Patuxent River basin water budget is shown in figure 3.

Most of the ground-water storage in the Piedmont is within the regolith above unweathered bedrock, with minor storage potential in joints and in foliation partings within fresh rock. The saprolite acts as a relatively porous reservoir for ground water.

The water that infiltrates to recharge the Piedmont ground-water reservoirs and that eventually reaches the surface streams does not follow straight flow paths. The anisotropic structure of the Piedmont rocks and saprolites causes water to flow faster in some directions than in others; therefore, rock structure, in large part, determines the amount of water flowing through any part of the regolith and bedrock. The steeply dipping foliation and joint sets of Piedmont rocks in this area facilitate downward movement of water.

BEDROCK CONTROL OF WEATHERING PROFILE

Parent bedrock mineralogy, texture, and structure- and rock-controlled drainage conditions directly affect the characteristics of the weathering profile. Studies of weathering of upland crystalline rocks (Sowers, 1954, 1963; Cleaves, 1973) revealed that weathering products depend primarily on the mineralogy of the parent bedrock and on drainage conditions. Pelitic schists, granites, and other felsic rocks in well-drained sites are typically weathered to a greater depth than are ultramafic rocks. In well-drained environments, rocks containing abundant feldspar and quartz (quartzofeldspathic rocks) weather to kaolinitic sandy saprolite; highly micaceous feldspathic rocks weather to kaolinitic silty saprolite, and rocks containing abundant mafic miner-

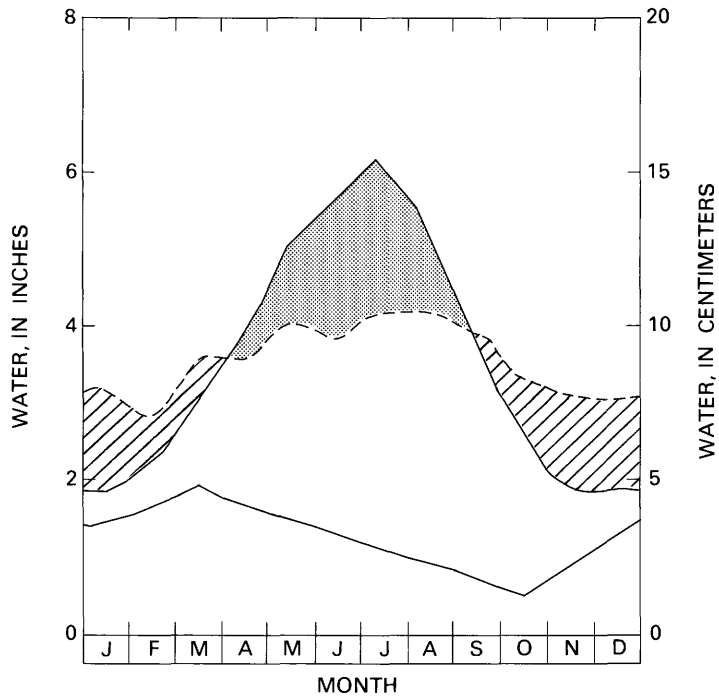

FIGURE 3.—Average annual water budget for the Patuxent River basin above Unity gaging station (adapted from Crooks and others, 1967). Dashed line represents rainfall; upper solid line represents evapotranspiration; diagonal lines represent recharge; shaded area represents deficiency; lower solid line represents runoff. In an average year, precipitation equals 109 cm; runoff equals 38 cm, and evapotranspiration equals 71 cm.

als weather to vermiculitic-kaolinitic silty saprolite. Most weathering products of ultramafic rocks are removed by solution (Leo and others, 1977; Cleaves, 1974). The clay content of the most highly weathered felsic saprolite is generally from 5 to 10 percent, but, for mafic rocks, it is as much as 20 percent.

In massive equigranular rocks such as granite and diabase, weathering occurs primarily along joints; in schistose and gneissic rocks, weathering also occurs along planes of schistosity, mineral layering (foliation), and cleavage. Saprolite derived from schistose rocks has more parting planes and may contain hard residual layers of primary quartz-rich strata.

In Fairfax County, the regolith is generally thickest on medium- to coarse-grained metasedimentary and igneous rocks of felsic or intermediate composition and is notably thinner on mafic rocks (pls. 1, 2). Regolith is very thin or absent on ultramafic rocks. Regolith is generally thicker and is developed more distinctly on medium-grained, biotite-bearing pelitic schists than it is on finer grained, sericite-chlorite phyllites. Unaltered quartz pods and veins are preserved in saprolite profiles, and larger quartz clasts are concentrated in masses of residual gravel and boulders that commonly cap hills.

The maximum thickness of regolith is beneath flat upland hilltops. On schistose, gneissic, and granitic rocks, regolith thickness locally exceeds 50 m, but more commonly it is 15–30 m thick (pls. 1, 2). Ultramafic rocks such as serpentinite exhibit a thin weathering profile and, with quartz veins, often crop out as fresh bedrock. Throughout the Fairfax County Piedmont, unweathered bedrock of any composition crops out in streams, and regolith is generally thin or absent in valleys of perennial streams.

At most places in the Piedmont, saprolite is thicker than weathered rock; however, in some places, no saprolite is present on weathered rock. In general saprolite is thickest beneath interfluves, and it is thin or absent in valleys where erosion is rapid. The contacts between saprolite and weathered rock and between weathered and unweathered rock are typically gradational, highly irregular, and difficult to define precisely. The contact between weathered and unweathered rock can be estimated closely on side slopes by the location of heads of perennial streams at minor springs. Because the rela-

tively impermeable unweathered rock forms a barrier to downward flow of water, except in areas where the rock is intensely jointed, ground water drains along the surface trace of the contact. Furthermore, the contact is readily discerned in water wells that are commonly cased and grouted at this horizon.

SHEAR STRENGTH AND COMPRESSIBILITY

Soil, massive subsoil, and the uppermost part of saprolite typically disintegrate easily and are much weaker than saprolite at depth and weaker than weathered rock. Soil is commonly so weak during wet seasons that it can be penetrated easily or indented by the thumb with moderate effort. Soil cohesion increases during summer and autumn drying. Wet massive subsoil generally can be penetrated with moderate effort, whereas wet saprolite immediately beneath the subsoil can be penetrated or indented with the thumbnail only with great effort. The lower part of saprolite is commonly so strong that it can be broken apart only by chopping with a shovel. Weathered rock is highly variable in strength; more intensely weathered rock can be broken apart only by chopping, and less weathered rock can be broken only by using a rock hammer.

Massive subsoil is highly compressible, and lightly loaded structures such as houses and small industrial buildings founded on this material can settle so much that the buildings may be damaged. The uppermost saprolite commonly is also highly compressible, but saprolite at depth is typically so much less compressible that it can be used to found caissons for multistory buildings.

Quantitative evaluations of compressibility for designing building foundations can be made in the laboratory by testing undisturbed samples in the consolidometer (Obermeier, 1979). In many places, however, foundation engineers have difficulty in getting good-quality specimens for laboratory testing. Field-sampling tubes are obstructed by thin, hard quartz veins or by quartz-rich metasedimentary layers, and samples commonly disintegrate along parting or joint planes. To circumvent this sampling problem, standard penetration test (SPT) blow-count data[1] often are taken in the field and then are used for designing building foundations. Low blow counts are obtained for highly compressible weaker materials, and high blow counts are obtained for relatively incompressible, stronger materials. Specific correlations have been developed that relate SPT blow counts to permissible foundation stresses for the Fairfax County area (Obermeier, 1979).

[1]SPT blow count equals the number of times a 140-lb (60-kg) hammer must be dropped 30 in. (75 cm) to drive a 2-in.- (5.1-cm-) diameter split spoon 6 in. (15.2 cm). For a 12-in. (30.4-cm) interval, an average of two drives is used.

SAMPLING AND ANALYTICAL PROCEDURES

Sampling sites for this study were chosen to obtain the thickest upland regolith profile on five representative crystalline rock types—metapelite, metagraywacke, gneissic granite, diabase, and serpentinite. At each of 19 sampling sites, a continuous core from the surface to unweathered rock was obtained; SPT blow counts were taken in an adjacent hole to a depth of about 6 m. Locations of the 19 core sites are shown on plate 1. Table 2 lists boring (core) numbers and a key to chemical analyses for the five representative rock types. Chemical analyses of ten cores are listed in the appendix tables.

Samples were extruded from Shelby tubes and core liners, were wrapped in plastic, and were labeled and stored in core boxes before description and sampling for analyses. Each of the 19 cores was described in detail. Five of the cores, one from each representative rock type, were selected for detailed petrographic, textural, and chemical analyses. The remaining 14 cores were only partially analyzed. Samples were selected from each of the five representative cores on the basis of visible profile changes that appeared related to the degree to weathering. These changes included variations in color, texture, and hardness. Selected samples included the soil, as well as the freshest bedrock penetrated. For each sample, all analyses were done on splits of one core section 10–20 cm long. Table 3 summarizes the techniques used to obtain samples, and table 4 summarizes the analytical procedures used to determine texture, composition, fabric, and physical properties of the core samples.

REGOLITH PROFILES DEVELOPED ON QUARTZOFELDSPATHIC ROCKS

Regolith on quartzofeldspathic rocks, including metasedimentary rocks and granite, is relatively thick

TABLE 2.—*Rock types, boring numbers, and index of chemical data of investigated cores*

Rock type	Boring core number	Chemical analysis number (see appendix tables A1–A4)
Peters Creek Schist		
A. Metapelite	F2, F4	1–8, 21–28
B. Metagraywacke	F3, F5,	9–20, 29–34
Occoquan Granite	F10, F11	35–49
Serpentinite	F14, F15	50–57
Diabase	F18, F19	58–67

TABLE 3.—*Drilling and coring techniques used to obtain core samples*
[Drill was mobile B-61, truck mounted]

Samplers	Comments
Shelby tube	Sampled to refusal depths: 1.7–6 m—metapelite, metagraywacke. 1–15 m— granite. 0.45–0.60 m—serpentinite.
Denison sampler	Yielded nearly continuous core; sample too disturbed for physical properties testing.
Diamond core drill, water cooled	Water-cooling flushed the sample.
Sawtooth bit core drill, air-cooled, portable, air compression at 4.5 m^3/min; 35.3 nT/cm^3 at surface, increased to 82.4 nT/cm^3 at depth of 15 m.	Effective at penetration rate of about 1 cm/min; yielded continuous cores.
Diamond core drill, air cooled, as above.	Used at penetration rate of <1 cm/min.
Standard Penetration Test: 2-in. (5.1-cm) sampling spoon; 140-lb (60-kg) hammer; 30-in. (75-cm) fall (Lambe and Whitman, 1966).	Number of blows to drive spoon 12 in. (30.4 cm).

and exhibits similar zonation on a variety of rock types. The results of analytical tests for three cores (F2, F3, and F11) are summarized in plate 3*A*, *B*, and *C*, respectively. General characteristics of the cores from each of the rock types sampled were as follows:

(1) Regolith on metasedimentary rocks (metagraywacke and metapelite) tends to be thick. The depth to fresh bedrock in five core holes (F1–F5) in metasedimentary rocks ranged between 15 and 34 m. In the cores, the total thickness of A and B soil horizons was notably thin, typically less than 2 m. Commonly, saprolite was contacted within 3 m of the surface. Lower in the drill hole, resistance to coring was variable but, in general, increased with depth to an abrupt transition from saprolite to weathered rock.

(2) Regolith developed on foliated granite has a thickness similar to that developed on metasedimentary rocks. Depth of weathering in the granite was as much

TABLE 4.—*Analytical procedures used to determine texture, composition, fabric, and physical properties of core samples*

Engineering test and classification:

Bulk density—Oven-dried (100 °C), samples coated with impermeable spray coating; density from Archimedes principle.

Uniaxial compression test—Unconfined (Terzaghi and Peck, 1948); conducted on massive wet samples containing >20 percent clay; clay content so large that triaxial confinement would not influence shear strength.

Triaxial compression test—Undrained (Terzaghi and Peck, 1948); conducted on samples containing partings or joints or samples containing little clay; confining pressure set at ambient overburden pressure.

Engineering classification—Unified Soil Classification System (Terzaghi and Peck, 1948); visual estimates verified by standard tests.

Textural (grain-size) analysis:

Hydrometer—

<63-μ fraction—50-g whole sample disaggregated and dispersed by using 125 mL of sodium hexametaphosphate solution (40 g/L); disaggregated by using Sonicator Cell Disrupter 10 min; grain-size distribution by soil hydrometer method of Casagrande (Lambe, 1951).

>63-μ fraction—wet sieve.

Petrography:

Thin section preparation—Regolith material dried 24 hr at 50 °C; placed in dishes with low-viscosity epoxy under vacuum 1.4–1.7 kgf/cm^2 at 40–50 °C, breaking and restoring vacuum filled voids and removed bubbles; hardened blocks slabbed and polished; reimpregnation of surfaces required. Final polish sequence of diamond spray compounds of 15–6–3–1; blocks mounted on glass slides with epoxy and slabbed and polished; slides left uncovered. Uncovered slides provide clear visibility and sharp resolution, can be studied by reflected light and electron microprobe analysis, and can be plucked for X-ray diffraction samples.

X-ray diffraction analysis:

Slide preparation—<2-μ fraction suspended in 0.1 *N* NaOH with Sonicator Cell Disrupter; suspension pipetted and dried on glass slides; slides prepared as (1) untreated, (2) solvated with ethylene glycol, (3) heated 1 hr to 300 °C, and (4) heated 1 hr to 500 °C.

Diffraction scan—Slides scanned from 32° to 2°/20, at 2°/20 min^{-1} CuK radiation; mineralogy and proportions of phases by methods of Carroll (1970).

Chemical analyses:

Major element oxides—Rapid rock analysis (Shapiro, 1975).

Major and trace elements—65 elements determined semiquantitatively by emission spectroscopy (but data not reported here).

as 30 m but averaged about 15 m. The soils obtained by coring were generally less than 1 m thick. In the longer of the two cores obtained, massive subsoil extended to 4 m below the surface. The saprolite became harder and less weathered with depth.

METAPELITE

The F2 core (metapelite) was taken on a ridge crest that trends south from the confluence of Difficult Run and Wolf Trap Creek in north-central Fairfax County. The site is located on the west side of a private road about 200 m north of Browns Mill Road (pl. 1). A cross section of the core site is shown on figure 4.

PROFILE ZONATION AND PETROGRAPHY

The zonation of the weathering profile and details of macroscopic inspection of core F2 are presented in plate 3*A*. Most of the profile characteristics that are described macroscopically in plate 3*A* are analyzed in more detail in the photomicrographs presented in figure 5. Saprolite constitutes 75 percent of the weathering profile; the weathered rock zone and the subsoil zone constitute 10 percent and 7 percent, respectively, of the profile. The inherited bedrock structure in the saprolite persists to within 2.4 m of the surface, and patches of coherent saprolite are present to within less than 1 m of the soil surface.

The fresh rock at the base of the profile consists of quartz (≈30 percent), muscovite (≈40 percent), plagioclase (≈25 percent), biotite (≈5 percent), and accessory magnetite. Alternating quartz- and mica-rich folia are the dominant structural features that are seen in thin section.

Muscovite and quartz persist upward through the profile and show signs of alteration only in the upper 1 m. Quartz grains show surface etching and embayment due to dissolution in the upper meter of the profile. Plagioclase grains show etching at the base of the profile and progressive alteration upward in the saprolite. Biotite shows increasing alteration from the base to the top of the saprolite.

MECHANICAL PROPERTIES

SPT blow counts and density for the upper 6 m of the F2 profile are shown in plate 3*A*. The comparison of blow counts with density shows that a direct relation exists among regolith zonation, density, and mechani-

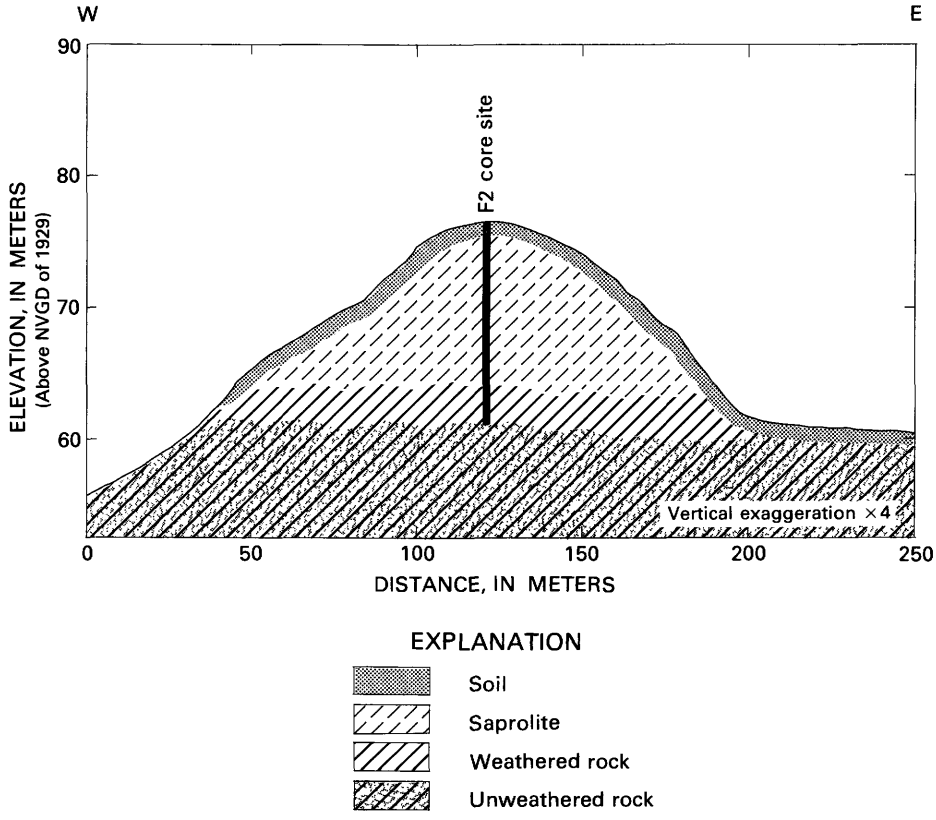

FIGURE 4.—Cross section of metapelite regolith, F2 core site.

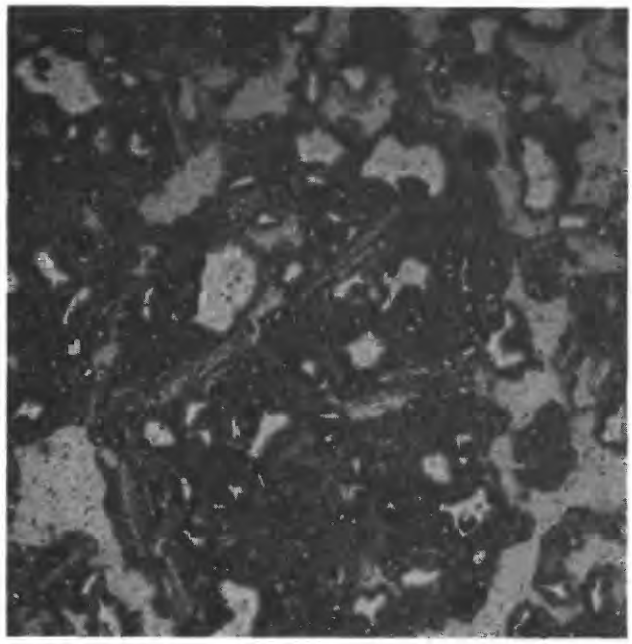

A. Sample 1a at 0.3-m depth. Soil consisting of fine, opaque, sesquioxide matrix containing scattered grains of quartz, muscovite, and saprolite fragments. Quartz grains are angular and etched. (Reflected light, 32×.)

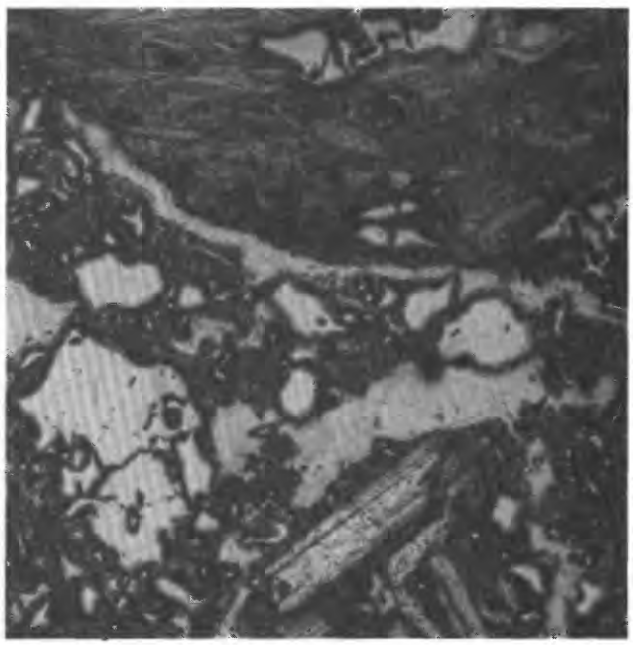

B. Sample 2b at 0.9-m depth. Soil consisting of fine, opaque matrix containing scattered grains of quartz, muscovite, and saprolite fragments. Quartz grains are angular and etched. Mica flakes are randomly oriented and more numerous than in sample 1a. (Reflected light, 32 ×.)

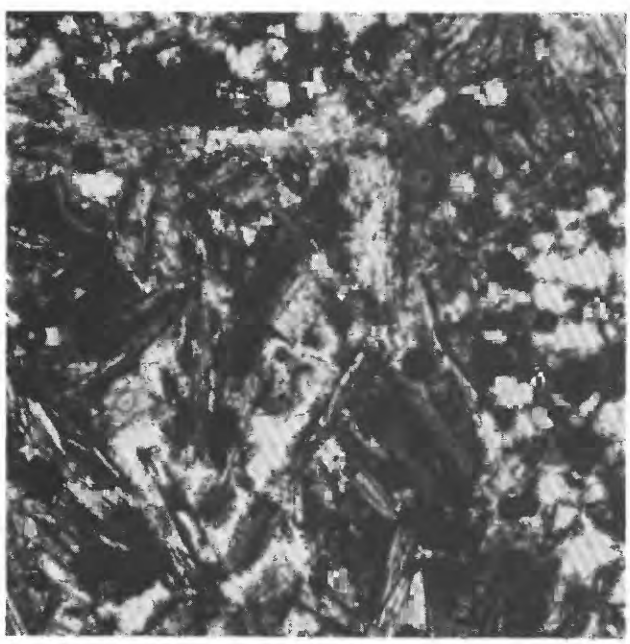

C. Sample 2c at 1.2-m depth. Massive zone consisting of quartz, muscovite, and biotite grains with a small amount of fine-grained opaque matrix. Muscovite flakes appear clouded and stained by alteration. No preferred orientation of the micas. Quartz does not appear etched and occurs in polycrystalline aggregates, some of which are disaggregating. (Transmitted light, 32 ×.)

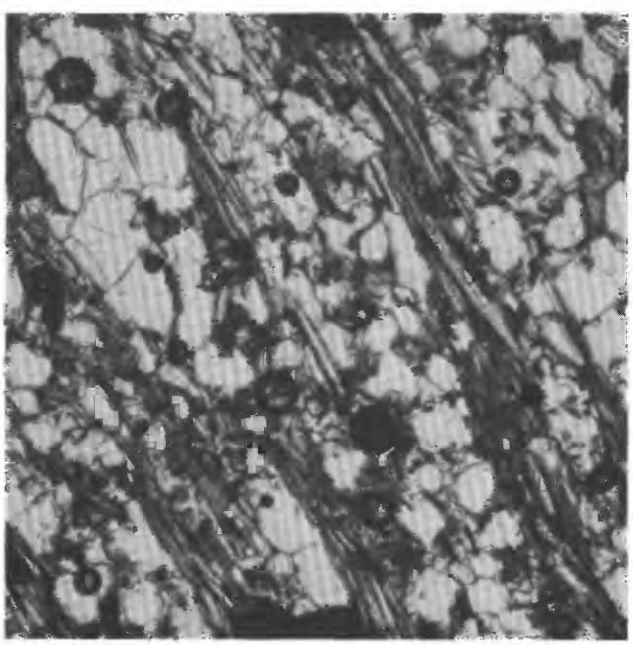

D. Sample 4d at 2.4-m depth. Saprolite composed of foliated muscovite and quartz. Fine-grained opaque matrix occurs between quartz and muscovite grains. Muscovite appears altered at edges of grains. Quartz occurs mainly in polycrystalline aggregates. The outlines of individual quartz crystals are enhanced by sesquioxide stain. (Transmitted light, 32 ×.)

FIGURE 5.—PHOTOMICROGRAPHS OF THE PETERS CREEK METAPELITE REGOLITH, F2 CORE SITE

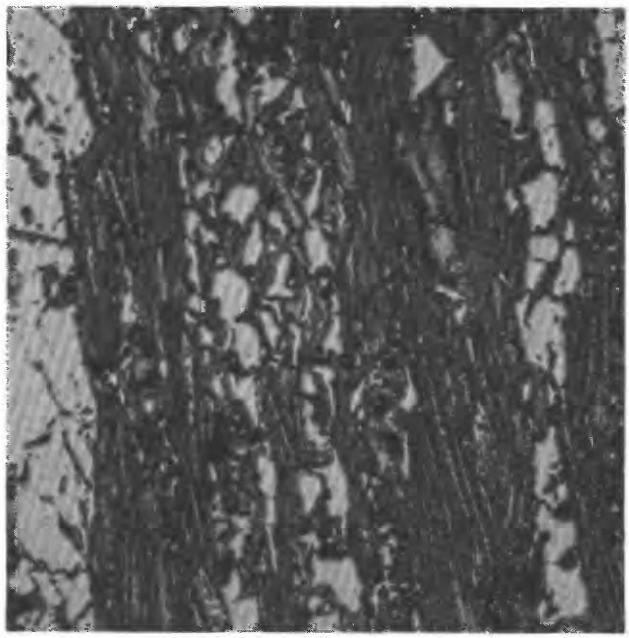

E. Sample 14 at 10.0-m depth. Saprolite composed of foliated muscovite, quartz, biotite, and plagioclase. Plagioclase (first appearance in this profile) is extensively altered; muscovite is unaltered. Boundaries between quartz crystals in polycrystalline aggregates are stained. (Reflected light, 32 ×.)

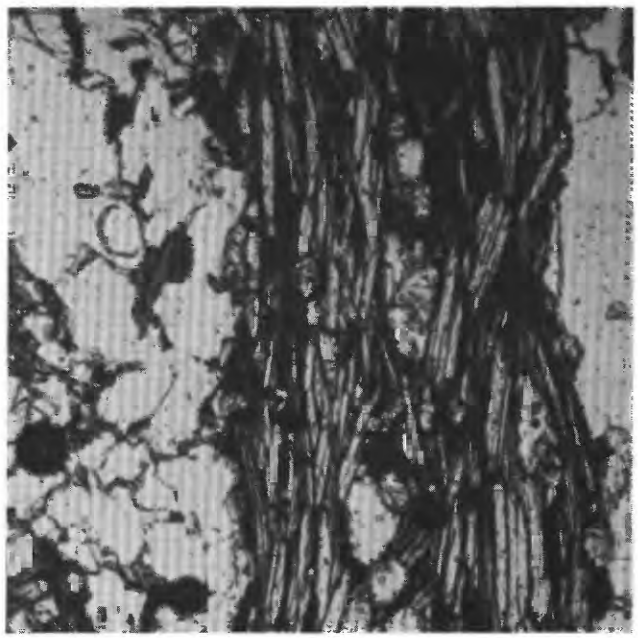

F. Sample 16 at 13.4-m depth. Weathered rock composed of muscovite, quartz, biotite, and plagioclase. Dark stain in micaceous folia is due to oxidation of iron in biotite. (Transmitted light, 32 ×.)

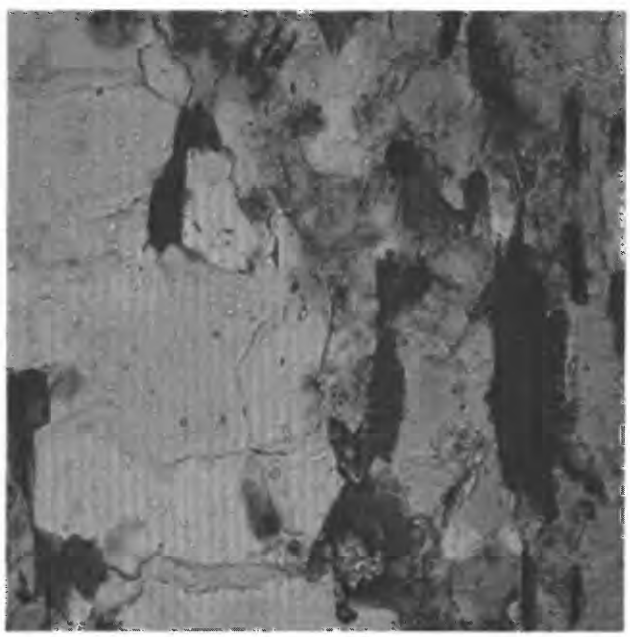

G. Sample 17 at 15.6-m depth. Foliated rock containing unaltered muscovite, biotite (dark), quartz, and plagioclase. Quartz occurs in bands of polycrystalline aggregate; crystal boundaries are faint. (Transmitted light, 88 ×.)

FIGURE 5.—CONTINUED

cal strength. Near the top of the saprolite in sample 6a (p. 3*A*, 3.2-m depth), the density is lowest (1.7 g/cm^3), and the blow counts are low, relative to more dense saprolite at 5.3- to 5.6-m depths. Sample 4d (pl. 3*A*, 2.4-m depth) is in the transitional zone between saprolite and massive subsoil. The loss of structure going from saprolite to the massive zone is associated with a decrease in mechanical strength, as is indicated by the blow counts. The mechanical reorganization is more complex in sample 2b (pl. 3*A*, 0.9-m depth) in the soil's B horizon. The B horizon exhibits the highest density in the upper 5 m of the regolith and is mechanically stronger than is the underlying massive material at 2 m. Therefore, the weak upper part of the saprolite (samples 6a and 4d on pl. 3*A*) apparently has undergone a mechanical disintegration, and the constituent grains have been reorganized into a denser, stronger material (the B horizon) than the original. The density change, assuming little mass addition from superjacent zones, is accomplished by a reduction in volume.

TEXTURE

The texture profile (pl. 3*A*) shows that samples from the upper 2 m are significantly finer grained than the lower samples are, particularly in total <2-μ content. The samples from below 2 m do not show significant textural differences related to weathering. For example, sample 4d from saprolite at 2.4 m is coarser than sample 14 at 10 m, a difference probably related to primary rock textures and unrelated to weathering.

Data indicate that, below 2 m in the saprolite zone, no significant diminution in grain size occurs in the silt-to-fine-sand fraction because of weathering, despite an overall increase in the <2-μ fraction between 10 and 3.2 m. The textural evidence that the remnant coarser fractions are not greatly affected by weathering below 2 m supports the petrographic observations that sand-sized grains of quartz and mica are resistant to chemical attack, while sand-sized plagioclase is removed completely.

Comparison of the changes in texture and density indicates the nature of the processes operating in the upper 3 m. Between 3 and 1.5 m in the massive zone, density increases with minor textural alteration. The lack of significant textural change suggests that, in the massive zone, the density increase is due to volume reduction and that consequent reduction of voids by compaction is due to rearrangement of the regolith structure. Comparison of photomicrographs in figure 5 of samples 4d (2.4-m depth) and 2c (1.2-m depth) demonstrates the loss of parallel mica folia in this zone, which corroborates the evidence for compaction.

Between 1.2 and 0.9 m in the B horizon of the soil, texture changes significantly, and density increases. The density change in this zone is the result of a decrease in void space caused by an increase in the <2-μ fraction, as well as by further compaction. The increase in the clay fraction may be due to genesis of clay minerals derived by chemical alteration of coarser parent minerals, chiefly muscovite and biotite, in this zone or to translocation of clay minerals from zones above. The absence of a well-developed eluviated A horizon in the soil zone (above 0.9 m) contraindicates translocation.

CLAY MINERALOGY

The X-ray diffraction patterns for <2-μ samples from the F2 core are shown in figure 6. The changes in clay mineralogy show progressive trends from the lower to the upper part of the saprolite. Sample 14, from 10-m depth in the saprolite, shows strong quartz and weak feldspar peaks. The broad peak centered at 7.25 A is produced either by a poorly crystallized kaolinite or by halloysite, a hydrated kaolin mineral. The small 10.0-A peak represents muscovite.

At 0.9-m depth in the soil B horizon in sample 2b, significant sharpening of the 7.25-A peak indicates

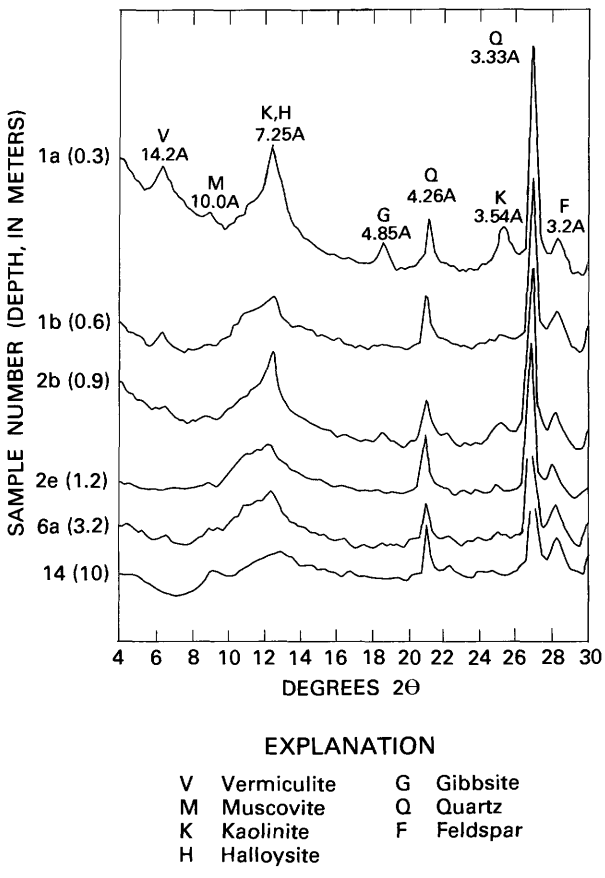

FIGURE 6.—X-ray diffraction patterns for untreated <2-μ samples from the F2 core site.

dehydration of the halloysite, relative to sample 14. A small peak of 4.85 A indicates the presence of a small amount of gibbsite. The small peak at 14.2 A is produced by dioctahedral vermiculite, an aluminous 2:1 layer clay derived from the alteration of muscovite (Rich and Obenshain, 1954).

In sample 1b at 0.6-m depth in the soil zone, the dioctahedral vermiculite peak is stronger than in sample 2b; the gibbsite peak is absent, and the 7.25-A peak is broad. In the shallowest sample, 1a (from 0.3-m depth), sharpening of the kaolin peak suggests dehydration of halloysite. The gibbsite and dioctahedral vermiculite peaks are stronger than in the deeper samples and indicate much more intense chemical alteration of this horizon than in the horizon below. The weak feldspar and the strong quartz peaks persist through the profile.

The change in soil clay mineralogy at 0.9-m depth indicates that chemical alteration is partly responsible for the textural change of the weathering profile relative to the lower samples. The dehydration of halloysite to kaolinite and the appearance of gibbsite and dioctahedral vermiculite (sample 2b) indicate more intense chemical weathering of parent minerals at this depth than in the lower samples. The reaction mechanism of muscovite to dioctahedral vermiculite probably involves removal of interlayer K^+ and replacement by H^+. SiO_2 also may have been removed from octahedral layers. This structural alteration fits the description of the transformation of a mica into a clay mineral as suggested by Rich and Obenshain (1954). The 10-A peak in sample 1a shows that, between 0.9 m and the surface, muscovite is altered; in the saprolite, however, muscovite is not altered. Muscovite appears to be the predominant source of the clay being formed in the soil. A relatively small amount of very fine grained plagioclase or potassium feldspar is present in the soil zone. Diffractograms from all samples contain minor 3.20-A feldspar peaks. However, no potassium feldspar was seen in thin sections, and the untwinned plagioclase was not identified in zones higher than the weathered rock. The 3.20-A peak may be caused by very fine grained albite or by potassium feldspar that was not observed in thin section.

CHEMICAL ZONATION

The chemistry of the metapelite weathering profile is shown in plate 3*A*. Note that interpretation of the gain or loss of any element relative to a higher or lower sample must take into consideration changes in bulk density, which are related to relative proportions of mineral species, and changes in abundances of other elements. Simple comparison of the slopes of lines on the semilog plot may be misleading.

Data points for samples between 3- and 15.3-m depth (pl. 3*A*) are connected by solid lines and are considered to represent isovolumetric saprolite, on the basis of the retention of fabric and structure, and therefore the volume of the parent material. Above 3 m, disruption of the original structure indicates that the apparent gains and losses of elements are not due simply to chemical reactions, but that mechanical processes such as translocation of clays may also affect the concentration of a particular element (for example, iron and aluminum). The major intervals of chemical change are in the lower part of the saprolite and in the soil. In the saprolite, the losses are absolute, and the gains, except for H_2O^+, are relative. In the nonisovolumetric zone, the losses are still absolute, but certain horizons appear also to have absolute gains in mass due to translocation of mineral constituents.

In the saprolite, three main trends are seen: (1) absolute loss of CaO and Na_2O and some SiO_2, (2) absolute gain in H_2O^+, and (3) relative gains or constancy of Al_2O_3, Fe_2O_3, K_2O, MgO, and TiO_2. The virtually complete loss of CaO and Na_2O and some of the SiO_2 loss can be accounted for by the dissolution of plagioclase feldspar. Assuming a plagioclase composition of $Ab_{60}An_{40}$, the stoichiometry of this reaction can be written as:

$$2.5\ (Na_{0.6}Ca_{0.4}Al_{1.13}Si_{2.8}O_8)+0.5\ H^+ +3.0\ CO_2+ (12.4+X)\ H_2O=$$

$$1.4\ Al_2Si_2O_5(OH)_4\cdot XH_2O+1.5\ Na^+_{(aq)}+ 1.0\ Ca^{+2}_{(aq)}+$$

$$13.0\ HCO_{3(aq)}+4.2\ H_4SiO_{4(aq)}.$$

This reaction accounts for some but not all of the mass loss in the zone between 10 and 3 m. The stoichiometry also demonstrates that this reaction will be favored by an excess of water and by an acidic pH. Because the weathering environment is generally acidic, the flux rate of H_2O through the weathering profile may be the limiting factor on the reaction rate.

The mineral species that contribute to mass loss in the saprolite also can be demonstrated by comparison of the observed mole ratios of CaO, Na_2O, Al_2O_3, and SiO_2 lost during weathering. Between 10 and 3 m, the moles of constituents lost per cubic centimeter are

CaO $0.036\ g/cm^3 \div 56\ g/mol = 6.4\times10^{-4} mol/cm^3$
Na_2O $0.034\ g/cm^3 \div 62\ g/mol = 5.5\times10^{-4} mol/cm^3$
Al_2O_3 $0.09\ g/cm^3 \div 102\ g/mol = 8.8\times10^{-4} mol/cm^3$
SiO_2 $0.29\ g/cm^3 \div 60\ g/mol = 4.8\times10^{-3} mol/cm^3$

These figures indicate that Al_2O_3 is not totally conserved in the solids and that substantial SiO_2 is lost. Roughly twice the amount of silica is lost when compared with the total amount lost of the other elements.

All this silica loss cannot be accounted for solely by plagioclase dissolution. Reactions such as biotite or quartz dissolution also must contribute to the silica loss.

Above the saprolite, the weathering process cannot be considered to be isovolumetric. Except for silica, the chemical trends developed upward through the saprolite change dramatically in the nonisovolumetric subsoil and soil (pl. 3*A*). In the soil and subsoil, the absolute loss of silica is large. Al_2O_3, Fe_2O_3, and H_2O^+ show overall gains; K_2O, MgO, and TiO_2 show gains relative to the saprolite but losses relative to Al_2O_3, Fe_2O_3, and H_2O^+.

The gain in Al_2O_3 in the zones of high bulk density is due largely to compaction of material in the B horizon relative to the saprolite. If no chemical processes were taking place in the B horizon of the soil, proportions of all the oxides would remain similar in the zone between 1.2- and 0.6-m depth, even though the density increases 17 percent. The changes in proportions indicate, however, that the B horizon is extremely active both chemically and mechanically.

The weathering processes of the soil zone most clearly identified by the chemical data are alteration of muscovite and dissolution of quartz. The alteration of muscovite to dioctahedral vermiculite that was indicated by X-ray diffraction also is indicated by the chemical analyses. The relatively slight gain of K_2O in the upper 1.5 m of the soil indicates that potassium is being leached and removed relative to Al_2O_3 and H_2O^+, the chief constituents that are involved in the alteration of muscovite to dioctahedral vermiculite. Some silica may be leached from muscovite in this transformation, but most of the SiO_2 loss is due to quartz dissolution.

METAGRAYWACKE

The F3 core (metagraywacke) was taken at Hazleton Laboratories 100 m northeast of the intersection of Route 7 and Towlston Road, north-central Fairfax County. A cross section of the site is shown in figure 7.

PROFILE ZONATION AND PETROGRAPHY

The F3 core encountered regolith that is relatively siltier and thicker (28 m) than that of the core of metapelite regolith (15 m). Despite differences in geomorphology, drainage, parent texture, and regolith thickness, metagraywacke regolith shows many petrographic features that are similar to those of the metapelite regolith (pl. 3*B*). Saprolite constitutes 55 percent of the profile, and weathered rock constitutes 35 percent. The details of macroscopic features described on plate 3*B* can be seen in the photomicrographs in figure 8.

The fresh rock is composed of quartz (≈65 percent), plagioclase (≈25 percent), muscovite (≈5 percent), biotite (≈5 percent), and accessory epidote and magnetite. Plagioclase is the only mineral visibly altered in the

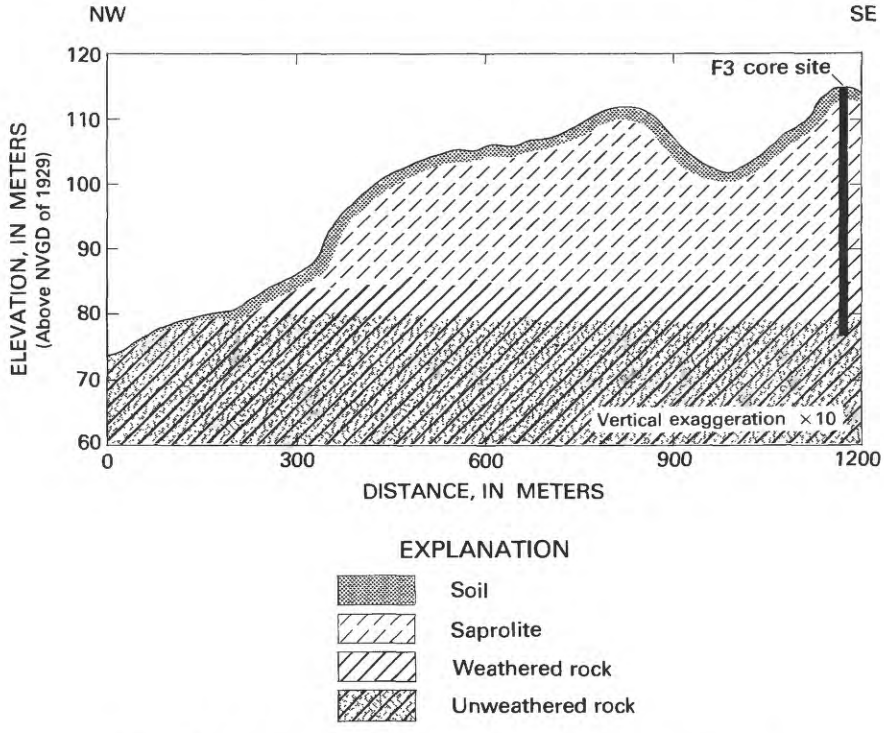

FIGURE 7.—Cross section of metagraywacke regolith, F3 core site.

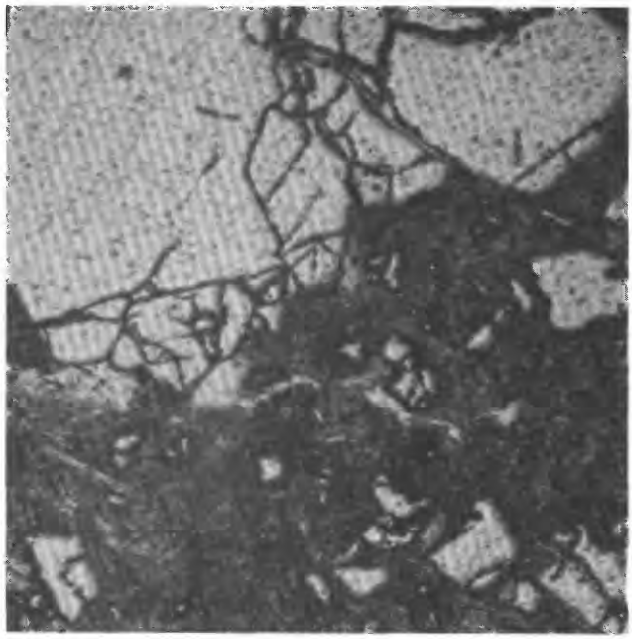

A. Sample 1c at 0.6-m depth. Soil consisting of angular quartz grains scattered in a cryptocrystalline-to-amorphous limonitic matrix. Muscovite grains are randomly oriented. Opaque areas are iron stained. (Reflected light, 32 ×.)

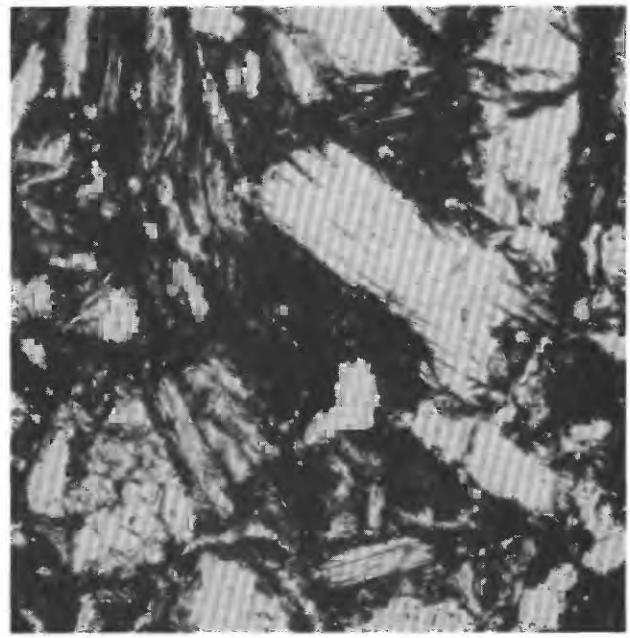

B. Sample 2e at 1.2-m depth. Massive zone containing angular quartz grains and scattered muscovite flakes. (Reflected light, 32 ×.)

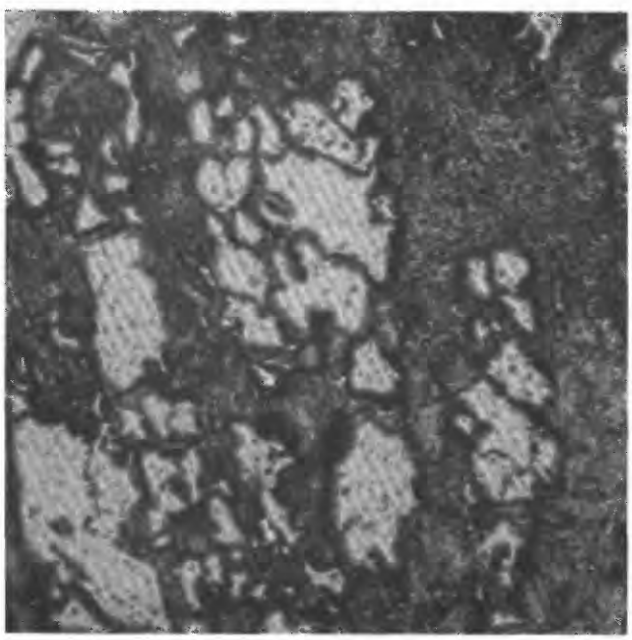

C. Sample 7b at 4.0-m depth. Saprolite containing laminae of quartz and muscovite with some opaque amorphous material. Quartz grains are distinctly etched. (Reflected light, 32 ×.)

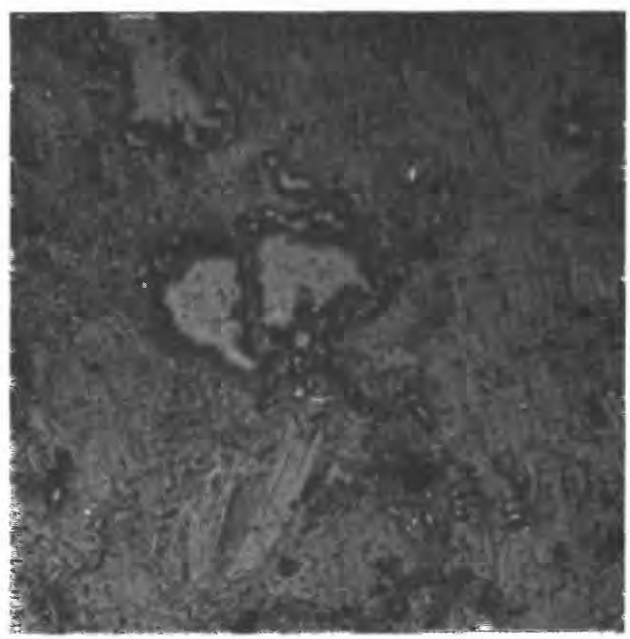

D. Sample 10b at 5.8-m depth. Micaceous saprolite containing muscovite, quartz, and opaque amorphous matrix (Reflected light, 88 ×.)

FIGURE 8.—PHOTOMICROGRAPHS OF METAGRAYWACKE REGOLITH, F3 CORE SITE

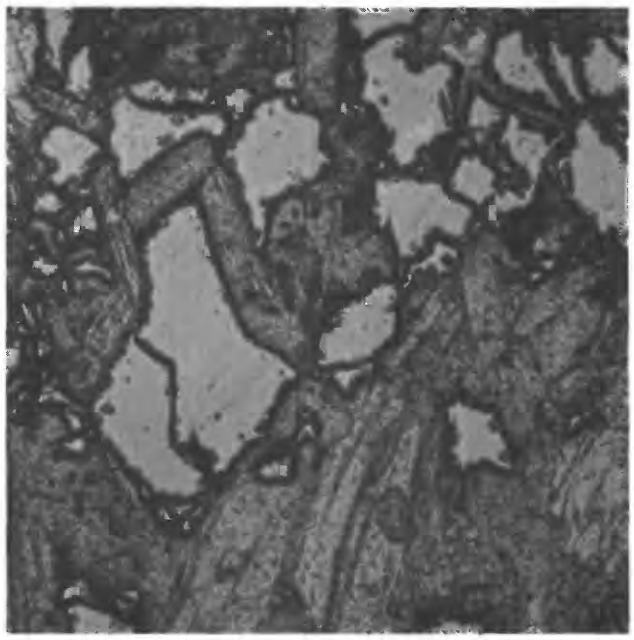

E. Sample 13 at 7.0-m depth. Micaceous saprolite containing muscovite, quartz, altered biotite, and opaque mottles. (Reflected light, 88 ×.)

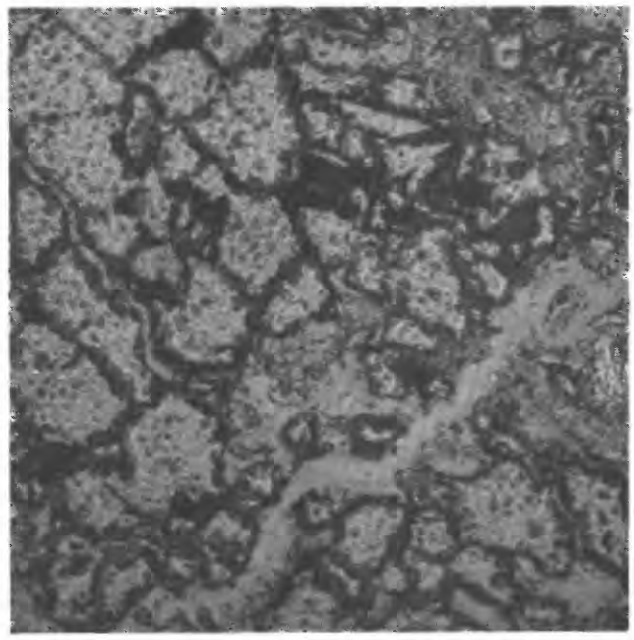

F. Sample 31 at 18.0-m depth. Quartz-rich saprolite containing a small smount of muscovite having chloritized boundaries. Quartz shows little etching, but polycrystalline boundaries are distinct. (Reflected light, 88 ×.)

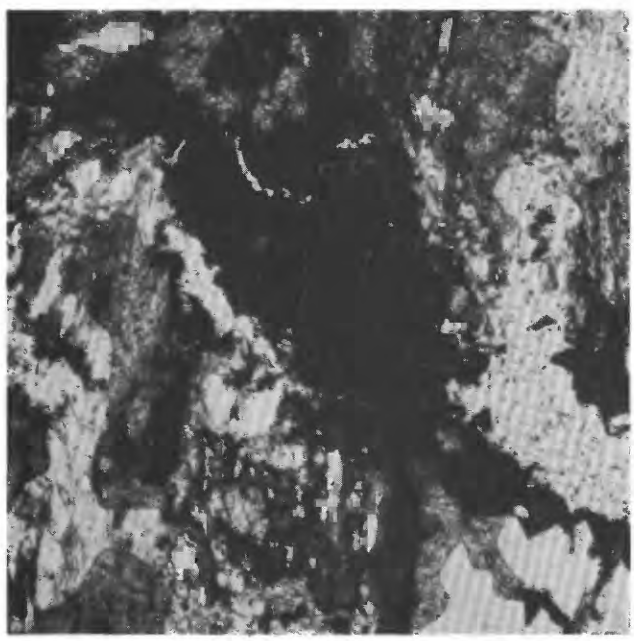

G. Sample 40 at 22.0-m depth. Foliated quartz and muscovite metagraywacke saprolite, subordinate altered biotite, and accessory magnetite. This zone is less altered than material above. (Transmitted light, 32 ×.)

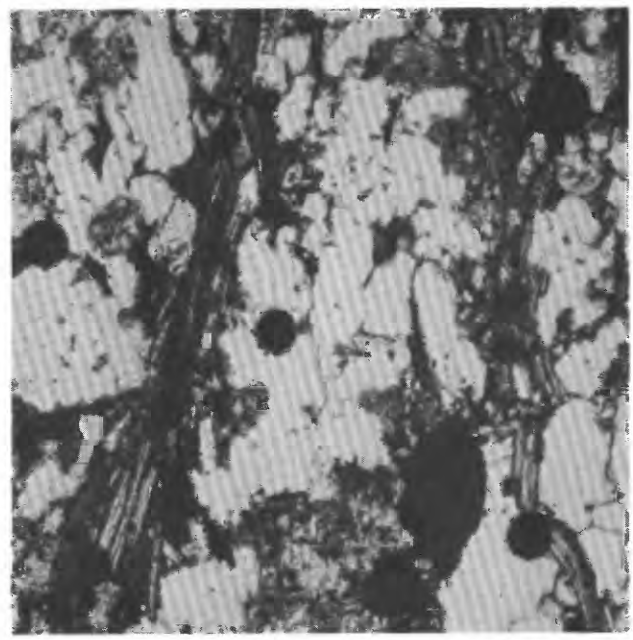

H. Sample 46b at 28.3-m depth. Weathered, quartz-rich metagraywacke containing plagioclase. Plagioclase and biotite show slight alteration. Polycrystalline quartz boundaries are faint. (Transmitted light, 32 ×.)

FIGURE 8.—CONTINUED

I. Sample 47a at 33.5-m depth. Mica schist with abundant muscovite and biotite; lesser amounts of quartz and unaltered plagioclase (about 5 percent of rock). (Transmitted light, 32 ×.)

FIGURE 8.—CONTINUED

weathered rock zone. Plagioclase decreases in abundance upward through the saprolite, but the muscovite appears to be unaltered. Iron-oxide stains on quartz grains are common to a depth of 20 m, and irregular veins of iron-stained material extend through the saprolite to that depth.

Rock structure is preserved to within 3 m of the surface. Between 3- and 4-m depth, the quartz folia are disintegrated slightly; the limonitic accumulation between quartz folia is extensive, and the micas appear slightly altered.

Above 3 m, the parent rock structure is lost, and a 2-m-thick massive zone occurs between the saprolite and soil. The massive zone is composed predominantly of quartz and muscovite. The soil zone is significantly finer grained than the massive zone is and exhibits a high proportion of etched and embayed quartz grains.

MECHANICAL PROPERTIES

Plate 3*B* shows bulk density and SPT blow counts for the F3 core. The maximum strength measured is at about 6-m depth; the upper part of the saprolite at 3-m depth is significantly stronger than is the massive zone at 2.4-m depth. The blow counts do not increase with the density increase in the soil; although the soil is formed partly by compaction of the massive zone, the compaction of metagraywacke regolith is less than that of the metapelite regolith. The F3 profile shows that structure loss and volume reduction are not restricted totally to the upper few meters of the profile. At 18-m depth, macroscopic features of the core revealed massive zones almost or entirely lacking the foliated structure of the parent rock. Sample 31 from 18-m depth was the lowest density sample tested. The high degree of alteration of the zone probably is due to intersecting joints or fractures. Furthermore, the density increase above 18 m might also be due to some volume reduction. The predominance of saprolite structure between 18 and 4 m indicates, however, that most of this zone has undergone isovolumetric weathering. The major zone of structural reorganization occurs above 4 m.

TEXTURE

The texture of the metagraywacke parent material is heterogeneous. In the intervals from 5.5- to 12.2-m depth and 15.9- to 20.4-m depth, the rock varies between a fine-grained micaceous schist and a sandy quartz-rich schist. Thus, separating the textural effects of weathering from those of variation in parent grain size is difficult.

The grain size data in plate 3*B* indicate that major textural changes occur at the top of the profile because of chemical weathering and soil formation. Sample 1c at 0.6-m depth is significantly finer grained than any of the lower samples; this observation strongly suggests that in-place fining is due to chemical weathering and (or) translocation. Translocation of clay-sized material from the overlying soil does not seem a sufficient explanation of the soil texture because of the thinness of the A horizon and because of the observed increases of both clay and silt content that occur between 1.2 and 0.6 m.

The texture of deeper samples from saprolite is inherited from the parent material. The textural variations among bulk samples that were measured by the hydrometer method correspond to macroscopic variations of grain size within different horizons of the saprolite. The texture data show that clay content of saprolite is low; this level of clay content suggests that weathering in the saprolite and weathered rock zones produces very little clay-sized material.

Density and textural changes correspond closely from the saprolite zone to the soil zone. Except for sample 10d at 5.8-m depth, the saprolite exhibits a density well below 2 g/cm^3. The density and clay content of the massive zone at 1.2-m depth are slightly

greater than those of the saprolite at 4-m depth. Between 1.2 and 0.6 m, the increase in both density and clay content is significant. This density increase is attributable to volume reduction.

CLAY MINERALOGY

The principal clay mineral in the saprolite is a hydrated kaolin phase having a broad peak centered at 7.25 A (fig. 9). Kaolin that is present in the soil in the upper 1 m produces a narrow and sharp 7.25-A peak, which indicates that the kaolin has undergone dehydration and has increased in crystallinity. No evidence of dehydration of this phase is present lower in the profile, although the upper part of the saprolite is above the phreatic zone.

A 3.20-A feldspar peak is present in all samples of the saprolite and is diminished in the soil. This peak is interpreted to be due to submicroscopic plagioclase or potassium feldspar. Separation and accurate identification of the feldspar were not attempted.

Below 0.6-m depth, halloysite is the predominant clay mineral; a small amount of muscovite also is present. In the soil at 0.6-m depth, the muscovite peak is more pronounced than it is lower in the profile. Muscovite occurs as one end member of a mixed-layer complex, as is shown by the high background between 10 and 14.2 A. Gibbsite is absent.

Both the texture data and clay mineralogy indicate that pedogenic clay-sized material is present in the soil zone and that the soil is composed predominantly of quartz plus the aluminous residue of intense chemical alteration of micas. Alteration of muscovite by grain size reduction is shown by the presence of the 10.0-A peak. The muscovite is the precursor to 14.2-A vermiculite that is produced by transformation. In the saprolite, the muscovite is not affected by chemical weathering, but, in the soil, it is the major source of clay-sized material.

CHEMICAL ZONATION

Despite the heterogeneity of the parent material, changes in chemical composition (as shown in pl. 3*B*) are progressive with depth. Oxidation of Fe^{+2} to Fe^{+3} takes place at the base of the profile; Fe_2O_3 content increases upward from the weathered rock zone. CaO and Na_2O decrease notably in the weathered rock zone at the base of the profile, and they are completely leached in the lower part of the saprolite. The other major-element constituents are proportionately constant from the base of the profile to the top of the saprolite. In the massive zone and soil, the relative proportions of constituents are greatly changed. This

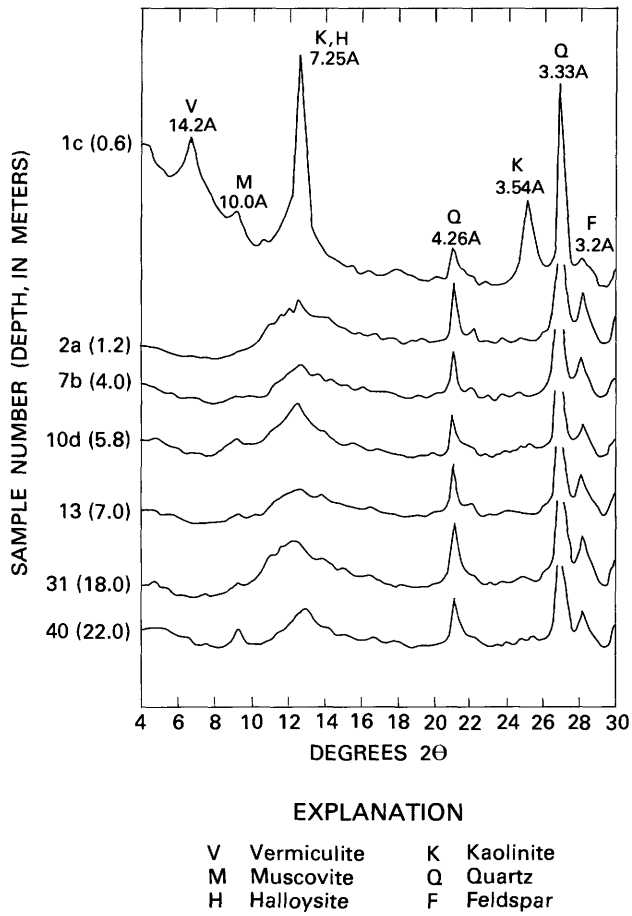

FIGURE 9.—X-ray diffraction patterns for untreated <2-μ samples from the F3 core site.

change is due, in part, to a loss of silica from the near-surface zones.

Along with the gross trends, other variations in individual constituents suggest three main zones of alteration. The weathered rock zone between 33.6- and 33.9-m depth contains ferric iron and shows decreases in CaO and Na_2O associated with plagioclase alteration. The variations in CaO and Na_2O in the bottom four samples appear to be directly related to the variation in plagioclase content of the unweathered rocks. Between 18- and 33.6-m depth, CaO and Na_2O are virtually nil and evidently have been completely leached. In addition, both Al_2O_3 and SiO_2 show relative decreases. At the top of the saprolite zone between 4- and 5.8-m depth, concentrations of Al_2O_3, Fe_2O_3, K_2O, and MgO decrease significantly. In the main body of saprolite between 5.8- and 18-m depth, the changes in bulk chemistry are minor, relative to these main leaching zones.

Through roughly half of the profile, the main chemical changes are an increase in SiO_2 and a loss of Fe_2O_3 and H_2O^+. In the main body of saprolite, therefore,

except for plagioclase dissolution, chemical weathering does not produce much alteration.

At the top of the profile, in the massive zone and the soil, mineral and chemical constituents vary nonisovolumetrically. The main variations involve an increase in Fe_2O_3 and Al_2O_3 and a loss of SiO_2. The Al_2O_3 increase reflects larger amounts of clay, and the decrease in SiO_2 is due to dissolution of quartz and alteration of muscovite and possibly of biotite.

GRANITE

The site of core F11 (granite) is the highest upland immediately north of the Occoquan River just west of the intersection of Ox Road (Route 123) with Hampton Road (Route 647). A cross section of the site is shown in figure 10.

PROFILE ZONATION AND PETROGRAPHY

The details of the macroscopic character and profile zonation of core F11 are shown in plate 3*C*. This core shows a continuous progression upward from fresh rock through saprolite, 75 percent of the core, to a highly weathered massive zone, 15 percent of the core, and soil, 10 percent of the core. Mineral alteration, mainly of plagioclase and epidote, occurs deep in the profile in the weathered rock zone. Plagioclase and epidote are less abundant upward in the saprolite, but potassium feldspar persists to within 4 m of the surface.

Because of the uniform texture of the coarse-grained parent rock, which consists of quartz, plagioclase, potassium feldspar (orthoclase), and biotite, photomicrographs (fig. 11) of the F11 core clearly illustrate the effects of mineral alteration and display the progressive nature of the weathering effects from fresh rock to soil. In the deepest of the core F11 samples (sample 9), mineral alteration is not evident. Abundant idiomorphic epidote in poikiloblasts within plagioclase is of metamorphic origin. In the weathered rock zone, plagioclase (sample 8) is slightly clouded. In comparison, the basal part of the saprolite (sample 7) exhibits greater plagioclase alteration, limonite staining along grain boundaries, and 50-mm-wide limonite veins that traverse the saprolite. In areas higher in the saprolite zone (samples 6, 5, and 4), the photomicrographs show strong etching of the feldspars along cleavage or twinning planes; the micas are exfoliated. The expansion of the mica in sample 4 appears to have caused the disaggregation of adjacent polycrystalline quartz aggregates. Voids between quartz grains are open, and the quartz grain boundaries are etched locally. In the highest part of the saprolite (sample 3), the original fabric and grain relations have been disrupted severely. The micas and clays form a fine matrix in which the polycrystalline quartz clusters are disaggregated. Some of the disaggregation may be due to thin section grinding, but

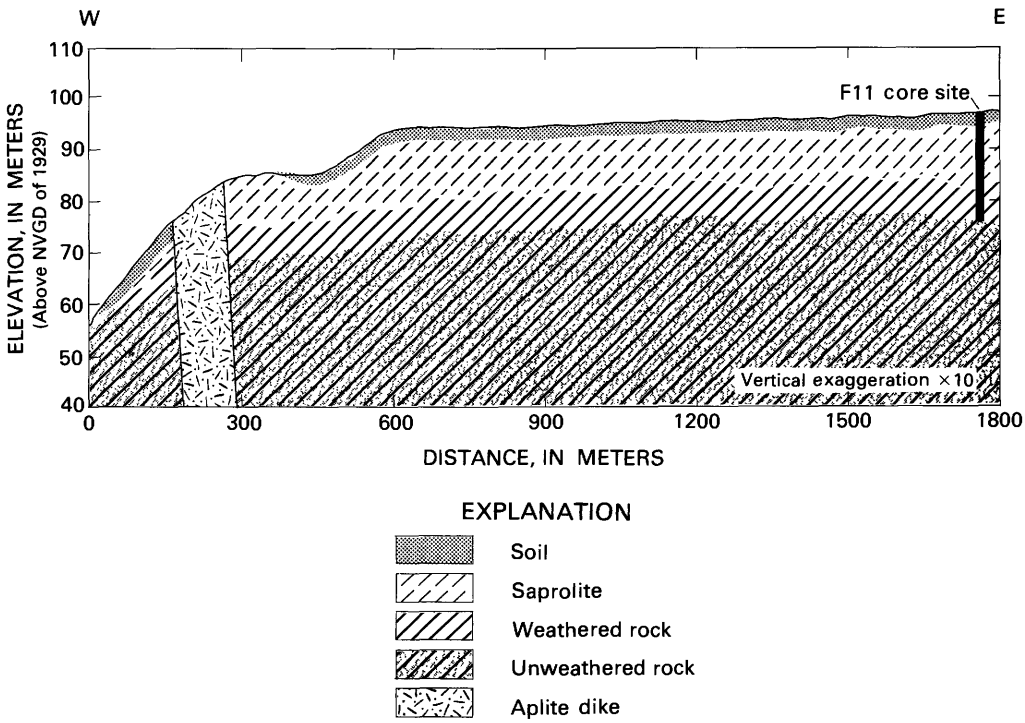

FIGURE 10.—Cross section of granite regolith, F11 core site.

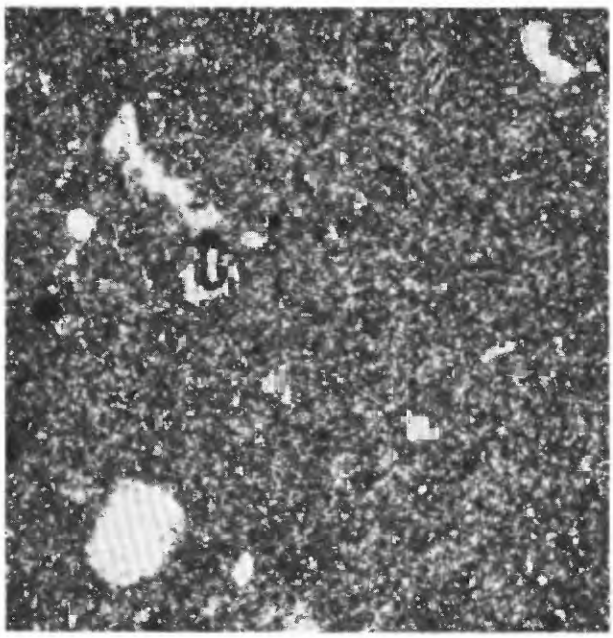

A. Sample 1 at 0.6-m depth. Soil consisting of subangular fragments of quartz in fine limonitic matrix. (Reflected light, 32 ×.)

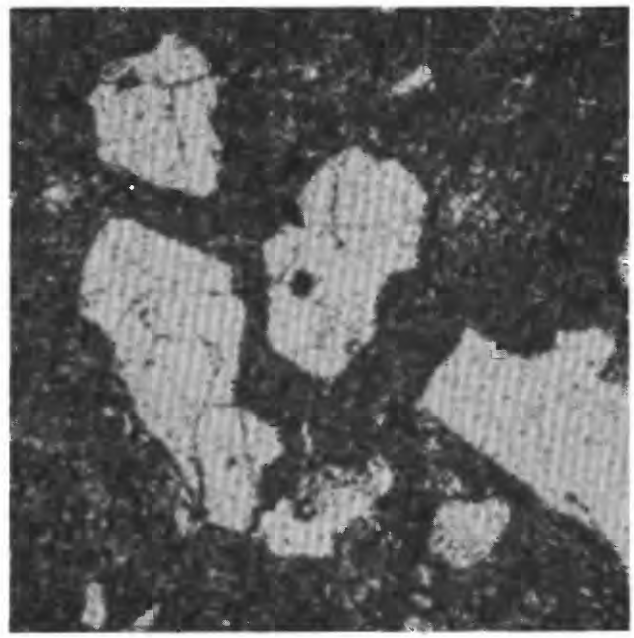

B. Sample 2 at 1.5-m depth. Massive zone in which quartz grains are much more abundant than in sample 1. The matrix is coarser and appears to contain more crystalline, altered mica. The mica flakes are small and randomly oriented. (Reflected light, 32 ×.)

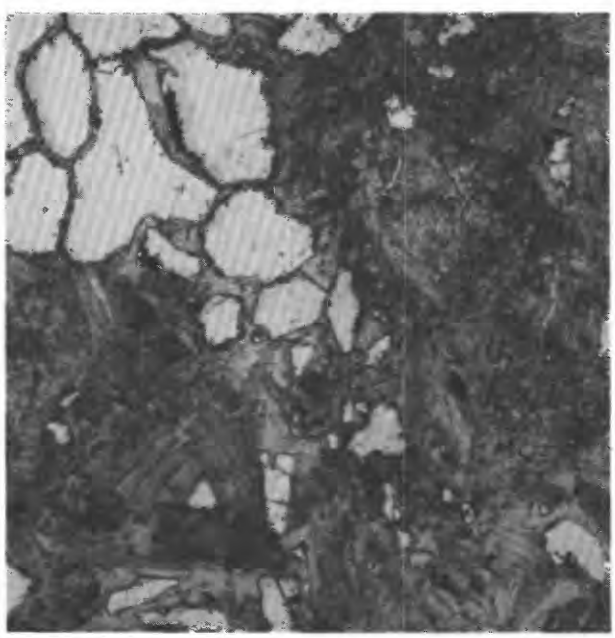

C. Sample 3 at 4.3-m depth. Saprolite containing disaggregated clusters of small quartz grains and several large potassium feldspar grains in an oriented matrix of altered micas. Rock structure visible. (Reflected light, 32 ×.)

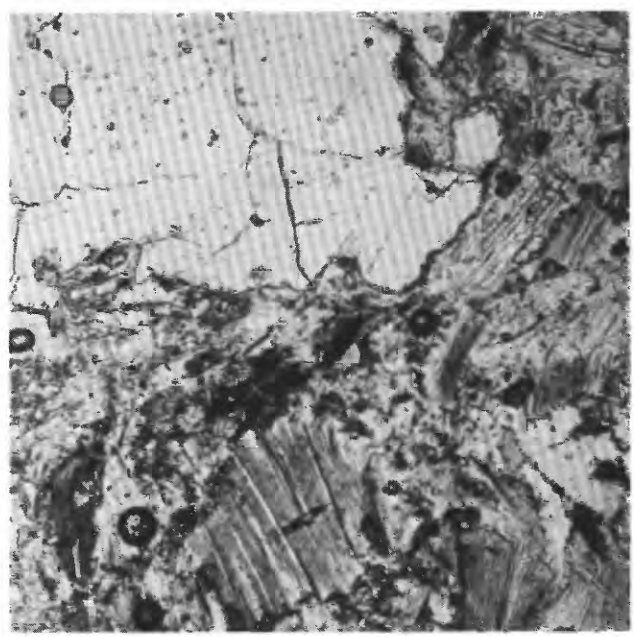

D. Sample 4 at 6.7-m depth. Saprolite containing quartz clusters that are less disaggregated than the clusters in sample 3. Micas are less altered, although visibly expanded along C axes. No feldspar is identified, and very little clay is present. (Transmitted light, 32 ×.)

FIGURE 11.—PHOTOMICROGRAPHS OF OCCOQUAN GRANITE REGOLITH, F11 CORE SITE

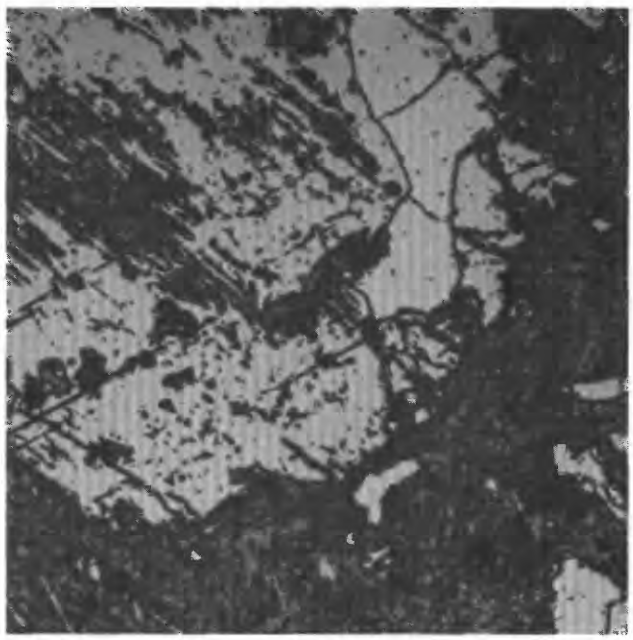

E. Sample 5 at 11.0-m depth. Saprolite containing quartz clusters that are not disaggregated. Micas look fresher than those in sample 4. Large plagioclase grain shows alteration at edges and etching of cleavage planes. (Reflected light, 32 ×.)

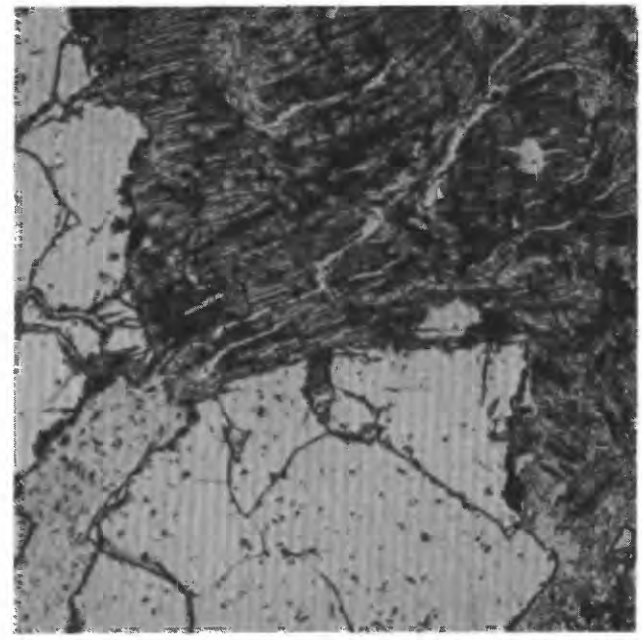

F. Sample 6 at 14.9-m depth. Saprolite with some quartz clusters showing evidence of disintegration; others are unaltered. Micas are altered and expanded. Plagioclase and potassium feldspar are present. (Transmitted light, 32 ×.)

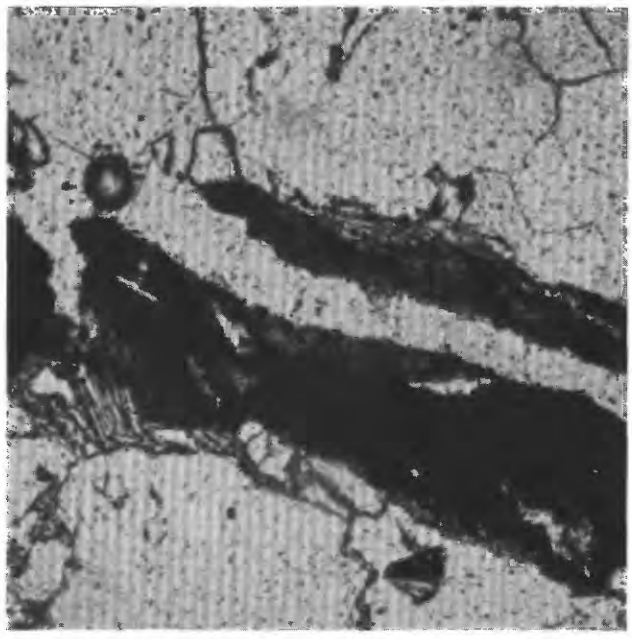

G. Sample 7 at 19.8-m depth. Saprolite in which quartz clusters are unaltered. Cloudy plagioclase contains metamorphic sericite; epidote is abundant; potassium feldspar is clear and unaltered. The photomicrograph shows one large, iron-stained fracture traversing the saprolite. (Transmitted light, 32 ×.)

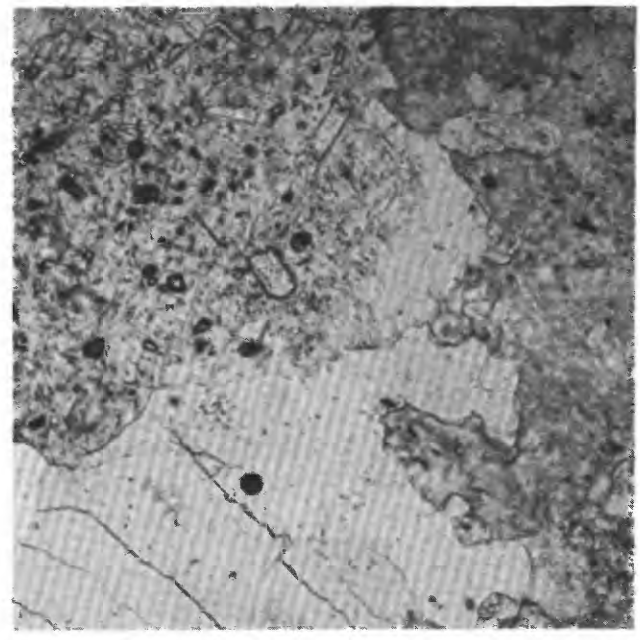

H. Sample 8 at 21.10-m depth. Weathered rock that is microscopically similar to sample 7. Petrographically the rock is a tonalite. Inclusions of sericite and epidote in plagioclase are of metamorphic origin. (Transmitted light, 32×.)

FIGURE 11.—CONTINUED

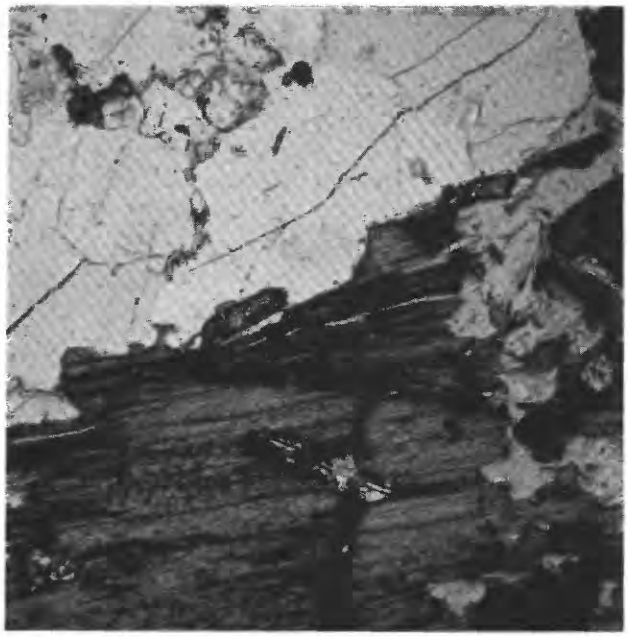

I. Sample 9 at 21.9-m depth. Fresh rock consists of unaltered plagioclase (approximately 30 percent of section), mica (5 percent), potassium feldspar (5 percent), and quartz (60 percent). Micas (muscovite and biotite) are unaltered. Some iron staining is present along joint planes. (Transmitted light, 32 ×.)

FIGURE 11.—CONTINUED

there is evidence of chemical alteration of quartz along crystal boundaries. Small embayments in individual quartz crystals show evidence of leaching. In the massive zone (sample 2), the quartz is present as individual monocrystalline grains in a very fine clay matrix. The grains are generally angular and deeply embayed, probably due to dissolution. In the soil (sample 1), the amount of quartz in sand-sized grains is greatly reduced relative to the massive zone (sample 2). The soil grains are smaller than those in the massive zone, and they are generally angular.

MECHANICAL PROPERTIES

The blow counts shown on plate 3*C* indicate that material from the massive zone, from 1.5- to 3.6-m depth, is mechanically weaker than that of the upper part of the saprolite at 4.3 m. The B horizon of the soil is much stronger than the underlying massive material. The blow counts further indicate that the massive subsoil zone is a relatively weak zone, that the soil is denser and more compact than is the massive zone, and that the soil is mechanically stronger.

TEXTURE

The textural data for the granite weathering profile (pl. 3*C*) indicate an overall upward fining of the regolith from weathered bedrock to the soil. Variations within the saprolite zone (notably in samples 6, 5, and 4) may be due partly to variation in parent texture, but the increase in the <2-μ fraction upward through the saprolite is consistent.

Sample 2 from the massive zone shows a large increase in silt and clay relative to the lower samples. Clay increases markedly from 6 to 24 percent between samples 3 and 2. The soil zone (sample 1) shows an even more pronounced fining relative to the massive zone. The clay content of the soil zone is nearly twice that of the massive zone.

Within the entire profile, much of the increase in the fine sand and silt grain sizes is due probably to chemical etching and exfoliation of coarser grains rather than due to the disintegration of polycrystalline quartz aggregates into monocrystalline grains. Photomicrographs of samples 3 and 4 in the saprolite zone (fig. 11) illustrate progressive effects of etching and exfoliation. Most of the quartz disaggregation takes place within the upper part of the saprolite, above 7 m.

The density changes correspond well with the observed regolith structure and texture analyses. The density decreases systematically from fresh rock (sample 9) to near the top of the saprolite at a depth of 6.7 m (sample 4). The density of the uppermost saprolite, 2.2 g/cm^3 (sample 3), is close to the minimum density of the saprolite, 2.1 g/cm^3 (sample 2 in the massive zone). Although the increase in the percentage of clay in sample 2 relative to sample 3 is large, evidently little volume reduction in the massive zone has occurred. The clay increase is due to translocation of clays from above or due to alteration of parent minerals in place. The soil B horizon (sample 1) shows a major increase in density relative to the massive zone. This increase is due to volume reduction, as well as to in-place formation of clay-sized material.

CLAY MINERALOGY

The large increase in clay and silt content in the soil relative to the massive zone may suggest a difference in parent material for the soil. The X-ray diffraction patterns from the F11 core site (fig. 12), however, show that the clay mineral phases in the soil were derived from weathering of the underlying granitic saprolite. The soil contains little if any transported (that is, aeolian or

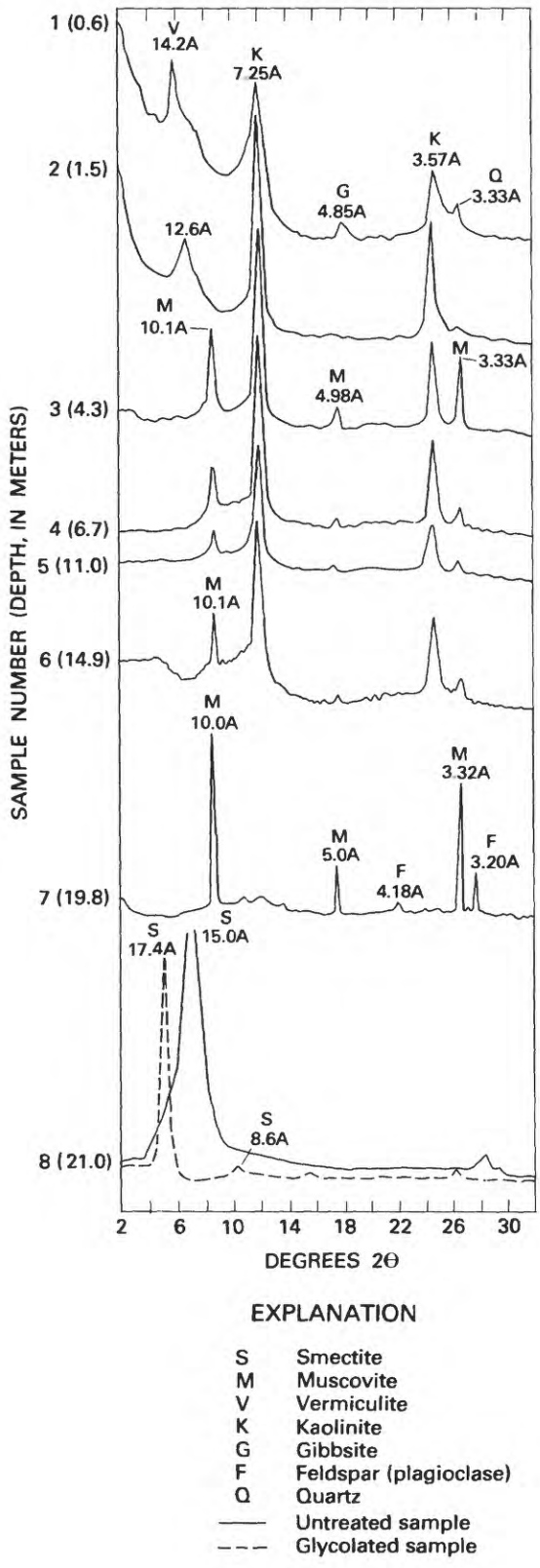

FIGURE 12.—X-ray diffraction patterns for untreated and selected glycolated <2-μ samples from the F11 core site.

colluvial) clay derived from other source rocks. Similarly related clay phases of the massive subsoil show that the subsoil is a zone of mechanical compaction of the saprolite and is a transitional zone between the saprolite and the soil.

In the upper 2 m of the profile, 10.0-A muscovite is transformed into 14.2-A vermiculite. The similarity of the kaolinite traces above and below 4.3-m depth and the progressive alteration of muscovite to vermiculite above 4.3 m seem to indicate that all the clay in the soil is derived from in-place weathering.

The clay in the saprolite below 4.3-m depth is predominantly kaolinite. The sharp and narrow 7.25-A peak indicates that kaolinite is not hydrated. A small proportion of halloysite, determined from the broad valley between the 7.25-A and 10.0-A peaks that forms a high angle shoulder on the 7.25-A peak, however, is evident from 4.3 m downward.

Below 4.3 m, muscovite is a minor constituent relative to kaolinite. The muscovite shows some evidence of alteration relative to the very sharp muscovite peaks in sample 7 at 19.8-m depth. The alteration is mainly a hydration that causes broadening of the peak and a slight shift from 10.0 A to 10.1 A (for example, compare samples 7 and 6). Sample 7 also contains a small amount of plagioclase feldspar that is not detected in the clay fraction higher in the profile. Sample 8 at 21 m is unique because the <2-μ fraction is entirely smectite, as determined from glycol solvation. This smectite is derived by alteration of biotite, as seen in thin section. The smectite is apparently unstable higher in the profile where it does not occur in association with kaolinite.

CHEMICAL ZONATION

The changes in bulk chemistry in the profile are shown on plate 3*C*. Predominant chemical changes include oxidation of Fe^{+2} to Fe^{+3} in the weathered-rock zone, loss of Na_2O and CaO in the saprolite due to the dissolution of plagioclase, and relative increases of Fe_2O_3, TiO_2, H_2O^+, and Al_2O_3 in the massive zone and soil due to the loss of MgO, K_2O, and SiO_2.

Because of the uniformity of the parent rock, trends of particular elements in core F11 saprolite can be considered in more detail than trends of particular elements in saprolite derived from the metasedimentary rocks. Silica is the major constituent. Assuming 2 g/cm^3 silica in the parent rock, about one-fourth (0.5 g/cm^3) is lost in the saprolite. Although silica content shows a slight relative increase in the soil, some absolute loss of silica relative to the increases in bulk density and relative to TiO_2 occurs. Petrographic examination of the soil suggests that silica loss is due, at least in part, to quartz dissolution.

Al_2O_3 content decreases in the saprolite relative to the fresh rock and decreases further in the massive zone. An increase of Al_2O_3 content in the soil is due to the increase of clay in the soil relative to the massive zone.

Fe_2O_3 shows a major increase in the weathered rock zone due to the oxidation of ferrous iron in silicates or sulfides. Fe_2O_3 is relatively constant throughout the saprolite and increases markedly above 4.3-m depth. The trend of the Fe_2O_3 increase from 4.3 m to the surface suggests that ferric iron is concentrated relative to the loss of other major elements, particularly SiO_2, MgO, and K_2O. No evidence exists of an additional outside source of iron.

CaO and Na_2O both show a major decrease between 15- to 20-m depth in the saprolite due to plagioclase dissolution. CaO shows a slight increase at 4.3-m depth; this increase is not explicable from reactions observed. The upward constant increase of Na_2O above 6.7 m may be due to its retention as an exchange cation in a clay mineral. No persistent primary mineral phases contain Na_2O. MgO content appears to remain constant throughout the profile, but, relative to TiO_2, Fe_2O_3, and Al_2O_3, MgO is lost in the upper part of the profile. K_2O, like MgO, appears to be relatively stable in the lower part of the profile. K_2O is lost due to potassic-feldspar dissolution in the upper part of the saprolite. K_2O decreases relative to TiO_2, Fe_2O_3, and Al_2O_3 in the massive zone and in the soil.

Water (H_2O^+) shows a steady upward increase from fresh rock to 11-m depth due to hydration of micas and to formation of hydrated clay minerals, particularly halloysite. Between a depth of 6.7 and 1.5 m, H_2O shows a substantial decrease caused by dehydration of the kaolin minerals. In the soil, H_2O increases due to the increase in total clay.

DISCUSSION OF WEATHERING PROFILES DEVELOPED ON QUARTZOFELDSPATHIC ROCKS

Data for cores F2, F3, and F11 indicate many similarities among the thick regolith profiles that are developed on the quartz- and mica-rich metasedimentary rocks and on the foliated granite. The profiles are most similar in the zone of isovolumetric weathering, the saprolite. This discussion of the features and weathering processes of the thick weathering profiles proceeds from the weathered rock, to the saprolite, to the subsoil, to the soil. The discussion is based primarily on data from the three weathering profiles (pl. 3*A*, *B*, *C*). Data and observations from other cores and surface exposures also are summarized.

WEATHERED ROCK

In the lowest zone of the weathering profile (weathered rock), a common weathering characteristic of all the quartzofeldspathic profiles is confinement of mineral alteration to joint and fracture faces. Most of the alteration consists of oxidation of ferrous iron to ferric iron in mafic minerals and of local etching of plagioclase along cleavage planes. In thin section, solution penetration into small intergranular boundaries appears to have been slight. Solution movement through the weathered rock zone is restricted to relatively large joints and to fractures of high permeability.

SAPROLITE

Data presented on plate 3*A*, *B*, *C* indicate that saprolite is the main component of the quartzofeldspathic profiles. In all cores, the isovolumetric zone was within 3 m of the surface. The properties of saprolite are not uniform as a function of depth from the geomorphic surface. The zonation of these properties is related to the differences in primary mineral stabilities and to the difference in duration of weathering between the bottom and top of the saprolite. The material most recently undergoing chemical weathering is at the lower boundary of the regolith.

In the lower part of the saprolite, muscovite and quartz maintain grain-to-grain contacts. Disruption of the mechanical bonding of these minerals inherited from the period of rock metamorphism is not evident. Macroscopic inspection of saprolite in road cuts, excavations, and cores gives few indications of volume change throughout the saprolite. Spacing of joints and of quartz veins shows no change relative to the lower saprolite and bedrock. These observations are taken as evidence that isovolumetric weathering extends to the top of the saprolite. The decrease in bulk density upward through the saprolite is due simply to mass loss to solution.

The lower few meters of the saprolite exhibit mineral alteration that is not restricted to grains adjacent to larger solution conduits such as joints and fractures. Plagioclase and mafic minerals including biotite are decomposed throughout the entire zone because of penetration of solutions along intergranular contacts and into individual crystal lattices.

The weathering characteristics of the lower saprolite that were observed in this study are commonly observed in a variety of surficial environments. They are invariably the incipient, or the most rapid, weathering reactions between igneous or metamorphic rocks and aqueous solutions. For example, Colman (1977) found that plagioclase was altered within 8,000 years in

weathering rinds developed on glacially deposited rhyolite cobbles in semiarid weathering conditions. Biotite, amphiboles, and pyroxenes also have been observed to alter readily in numerous weathering profiles (Loughnan, 1969; Goldich, 1938).

The most easily weathered mineral species disappear upward in the saprolite profiles studied here. The upper half of the saprolite is characterized by relatively inert minerals. Thus, the saprolite is zoned with respect to mineral stability.

The same mineral stability sequence has been related to time through Pettijohn's (1941) ranking of the persistence of minerals in sedimentary rocks of different ages. For example, he found that biotite and hornblende are of relatively low resistance and are lost in a short time, relative to muscovite. Muscovite is the most persistent of the major minerals through geologic time. The mineral stabilities in the saprolite also can be related to time by comparing them with laboratory experiments on the kinetics of silicate mineral dissolution.

Kinetics of Silicate-Mineral Dissolution

The relative instability of silicate minerals in acidic, oxygenated solutions involved in weathering processes has been quantified in laboratory experiments (such as Wollast, 1967) that were designed to measure the kinetics of solute exchange between minerals and solutions. The results of the experiments provide insights into the reaction mechanisms operating in the alteration of rock to saprolite. Mineral dissolution data, shown in figure 13, indicate several significant points:

(1) The mafic minerals dissolve more rapidly than do the feldspars, which dissolve more rapidly than does quartz.
(2) The dissolution rates are different for different plagioclase and potassium feldspars, particularly within the first 48 hours of reaction.
(3) Reaction rates for all minerals except quartz are initially fast but then decrease and become roughly linear over time.

Although not measured, the data point for silica release from biotite probably would fall between that of plagioclase and hypersthene shown on figure 13. Muscovite would probably plot close to the quartz curve.

Thus, the relative rates obtained from these experiments correspond to the relative mineral stabilities compiled by Loughnan (1969). They also correspond to the relative stabilities of silicate minerals within the weathered rock zone and lower saprolite observed in this study.

Both the persistence of minerals in sediments and the kinetics of mineral dissolution correspond to the sequence of mineral alteration observed from the base to the top of the saprolite. This correspondence indicates that the intensity and (or) duration of weathering increases from bottom to top in the saprolite. The most reactive minerals are altered first in the weathered rock and basal saprolite. The variability in reactivity of minerals and the difference in duration of weathering between the base and top of the saprolite produce a zonation in mineralogy, chemistry, and other properties. The zonation of saprolite is similar in the three weathering profiles of quartzofeldspathic rocks studied here.

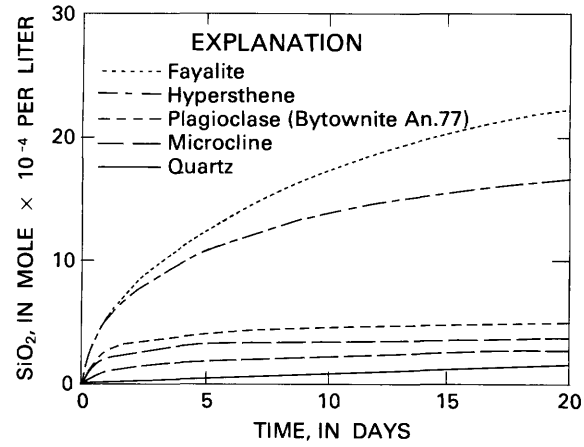

FIGURE 13.—Silica release from silicate minerals at 25 °C, starting with 50 g/L, initial pH of 4.0 to 4.5. Data from Siffert, 1962; Wollast, 1967; Luce and others, 1972; Busenburg and Clemency, 1976; Petrovic, 1976; and Siever and Woodford, 1979.

Saprolite Zonation

Within the saprolite, changes in density are generally transitional, but changes in mineralogy and chemical composition are distinct. The changes in density and chemical composition of the three quartzofeldspathic rocks define two principal subzones within the saprolite—a relatively inert upper half and a relatively reactive lower half. Despite differences in saprolite thickness, all three profiles show the same general subzones. Most of the mass loss occurs in the lower half of each of the profiles, and the average mass loss is about 35 percent in each of the profiles (fig. 14). The remaining 65 percent is roughly the combined percentage of quartz and muscovite in the parent rock. The maximum mass loss corresponds to the observed alteration of plagioclase and mafic minerals including epidote. Figure 15 shows trends of chemical loss or gain for the most mobile elements.

A loss of CaO (fig. 15*A*), which reflects dissolution of plagioclase, occurs in the lower parts of each of the

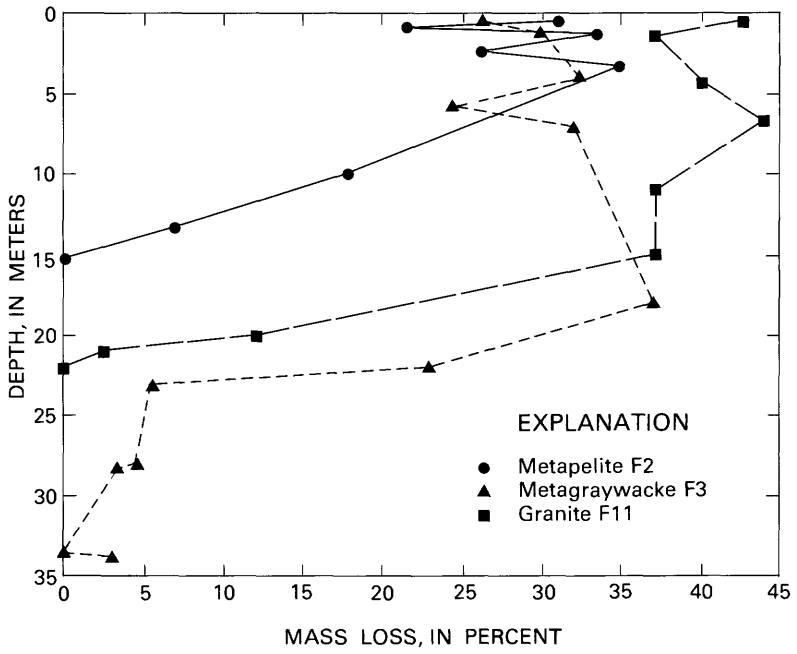

FIGURE 14.—Percent of mass loss versus depth for regolith developed on quartzofeldspathic rocks.

profiles. This loss suggests that two subzones may be defined within the profile. The first is an upper zone in which all the plagioclase has been dissolved, and the second is a lower zone in which the process of plagioclase dissolution and calcium loss is active. The plagioclase dissolution does not determine the position of the weathering front. The hydrolysis of the feldspar proceeds at a kinetically slower rate than does the oxidation of the iron-bearing minerals and the hydration of the micas. If all three rates were equal, the calcium would be lost at a relatively well-defined weathering front.

The amount of H_2O^+ increases in the lower 5 to 10 m of all three quartzofeldspathic rock profiles (fig. 15*B*). Although H_2O^+ also increases in the clay-rich B horizons relative to the massive subsoil, maximum hydration occurs in the middle of the saprolite. In the upper half of the saprolite in cores F2 and F11, however, the increase in H_2O^+ is small; in core F3, an absolute decrease in H_2O^+ occurs. The net gain in H_2O^+ roughly corresponds to the increase in Fe_2O_3.

The greatest increase of Fe_2O_3 (fig. 15*C*) is in the lower half of the profile. Fe_2O_3 content is either constant or declines slightly in the upper half of the saprolite. Solutions moving downward in the vadose zone may dissolve small amounts of Fe^{+3}, and Fe^{+3} may be reprecipitated in the phreatic zone.

On the basis of the overall trends of density and chemistry, saprolite is subdivided into a relatively inert upper half and a relatively reactive lower half. The details of the chemical changes in the reactive zone reveal that saprolite formation on the quartz- and muscovite-rich schists, gneisses, and granites of Fairfax County involves a mass loss equal to about one-third the mass of the parent rock. Plagioclase alteration, which was documented as a primary weathering process in saprolite by Bricker and others (1968), is confirmed here by observation of plagioclase alteration in thin section and by trends in CaO and Na_2O content within the saprolite. These observations and data show that dissolution of plagioclase feldspar is primarily responsible for the mass loss of CaO and Na_2O in saprolite.

Loss of Al_2O_3 and SiO_2 is striking when considered on a mole-per-cubic-centimeter basis. As shown in the metapelite profile (pl. 3*A*), a mass balance based on plagioclase dissolution does not account for all the observed silica loss. The dissolution of biotite and quartz may contribute significantly to the silica loss. Although a complete mass balance has not been constructed, chemical alteration of the lower half of the saprolite, the reactive zone, clearly is associated with mineral decomposition.

In contrast, the upper half of the saprolite is the least chemically active zone of the entire weathering profile and does not exhibit petrographic or chemical evidence of alteration of primary minerals such as muscovite. The clay mineral phases, however, show some changes

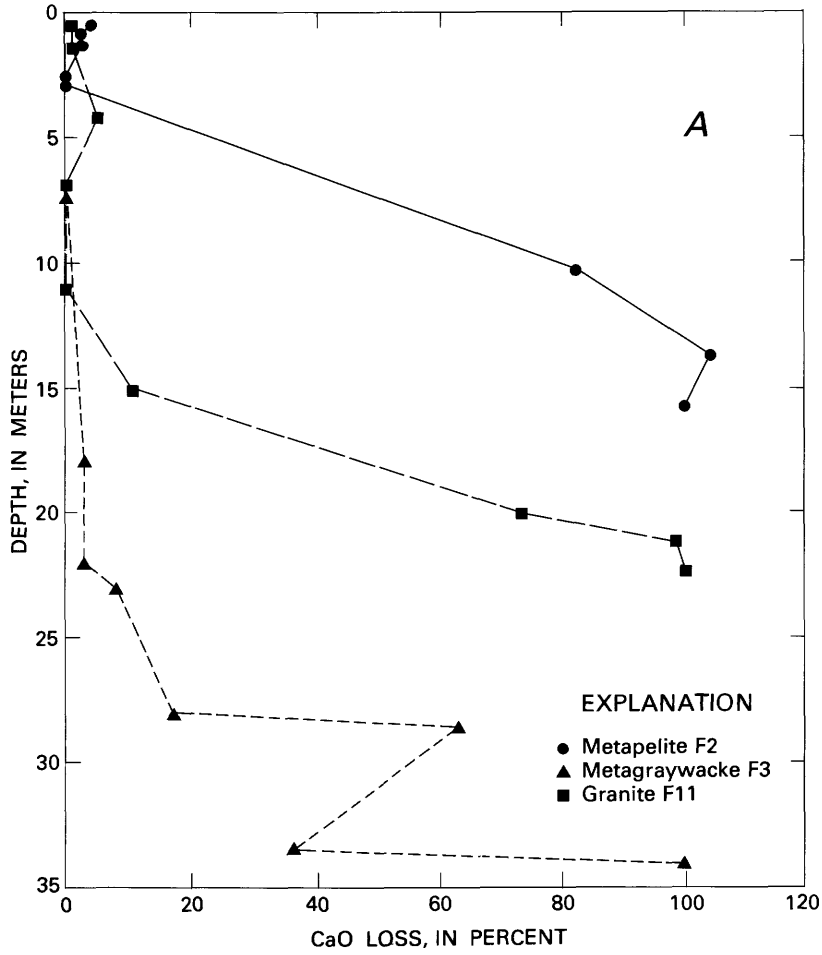

FIGURE 15.—Chemical loss or gain versus depth in regolith profiles. *A*. CaO loss.

in this relatively inert zone, as summarized in table 5. The main product of mineral alteration in the saprolite of each of the quartzofeldspathic rocks is a hydrated kaolin mineral probably close to halloysite in composition, as $Al_2Si_2O_5(OH)_4 \cdot 2H_2O$. This hydrated phase produces a broad peak on the X-ray diffraction patterns (figs. 6 and 9) that extends from about 7.25 A to 10.0 A. This characteristic band in the diffraction patterns indicates that the hydrated kaolin is probably a mixed-layer stacking of variously hydrated kaolin layers. Spacing of peaks varies with degree of hydration.

Other changes in clay mineralogy in the saprolite show that dehydration occurs in the relatively inert zone. Although initial weathering of micas and genesis of clays within the profile involve incorporation of H_2O^+ into the crystal lattice, the chemical data and clay mineralogy show that the dehydration of halloysite to kaolinite is an important process in the upper part of the saprolite. The 7.25-A kaolin peak is much sharper near the top of the saprolite, above the phreatic zone (figs. 6 and 9). The sharper peak results from an overall dehydration of the mixed-layer mineral and the formation of a more uniformly spaced kaolin phase.

The minerals that provide structural integrity and mechanical stability to the relatively inert zone, chiefly quartz and muscovite, react slowly with solutions, as indicated by laboratory kinetics studies. The rapid passage of water through this unsaturated zone probably further limits the amount of reaction that can take place. Although some chemical losses do occur in the upper half of the saprolite developed on the quartzofeldspathic rocks, the changes are relatively minor in comparison with losses in the lower half.

MASSIVE SUBSOIL

The boundary between saprolite and the overlying massive subsoil zone occurs at about 3-m depth in quartzofeldspathic weathering profiles and is transitional. The boundary is defined by three criteria. First,

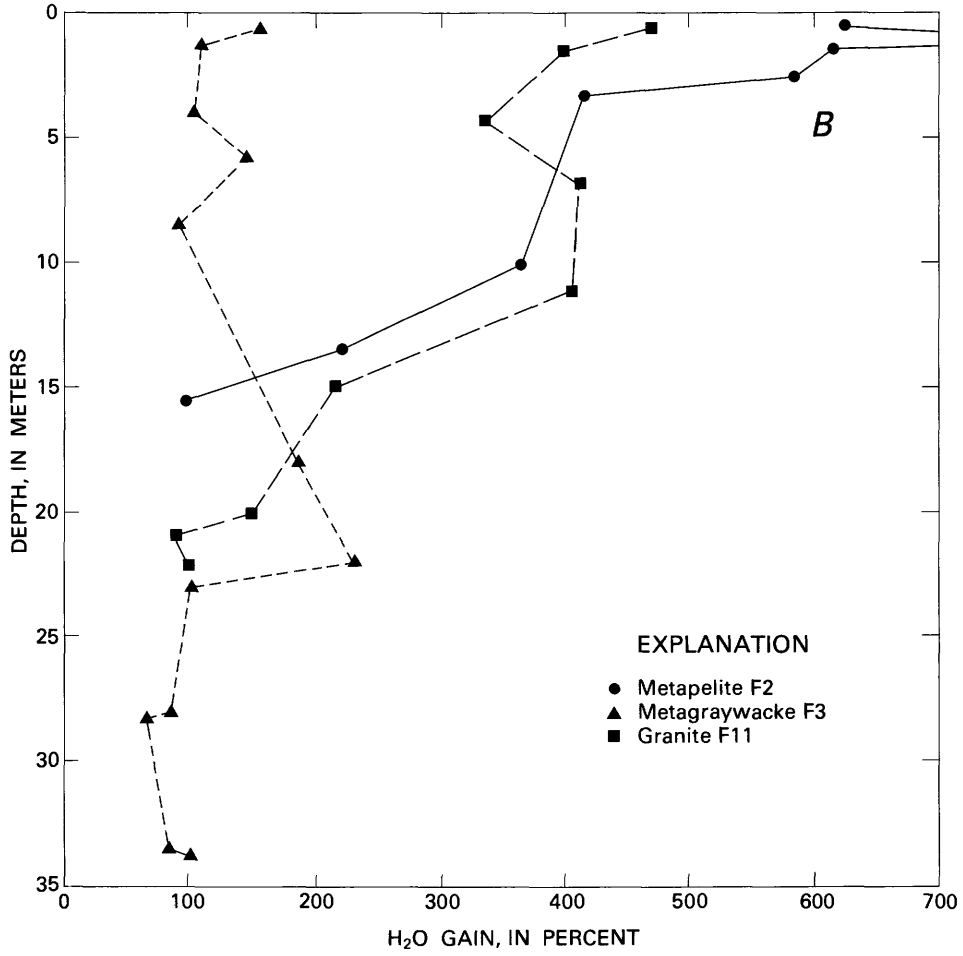

FIGURE 15*B*.—H_2O^+ gain.

the breakdown of saprolite structure is associated with the disruption of original grain-to-grain contacts between resistant residual framework minerals, chiefly quartz and muscovite, as seen in the photomicrographs (figs. 5, 8, and 11). Second, the bulk density increases upward, owing principally to volume reduction as suggested by the chemical trends. Minor loss of mass due to chemical weathering, notably quartz dissolution, continues in the massive zone; therefore, the density increase is effected by volume decrease rather than by mass increase. Third, the mechanical strength, as measured by the SPT blow counts (pl. 3*A*, *B*, *C*), is lower in the massive zone. The dominant physical feature of the saprolite is that, despite its chemical alteration, it possesses structural integrity and is thus stronger than the overlying disaggregated massive zone. The relative strengths of saprolite and subsoil are indicated by excavatability in outcrops and by differences in resistance to mechanical disruption, measured by SPT blow counts. Inspection of cores, road cuts, and excavations revealed that structured, mechanically resistant saprolite is present within 3 m below the surface. Above 3 m, residual structure is preserved only in a few discontinuous patches within the subsoil. The upper half of the subsoil preserves no inherited bedrock structure.

The disaggregation, compaction, and associated bulk density change that differentiate saprolite from the massive subsoil zone are related primarily to the low density and mechanical instability of the uppermost saprolite. Comparison of the bulk density of the upper saprolite (1.7 g/cm^3 in the F2 core and 1.8 g/cm^3 in the F3 core) to that of compacted, well-sorted quartz sand (1.9 g/cm^3) indicates that the uppermost saprolite is mechanically metastable and easily disrupted.

Disruption of the uppermost saprolite is generally restricted to a zone within 2 m below the surface and is due to the increase in the intensity of mechanical forces near the geomorphic surface. Mechanical forces that act at the base of the soil include burrowing organisms, roots, seasonal wetting and drying, and possibly frost

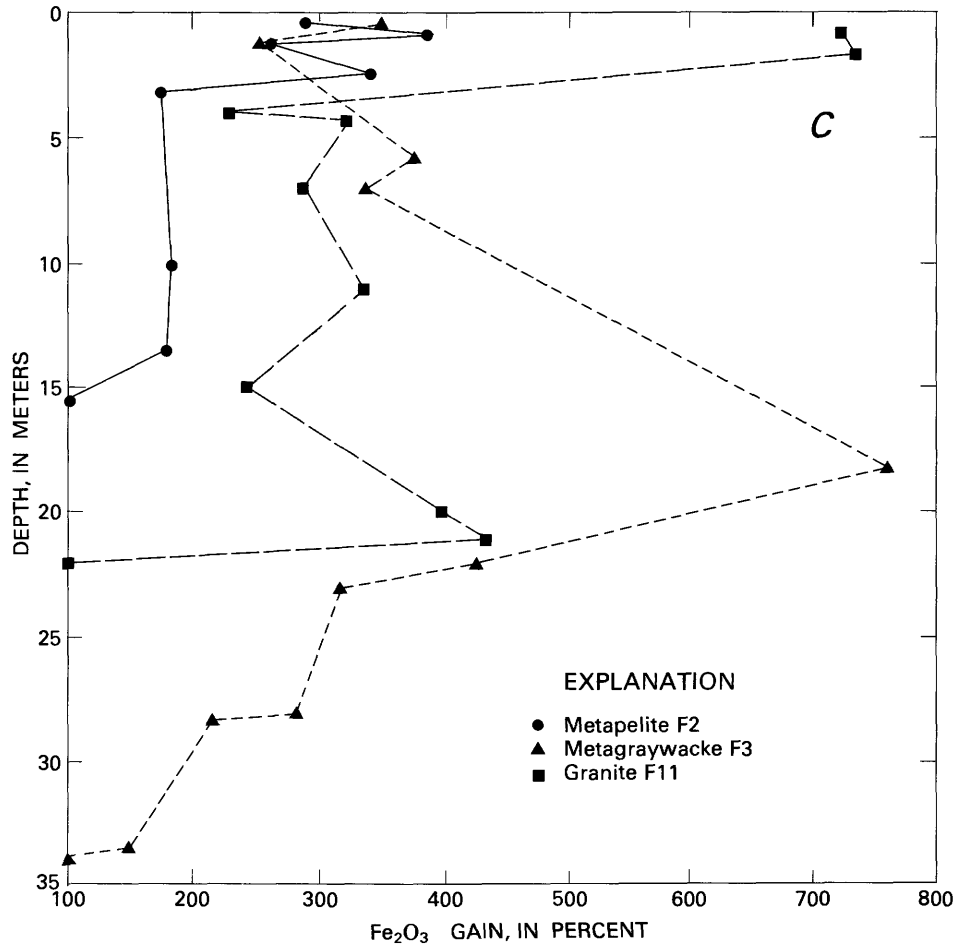

FIGURE 15C.—Fe_2O_3 gain.

action. These forces cause disturbance of the grain-to-grain contacts in the upper part of the saprolite. After disturbance of these contacts in the inherited bedrock fabric, the mineral grains assume a new, more closely packed fabric that possesses a higher density and lower mechanical strength than that of the undisturbed saprolite.

Deep, thin massive zones devoid of primary rock structures occur below 10 m, well below the depth of near-surface mechanical disturbance. For example, a massive zone was encountered in the F3 core of the metagraywacke profile in sample 31 at 18-m depth (pl. 3*B*). Such deep massive zones occur most commonly at the intersections of major joint sets. Chemical weathering and mass loss in zones of relatively high permeability apparently are responsible for formation of the deep massive zones. The massive subsoil zone that occurs between the uppermost saprolite and the soil is not produced, however, by simple mass loss in the way that these deeper massive zones are. Interpretation of the processes active in soil formation indicates the importance of mechanical, as well as chemical, processes in the upper 3 m of the regolith.

SOIL

The effects of mechanical disruption by wetting and drying, by biological activity including roots and burrowing animals, by freezing and thawing, and by creep are even more pronounced in the soil zone than in the massive zone. In the soil proper, which includes the pedogenic A and B horizons, mass and volume are constantly reorganized, so that, in contrast to the massive subsoil zone and saprolite, the soil is a zone of extremely active physical and chemical processes.

The soils developed upon the quartzofeldspathic profiles are similar in that they exhibit thin A horizons (generally less than 0.1 m thick) and dense, sesquioxide-rich B horizons about 0.6 to 1 m thick. Changes in texture, density, mineralogy, and chemistry between

TABLE 5.—*Relative abundance of clay mineral phases in weathering profile zones*
[XXX, abundant; XX, present; X, minor; —, absent. Relative abundance is based on method of Carroll (1970)]

Profile	Sample	Depth	Zone	Halloysite	Kaolinite	Muscovite	Smectite	Vermiculite
Metapelite	1a	0.3	Soil	—	XXX	XX	—	XXX
(core F2)	1b	.6		XXX	—	X	—	XX
	2b	.9		XXX	—	X	—	X
	2c	1.2	Massive subsoil	XXX	—	—	—	X
	6a	3.2	Saprolite	XXX	—	X	—	X
	14	10.0		XX	—	XX	—	X
Metagraywacke	1c	.6	Soil	—	XXX	—	—	X
(core F3)	2e	1.2	Massive subsoil	—	XX	—	—	XX
	7b	4.0		XX	—	—	—	XX
	10d	5.8	Saprolite	XX	—	X	—	XX
	13	7.0		X	—	X	—	XX
	31	18.0		XX	—	X	—	XX
	40	22.0		XX	—	XX	—	XX
Granite	1	.6	Soil	—	XXX	—	—	XXX
(core F11)	2	1.5	Massive subsoil	—	XXX	X	—	XX
	3	4.3		—	XXX	XX	—	—
	4	6.7	Saprolite	—	XXX	XX	—	—
	5	11.0		—	XXX	XX	—	—
	6	14.9		—	XXX	XX	—	—
	7	19.8		—	—	XXX	—	—
	8	21.0	Weathered rock	—	—	—	XXX	—

the soil and subsoil indicate that the processes acting within 1 m of the surface are biologically, mechanically, and chemically more energetic than are the processes that act deeper than 1 m in the profile.

SOIL TEXTURE

The soil contains much more clay and silt than does either the massive zone or the saprolite. This diminution in grain size is brought about, in large part, by chemical weathering. Quartz and muscovite, which were relatively unaffected by chemical alteration in the upper saprolite, have undergone significant chemical alteration in the soil zone. Thin sections show that quartz is etched and reduced in grain size. The decrease in the number of discrete mica grains in thin section corresponds to the increase in clay-sized vermiculite (table 5) that is derived from the mica. The increase in clay in the soil relative to saprolite is at least partially the result of transformation of the mica lattices.

SOIL MINERALOGY

Because of the complex biological and physiochemical reactions and the significant proportions of mica and transformed mica-clay species, the soil clays are chemically and crystallographically complex. Soil clays are not simply a chemically degraded product of clay from the saprolite parent material. We see no evidence for loss of crystallinity of kaolinite or for accumulation of amorphous oxyhydroxides of aluminum and iron. In the soil B horizon where the total weight percentage of clay is relatively large, the crystallinity of the soil clay increases relative to clay in the saprolite, and the hydration of the clay decreases. In the soil, for example, the 7.25-A kaolin mineral, which may be inherited from the saprolite clay fraction, is dehydrated from a halloysitelike mineral. As in the upper half of the saprolite, water loss from the clays appears to be an important process.

SOIL CHEMISTRY

Changes in soil texture and mineralogy are associated with major changes in chemistry relative to the uppermost saprolite. The trends of major element composition that are shown in plate 3*A*, *B*, *C* illustrate that the absolute, though nonisovolumetric, concentrations of the oxides vary in the soil and that the ratios among the major elements vary unequally as the soil density changes. Two possible mechanisms for the changes in chemical composition in the soil are contamination from an outside source and leaching of more soluble elements during mechanical compaction of the soil zone.

Evidence for minor contamination of the soil from outside sources is clearly indicated by the increase in CaO and Na_2O concentrations (pl. 3*A*, *B*, *C*). The CaO and Na_2O occurring in the soil apparently have been introduced by rainwater, atmospheric dust, fertilizers added by man, or the nutrient cycle of vegetation. CaO and Na_2O concentrations in rainwater are small (Fisher, 1968), and atmospheric dust composition includes only minor feldspar or calcite. Whatever the source, CaO and Na_2O can reside in the soil in exchange positions on clays, and long-term accumulation is likely.

In contrast with the chemical evidence for minor contamination of the soils, diffraction patterns of clay minerals (figs. 6, 9, and 12) show that, in all three weathering profiles, the changes affecting clay minerals from saprolite to soil are progressive. No evidence of any new clay phase being introduced to the soil exists. For example, none of the soils contain gibbsite, which was identified by Denny and Owens (1979) as a wind-transported component of soils on the Delmarva Peninsula, 100 km east of Fairfax County.

Zonation and Pedologic Processes

Concurrent chemical and mechanical processes have produced pedogenic A and B soil horizons by altering subsoil or saprolite within the upper 1 to 2 m of the profiles. The nature of these alteration processes is demonstrated by plotting chemical data that reflect bulk chemical, mineralogic, and mechanical changes within the soil horizons. Figure 16, which is a plot of the $(Fe_2O_3+Al_2O_3)/SiO_2$ ratio, shows similar trends for all three profiles. In the soil zone, above 1 m, iron and aluminum show a marked increase relative to silica, particularly in the metapelite profile core F2. The increase of these elements corresponds to the major increase in the weight percent of clay-sized material above 1-m depth in each of these profiles. Because much of the increase in clay is due to the increase of silica-rich (2:1 layer) vermiculite, however, the decrease in silica probably is not solely the result of this increase in clay. The relative decrease in silica probably reflects an absolute decrease in silica content. For example, thin sections showing pitted and embayed quartz grains indicate that much of the decrease in silica is due to dissolution of quartz. As a result of dissolution, quartz grains increase in angularity and decrease in diameter in the soil. Cores and exposures of soil B horizons exhibit a notable decrease in quartz-grain content relative to the massive subsoil and saprolite.

The quartz-water dissolution reaction that takes place in an acidic soil environment is written $SiO_{2(qtz)}+2H_2O=H_4SiO_{4(aq)}$. This dissolution reaction leaves no residual or transformation product (Stumm and Morgan, 1970). Due to the low solubility of quartz in acidic solutions (for example, $k=10^{-3.7}$ mol/L at 25 °C), the amount of silica released by any aliquot of soil water is small.

Quartz dissolution in soils has been noted elsewhere in the southeastern Piedmont (Cleary and Connolly, 1971). Despite evidence that clay-sized quartz is more soluble than phyllosilicates (Jackson, 1968), the significance of quartz loss from soils has not been considered fully. Quartz dissolution attests to the greater intensity of weathering in the soil than deeper in the regolith profile. This intensity might be caused by pH and organic acids as the soil is generally more acidic than

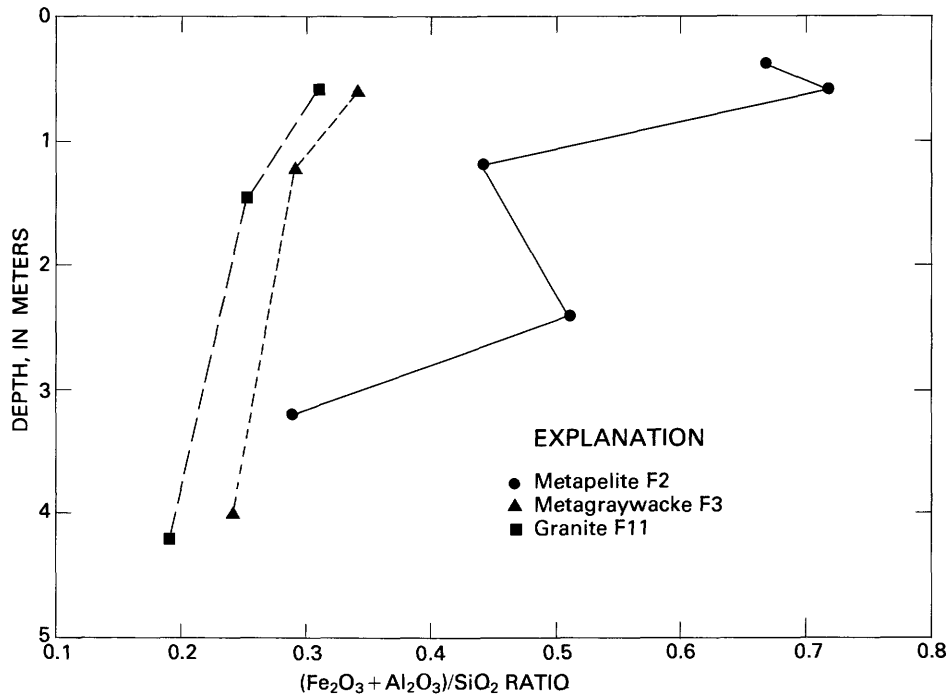

FIGURE 16.—$(Fe_2O_3+Al_2O_3)/SiO_2$ versus depth in soil developed on metasedimentary and granitoid rocks.

are the lower parts of the regolith. Review of quartz dissolution studies shows, however, that quartz solubility is independent of pH in the acidic range (Stumm and Morgan, 1970). Quartz dissolution is probably related to the total amount of water that fluxes through the soil. If so, quartz dissolution is more active in the soil than in the other regolith zones because the soil is hydrologically the most active zone of the regolith. The total water flux due to infiltration, interflow, and evapotranspiration may be several orders of magnitude greater than is the flux of water through the upper saprolite.

Accumulation of clay in B horizons appears to be chiefly from compaction and leaching of the underlying massive subsoil, rather than from translocation of clay from a superjacent A horizon. The cores and exposures corroborate other field observations (Porter and others, 1963) that A horizons of soils of the Fairfax County Piedmont are thin, generally less than 0.3 m. Furthermore, no eluviated, sandy A2 horizons that are possible sources for the clay in B horizons are found. Clay mineralogy shows, moreover, that most of the clay is inherited from the underlying parent material.

The diffraction patterns also show that the soil clays are less hydrated than are the clays of the underlying subsoil and saprolite. This difference in water content suggests that dehydration of the soil zone has been a significant process under the humid climate regime. The evidence for dehydration indicates that much of the mechanical force that causes volume reduction (compaction) of the soil during overall mass loss by dissolution and leaching is due to seasonal wetting and drying of the soil. The density increase in the soil relative to the underlying material indicates that a major volume decrease is concurrent with intense leaching. This balance of mass loss and compaction produces a zone that is the most dynamic part of the regolith. Thus, the alteration of the saprolite at its upper boundary to massive subsoil material and soil is dependent upon both mechanical and chemical processes that are important in controlling the overall thickness of the regolith.

SUMMARY AND GENERALIZED WEATHERING PROFILE

A generalized weathering profile for thick regolith developed on quartzofeldspathic rocks of the Virginia Piedmont is shown in figure 17. On the basis of data from core sites F2, F3, and F11 (pl. 3*A*, *B*, *C*), from other cores, and from surface exposures and the isopach map of regolith thickness of the Fairfax County Piedmont (pl. 2), the profile shows the average thicknesses of zones and subzones. Variations in thicknesses of zones are related to rock type and rock structure, as well as to local drainage conditions and to the degree of soil development. Zones in the lower part of the profile are differentiated on the basis of hardness, mineral alteration, and chemistry. These zones and the boundaries between these zones thus define chemical weathering fronts at the base of the saprolite and in the middle of the saprolite. In the upper part of the profile, zones are differentiated on the basis of density, standard penetration data, and texture. These zones, and the boundaries between these zones, are the result of complexly interrelated chemical and mechanical processes that act near the ground surface in the soil and subsoil.

In the isovolumetric zone between the fresh rock and the top of the saprolite, the following zonation is seen: weathered rocks, relatively reactive saprolite, and relatively inert saprolite. These zones are recognized in all three profiles on quartzofeldspathic rock. This zonation and the existence of a thick saprolite are dependent upon the presence in the bedrock of a mixture of minerals that will dissolve at different rates. The differences in kinetics of mineral dissolution allow for selective removal of the more reactive species. The more resistant minerals (such as quartz and muscovite) provide structural support for the saprolite. Structural support is essential for maintaining saprolite as an isovolumetric product of bedrock.

The soil contains mineral phases that apparently are solely derived from the alteration of saprolite. The soil, therefore, appears to be the result of volume reduction and mass loss due to intense chemical weathering reactions. In cores F2, F3, and F11, the major changes in volume occur in the upper 3 m. Volume reduction is evidenced by reorientation of micas from saprolite to massive zone (as seen in photomicrographs in figs. 5, 8, and 11) and by density increase in the soil relative to the uppermost saprolite during continued mass loss. Accompanying volume reduction in the upper 3 m of the profile is a major chemical alteration that includes the transformation of muscovite to vermiculite and the congruent dissolution of quartz.

The uppermost saprolite and massive zone are less dense and are mechanically weaker (as determined by SPT blow counts) than is the B horizon of the soil in two of the three profiles. This condition suggests that the uppermost saprolite reaches a condition of mass loss and low strength that makes it mechanically unstable relative to B horizon of the soil. The massive zone evidently represents a transitional zone in which mechanical reorganization is taking place.

Except for the lower half of the saprolite and weathered rock zone, most of the profile below the massive subsoil zone (that is, between 3 and 10 m) appears to be fairly stable mechanically, mineralogically, and chemically. Most of the mass difference between the saprolite and parent rock is due to plagioclase dissolution in the

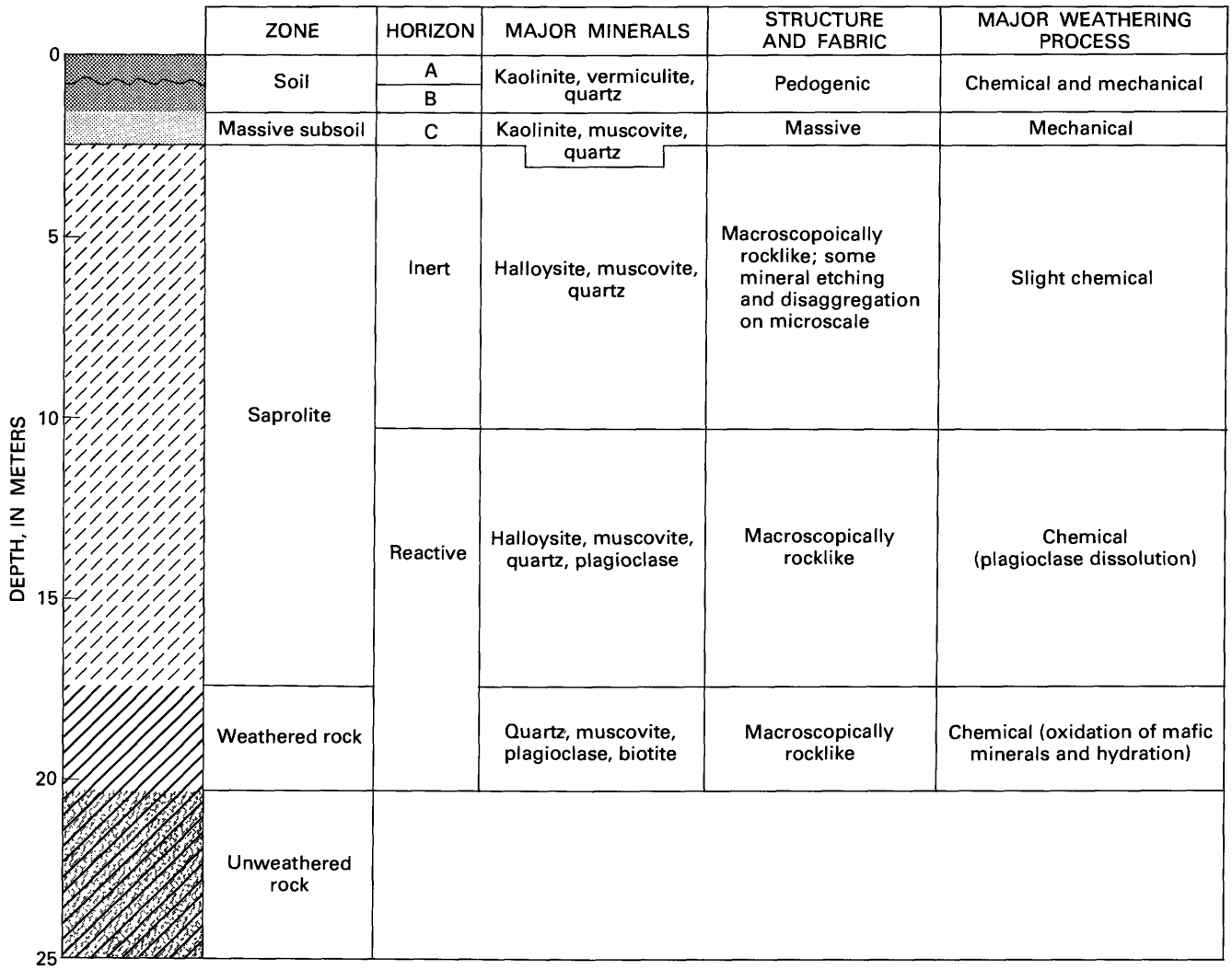

ZONE	HORIZON	MAJOR MINERALS	STRUCTURE AND FABRIC	MAJOR WEATHERING PROCESS
Soil	A	Kaolinite, vermiculite, quartz	Pedogenic	Chemical and mechanical
	B			
Massive subsoil	C	Kaolinite, muscovite, quartz	Massive	Mechanical
Saprolite	Inert	Halloysite, muscovite, quartz	Macroscopoically rocklike; some mineral etching and disaggregation on microscale	Slight chemical
	Reactive	Halloysite, muscovite, quartz, plagioclase	Macroscopically rocklike	Chemical (plagioclase dissolution)
Weathered rock		Quartz, muscovite, plagioclase, biotite	Macroscopically rocklike	Chemical (oxidation of mafic minerals and hydration)
Unweathered rock				

FIGURE 17.—Generalized weathering profile for thick regolith developed on upland quartzofeldspathic rocks.

weathered rock zone and in the lower saprolite. Above the middle of the saprolite, the predominant minerals (quartz and muscovite) appear to be chemically inert in the zone of isovolumetric weathering.

REGOLITH PROFILES DEVELOPED ON MAFIC AND ULTRAMAFIC ROCKS

Although relatively thin when compared to regolith developed on quartzofeldspathic rocks, regolith developed on mafic rocks, including diabase and serpentinite, shows an overall zonation within the weathering profile. The results of analytical tests of four cores are summarized in appendix tables A3 and A4.

Regolith developed on diabase in the early Mesozoic Culpeper basin ranges between 0 and 10 m in thickness and averages 6 m in thickness on interfluve areas (pl 2). In the cores and in the surface exposures, A and B soil horizons are thin, typically less than 0.2 and 0.8 m, respectively. Saprolite that immediately underlies the soil B horizon is notably thin and granular. Saprolite overlies a thin but distinct weathered rock zone that overlies fresh rock.

Regolith developed on serpentinite is less than 1 m thick and consists of a weakly developed soil, 0.6 m thick, and of a massive zone that overlies relatively strong and dense weathered rock.

DIABASE

The core of regolith developed on diabase, core site F18, was taken from a hill adjacent to a large diabase quarry off Route 29 in central western Fairfax County (pl. 1).

PROFILE ZONATION AND PETROGRAPHY

The zonation of the weathering profile and the macroscopic details of the F18 core are shown in plate 3*D*. The photomicrographs of core F18 are shown in figure 18. The fresh rock consists of labradorite, augite, and minor amounts of biotite and magnetite. The weathering profile is about 1.5 m thick, which is thinner than the average regolith developed on diabase of the early Mesozoic basins. The weathering profile developed on the diabase has very thin saprolite and weathered rock zones; the massive subsoil zone and soil rest almost directly on unweathered bedrock. Despite its relative thinness, the weathering profile shows distinct zones.

The weathered rock zone at the base of the profile is thin, but mineral alteration is evident along joints below the base of the cored profile. Petrography of the weathered rock zone shows that augite is more altered than plagioclase. The firm and slightly altered diabase grades upward from 1.5- to 1.0-m depth into saprolite. The saprolite is granular and consists mainly of disaggregated and variously altered fragments of diabase. The remnants of bedrock joints are the dominant structure preserved in the saprolite. The base of the massive subsoil zone is in abrupt contact with the thin saprolite horizon. The soil contains fragments of quartz and slightly altered diabase.

The uppermost horizon is a gray-brown soil containing fragments of quartz and slightly altered diabase. Iron- and manganese-rich concretions in the form of spheroidal nodules are abundant in the soil. Petrography indicates that the nodules commonly form around nuclei of quartz, other mineral grains, or rock fragments and that the nodules exhibit concentric rings, which suggest sequential growth in the soil. The concentration of concretions decreases downward toward the base of the soil at about 0.7-m depth.

MECHANICAL PROPERTIES

Bulk density and blow counts for the diabase weathering profile show that density and strength of the profile zones are related to structure. Mineral grain contacts are attacked during weathering and do not provide structural support in the saprolite. Mechanical disturbance of near-surface material by wetting and drying, freezing and thawing, and bioturbation cause the destruction of the saprolite structure.

The relative differences in density between the zones in this profile are unlike those observed in the thicker profiles developed on quartzofeldspathic rocks. The minimum density occurs in the soil; the saprolite is intermediate in density when compared with soil and bedrock.

TEXTURE

Textural data for the profile (pl. 3*D*) show that the bulk of the upper part of the regolith consists of coarse gravel-sized fragments that are slightly weathered rock in a fine matrix of clay. Most sand-sized particles are iron- and manganese-rich concretions and quartz grains.

The density data (pl. 3*D*) show that the nodular soil is much less dense than the weathered rock is. The bulk density of the saprolite (2.2 g/cm^3) is significantly lower than that of the fresh rock (3.0 g/cm^3). This difference reflects the degree of mineral alteration observed in photomicrographs.

CLAY MINERALOGY

X-ray diffraction patterns of samples from diabase profile F18 are shown on figure 19. Clay near the base of the profile, sample 2b, shows abundant reflections from diffraction spacings greater than 10 A; these spacings represent a mixed-layer clay assemblage (fig. 19). On the basis of expansion of the material to 17 A with glycolation (fig. 19), the mineral phase was determined to be a smectite, possibly nontronite. Peaks at 7.5 A and 3.5 A are interpreted to be the higher order spacings of a chlorite lattice.

Sample 1d from 0.43-m depth in the soil horizon contains distinct 14.3-, 7.5-, 4.75-, and 3.59-A peaks. These are produced by an ordered mixed-layer phase. Many of the layers expand to 17.0 A with glycolation, but the broad low-angle shoulder on the glycolated pattern indicates a high percentage of nonexpandable layers in this sample. The small 3.35-A peak is quartz.

Sample 1c at 0.25-m and sample 1a at 0.1-m depth show a change in the predominant clay phase to a nonexpandable 14.3-A mineral, probably trioctahedral vermiculite, on the basis of the presence of the 0.60-A peak (not shown on fig. 19) in a randomly oriented sample. The 3.35-A peak is quartz. The 7.2-A and 3.57-A peaks in the glycolated sample 1a are due to kaolinite. These peaks are not affected by heating to 300 °C, while the 14.3-A peak collapses to 13.4 A.

The alteration of the clay assemblage from a smectite-rich, mixed-layer assemblage at the base of the soil to a nonexpandable vermiculite higher in the soil indicates that the vermiculite is a product of the transformation of the mixed-layer assemblage. The loss of expandable interlayers may be due to formation of a stable interlayer complex of brucite ($Mg(OH)_2$) or of iron hydroxide ($Fe(OH)_3$), or of some combination of the two. A few soil nodules were picked for X-ray diffraction analysis. The analysis showed them to be noncrystalline. The quartz and kaolinite in the upper 10 cm of the profile may be aeolian additions.

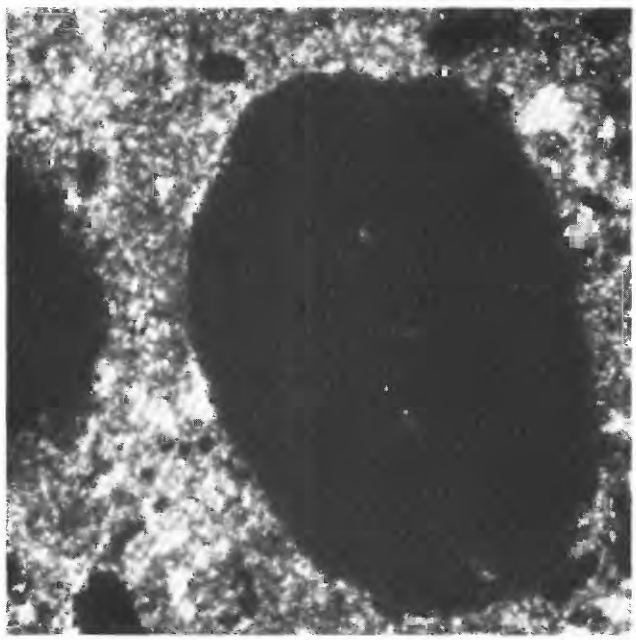

A. Sample 1a at 0.12-m depth. Soil consisting of fine crystalline matrix containing angular grains of quartz, plagioclase, and augite; dark, rounded, translucent to opaque nodules; and angular fragments of nearly fresh diabase. (Transmitted light, 32 ×.)

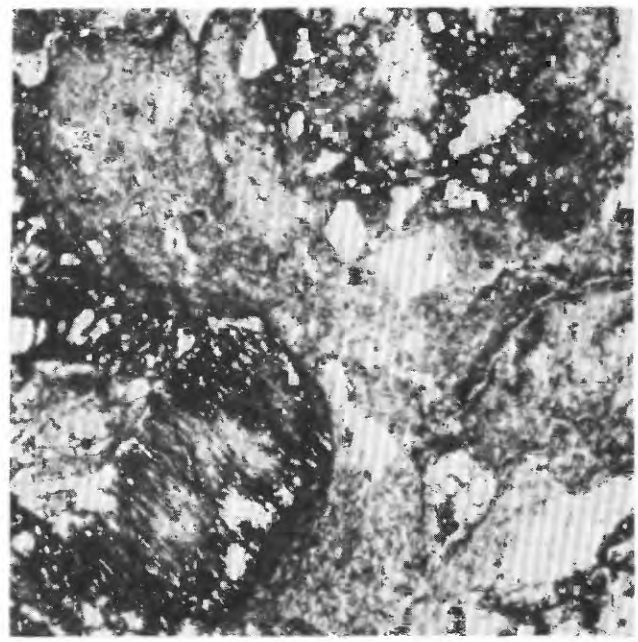

B. Sample 1c at 0.25-m depth. Soil consisting of fine crystalline matrix similar to sample 1a with rounded nodules, fewer rock fragments and less plagioclase and augite than in sample 1a. (Transmitted light, 32 ×.)

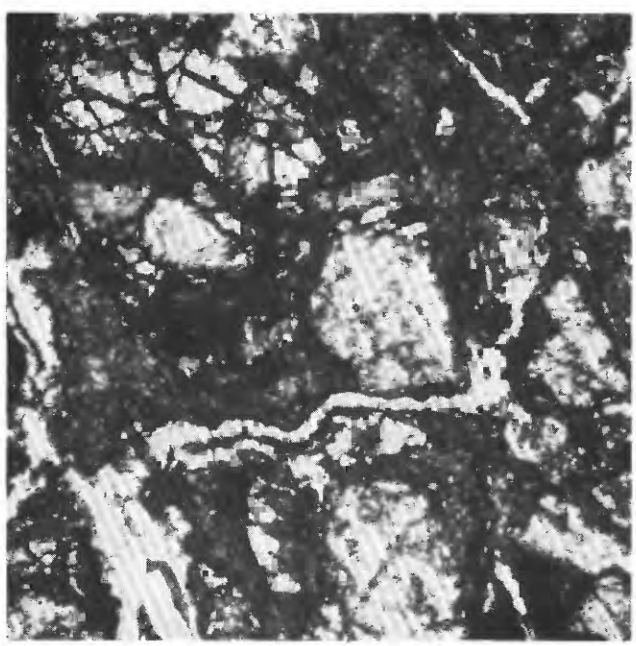

C. Sample 2b at 0.90-m depth. Saprolite containing abundant fragments of slightly altered diabase in an altered, cryptocrystalline matrix. Plagioclase is locally sericitized; augite is limonite stained and slightly chloritized. (Transmitted light, 32 ×.)

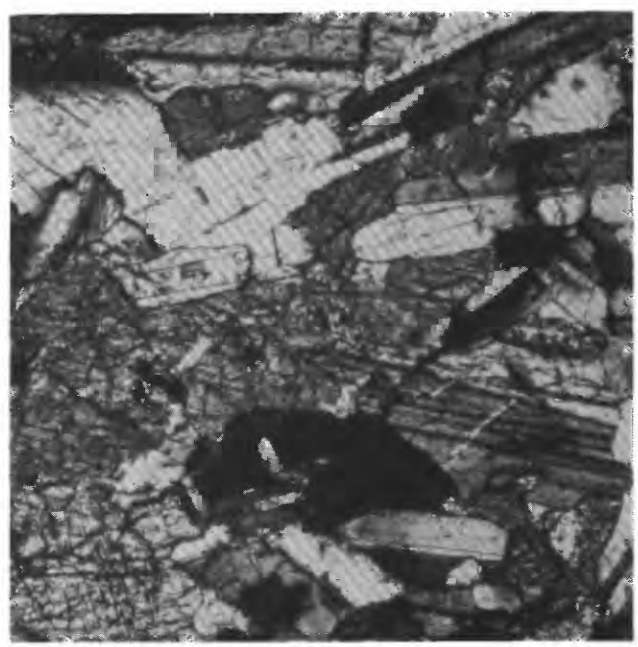

D. Sample 3 at 1.0-m depth in the weathered rock zone. Unaltered rock containing plagioclase feldspar (labradorite), augite, minor brown biotite, and minor magnetite (ilmenite?). (Transmitted light, 32 ×.)

FIGURE 18.—PHOTOMICROGRAPHS OF DIABASE REGOLITH, F18 CORE SITE

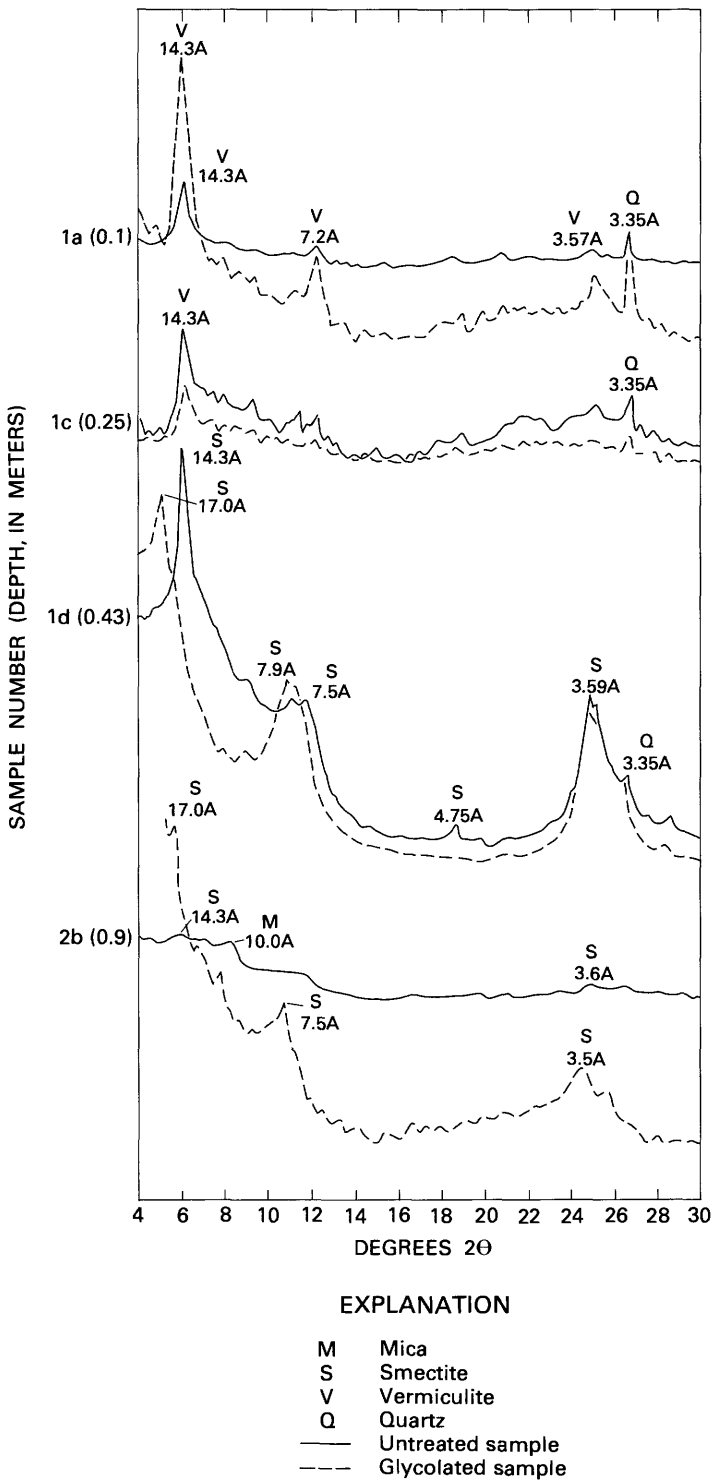

FIGURE 19.—X-ray diffraction patterns for untreated and glycolated <2-μ samples from the F18 core site.

CHEMICAL ZONATION

Chemical analyses of core F18 are shown in plate 3*D*. The absence of rock structure through most of the weathering profile indicates that the weathering is not isovolumetric above 0.86-m depth and therefore the chemical trends are complicated by mechanical disturbance of the samples. The individual elements show trends similar to those found in the weathering of the more silicic rocks. Large changes occur in concentration of elements in the solid phases between the fresh bedrock and the saprolite.

SiO_2 declines from 1.6 g/cm^3 to 0.9 g/cm^3 upward from fresh rock to saprolite. This decline, coupled with the large density decrease, attests to a considerable mass loss due to primary mineral decomposition and leaching of soluble elements. Al_2O_3 shows less, but still substantial, depletion in the saprolite. In the soil zone, SiO_2 remains constant. This constancy is possibly due to the predominance of siliceous 2:1 layer clays and to the increasing percentage of quartz, which is relatively resistant to weathering. The aluminum decrease in the soil above 20 cm is related to the continued alteration of the aluminum-rich calcic plagioclase and to eluviation of clay from the soil A horizon to the clay-rich B horizon below 40 cm.

SERPENTINITE

Several cores were taken from serpentinite regolith of Lake Fairfax Park off Route 606 in west-central Fairfax County (pl. 1).

PROFILE ZONATION AND PETROGRAPHY

The cores penetrated a thin (50-cm) regolith. Plate 3*E* depicts core F14, which is representative of several cores taken in the same vicinity. The photomicrographs in figure 20 show the main mineralogical and structural changes that occur in the profile. The weathering profile consists of thin soil and thin massive subsoil that directly overlie weathered rock. Most of the regolith consists of a dense, brown clay having spheroidal nodules that are similar to those formed over diabase. The spheroids are translucent to opaque in thin section. The finely crystalline matrix contains micaceous minerals and quartz grains. Fragments of unaltered serpentinite increase in abundance downward to an abrupt contact with unweathered bedrock.

Quartz is concentrated, along with iron hydroxides, in the weathered zone. The presence of quartz in the upper two samples is confirmed by a 3.35-A X-ray diffraction peak (fig. 21). All the quartz grains examined are subangular to subrounded and appear to be undergoing etching and dissolution. Because no quartz was identified in the two lower samples of weathered and fresh rock, the quartz grains in the upper part of the profile are not derived directly from the underlying parent rock. No evidence occurs of any authigenically precipitated quartz in the upper part of the profile. Cleaves (1974) showed, however, that silica dissolved during the alteration of serpentinite minerals was reprecipitated in veins in the bedrock. The quartz observed in this soil may be detrital from similar veins, although such veins have not been identified in the parent rock. An example of serpentinite weathering on a much larger scale and concomitant formation of quartz on the Anatolian plateau of Turkey has been described by Leo and others (1977). It is also possible that the quartz was introduced into the soil through aeolian deposition.

MECHANICAL PROPERTIES

Although the thinness of this profile precluded detailed analysis of mechanical strength, SPT blow counts (pl. 3*E*) indicate that weak, low-density soil and massive subsoil zones overlie relatively strong, dense weathered rock. As in the profiles developed from silicic metamorphic rocks, the B horizon of the soil is more dense than is the underlying nodular massive subsoil zone.

TEXTURE

Textural data for the profile (pl. 3*E*) are taken from U.S. Department of Agriculture Soil Conservation Service data (Porter and others, 1963). Most of the easily dispersed clay-sized material is in the weathered rock zone. Going upward from weathered rock, coarsening of the texture is due to the abundance of silt- and sand-sized nodules.

CLAY MINERALOGY

X-ray diffraction patterns of samples from serpentinite profile F14 are shown on figure 21. Clay minerals in slightly weathered rock at 0.66-m depth have a predominant X-ray diffraction peak of 7.31 A that is produced by a mixture of clinochrysotile, antigorite, and lizardite. The 7.31- and 3.63-A basal spacings and *hkl* reflections indicate that clinochrysotile is the dominant phase. The untreated sample from 0.66-m depth also shows a low, broad peak that is centered at about 14 A. Glycolation causes most of this material to expand to about 17 A. This expandability indicates the presence of smectite in the sample, possibly as an authigenic 2:1 clay layer in the weathered rock. A magnesium-montmorillonite was identified as a weathering product

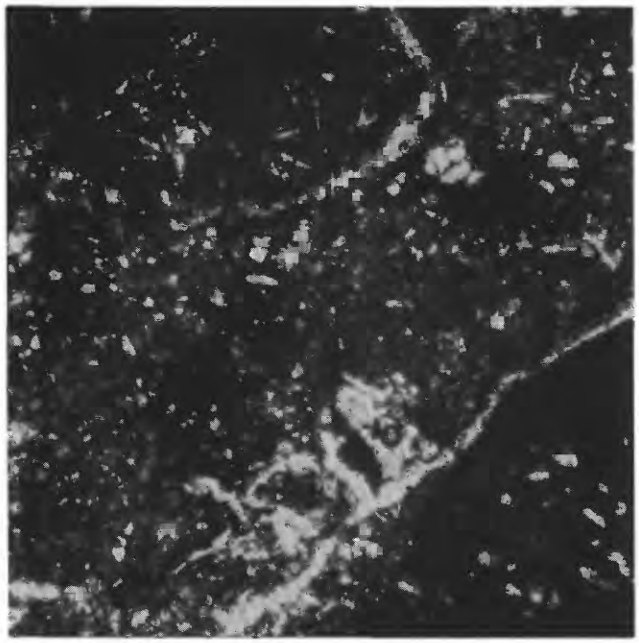

A. Sample 1b at 0.25-m depth. Soil containing dark, translucent to opaque spheroidal nodules and rounded fragments of weathered serpentinite in a cryptocrystalline matrix. Quartz grains and matted serpentine minerals are recognizable. Many of the quartz grains are deeply etched. (Transmitted light, 32 ×.)

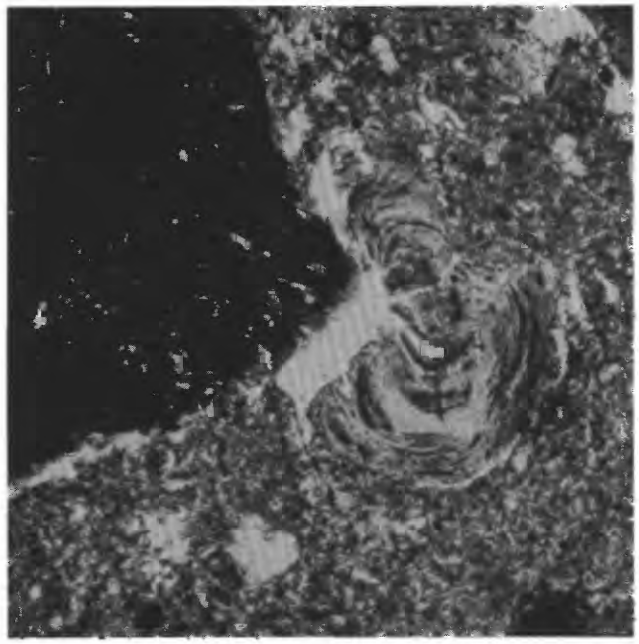

B. Sample 1d at 0.51-m depth. Massive subsoil containing serpentinite rock fragments having quartz grains, mica, and nodules similar to those observed in sample 1b. The nodules appear to be amorphous iron hydroxide yielding no X-ray pattern. Quartz grains are etched, but the serpentinite matrix is almost unaltered. (Transmitted light, 32 ×.)

C. Sample 2-1 at 0.66-m depth. Weathered rock containing unoriented serpentinite, primarily with lesser amounts of clinochrysotile and lizardite. The irregular cross-cutting vein near center of field is brucite; similar veins occur throughout the section. Quartz is absent. (Transmitted light, 32 ×.)

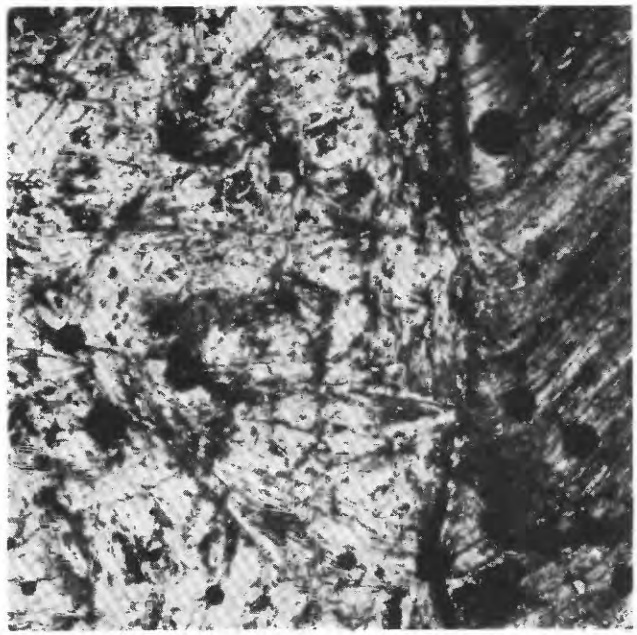

D. Sample 2-2 at 1.52-m depth. Unweathered, fibrous serpentinite with spheroidal and irregular patches and cross-cutting veinlets of brucite(?); veinlets and granular aggregates of magnetite. (Transmitted light, 32 ×.)

FIGURE 20.—PHOTOMICROGRAPHS OF SERPENTINITE REGOLITH, F14 CORE SITE

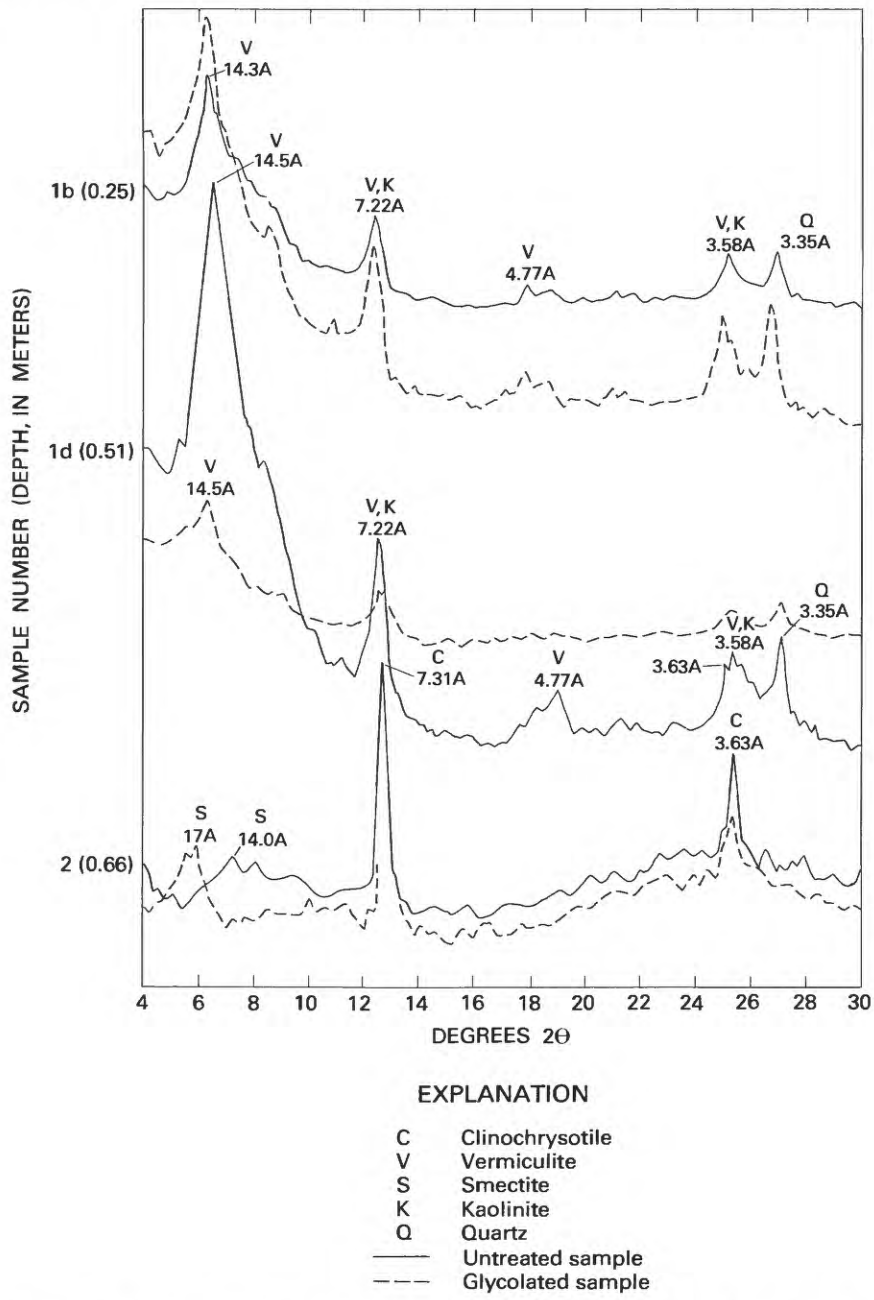

FIGURE 21.—X-ray diffraction patterns for untreated and glycolated <2-μ samples from the F14 core site.

of serpentinite in Maryland by Cleaves and others (1974). The reaction required to produce montmorillonite is not a simple transformation from another clay. The 7.3-A serpentine minerals cannot simply be stacked to produce a 14.0-A spacing. The in-place genesis of the montmorillonite involves solution: 7.31-A chrysotile → solution → 14.0-A montmorillonite. The synthesis of 14-A magnesium-montmorillonite was suggested by Cleaves and others (1974).

Higher in the profile, the percentage of original serpentine minerals decreases markedly, and 2:1 layer material is much less expandable. Although an expandable mixed-layer clay is identified in samples 1b and 1d, most of the clay is a nonexpandable 14.3-A vermiculite. The 14.3-A peak collapses to 10.5 A, on heating to 300 °C. This collapse did not always occur with the vermiculites obtained from the soils overlying the quartzofeldspathic parent rocks (for example, core F3,

sample 1c). The vermiculite in this soil overlying serpentinite may have been introduced by aeolian deposition, but the presence of an authigenic 14-A smectite lower in the profile (sample 2 at 0.66 m) suggests that the nonexpandable vermiculite is produced in place by alteration of the smectite.

The 7.22-A peak in the uppermost sample at 0.25 m is not affected by heating to 300 °C. This lack of effect indicates that this peak is produced by clinochrysotile and (or) by kaolinite. The presence of kaolinite(?) and quartz in the upper samples could be explained by aeolian deposition. The intensity of the 7.22-A peak does not increase, however, toward the soil surface as one would expect with a phase being deposited on the surface. The vermiculite, however, appears to be predominantly the result of in-place alteration. Unlike other vermiculites identified in the other profiles, this mineral exhibits a 4.77-A peak in sample 1d at 0.51 m. This peak is apparently a higher order spacing of a well-crystallized, possibly talc-composition, vermiculite. Equating this 14-A mineral with those observed in the upper meter of other profiles is difficult. Physical separation, if possible, and chemical analysis would yield useful results.

CHEMICAL ZONATION

Because the profile contains no saprolite and has a very thin weathered rock layer, the weathering of the serpentinite is predominantly nonisovolumetric. As noted by Cleaves and others (1974), the main process in serpentinite alteration is the congruent dissolution of magnesium silicate minerals. Clay mineralogy (fig. 21) suggests that the residual regolith develops because of the presence of dissolved silica that reacts to produce a stable talclike clay. The weathered rock at 0.66-m depth is considered to be isovolumetric with the fresher rock at 1.5-m depth. The weathered rock is slightly less dense than the fresh rock. In the massive subsoil zone above 0.66 m, the density declines markedly, and the photomicrographs in figure 20 show that the materials do not retain the bedrock structure above 0.66 m.

The chemical data in plate 3*E* show that MgO and SiO_2 are the principal constituents (80 percent) of the fresh rock. These oxides decrease in concentration in roughly equal amounts between the fresh and weathered rock. This equal decrease indicates that congruent dissolution of the serpentine minerals has taken place. Above the weathered rock, however, MgO declines rapidly, while SiO_2 remains relatively constant. Assuming that the vermiculite produced is close to an ideal talc composition ($Mg_3Si_4O_{10}(OH)_2$), this change reflects the decreasing ratio of Mg:Si in the vermiculite (3:4) when compared to the original serpentinite (3:2) and also indicates the presence of quartz.

The large change in Mg:Si, from 1:1 to 1:10, above the weathered rock indicates that the vermiculite includes few cations other than magnesium and that a large volume of serpentinite is dissolved to produce the thin regolith. An increase in Fe_2O_3 and Al_2O_3 relative concentrations (fivefold in the base of the soil) also indicates this volume change.

Other major oxides, including CaO, NaO, and K_2O, are minor constituents of the fresh rock. Concentrations of these oxides are less than 5×10^{-4} g/cm^3 in the fresh rock. All three oxides increase to concentrations of 0.001–0.003 g/cm^3 in the soil, but these levels are still minor relative to the other constituents.

The fresh serpentinite minerals are hydrated phases containing nonstructural H_2O^+. Decomposition of these minerals to dehydrated phases is accompanied by a decrease in H_2O^+ between 1.52- and 0.6-m depths. In the soil zone, which is dominated by vermiculite, the H_2O^+ decreases significantly to a value of less than 0.1 g/cm^3. This decrease of 75 percent results from the alteration of the serpentine minerals to less hydrous, magnesium-rich vermiculite. The constant concentration of Al_2O_3 between 0.5 and 0.25 m is evidence against aeolian deposition of an aluminum-rich vermiculite or kaolinite.

DISCUSSION OF WEATHERING PROFILES DEVELOPED ON MAFIC AND ULTRAMAFIC ROCKS

Data obtained from the weathering profiles of diabase and serpentinite indicate that, because only thin saprolite is produced by alteration of the parent rock, the entire regolith developed on these rocks is thin. Nonetheless, a zoned weathering profile shows progressive alteration of rock materials from bottom to top.

WEATHERED ROCK

The depth of weathering on the diabase is related to the intensity of jointing or fracturing of the rock (A.J. Froelich, oral commun., 1980). Numerous exposures in Loudoun Quarry, Route 606, east of Dulles International Airport, show that the depth of weathering on the diabase varies from a few meters to a maximum of about 10 m. Weathering alteration consists of oxidation of ferrous iron to ferric iron in mafic minerals, principally augite, and local etching of plagioclase along joint planes. Water movement through the weathering rock is restricted to joints.

Mineral stabilities during isovolumetric weathering of diabase correspond to the mineral dissolution data obtained for the quartzofeldspathic rocks (fig. 13). For example, the diabase in core F18 contains approximately equal amounts of plagioclase and augite. Petrog-

raphy of the diabase indicates that, in the weathered rock zone, the augite is altered more readily than is the plagioclase.

SAPROLITE

The cores and surface exposures of the weathering profiles of mafic rocks show that structured saprolite is developed only on diabase and that saprolite is virtually absent in serpentinite profiles. On diabase, saprolite is within 1 m of the surface (fig. 22). The thickness of saprolite is related to gross rock structure. Water moves through the saprolite predominantly along joints. Structural support of the saprolite zone in these weathering profiles apparently is provided by the large (boulder-sized) core-stones that weather spheroidally between intersecting joint planes. The diabase, unlike the quartzofeldspathic rocks, contains no chemically resistant minerals such as quartz and muscovite. Despite slightly greater resistance of plagioclase, both plagioclase and augite alter to structurally weak clay and iron oxyhydroxides. The absence of chemically resistant minerals precludes the formation of a mechanically stable saprolite such as that formed on quartzofeldspathic rocks and appears to limit the thickness of the saprolite.

The serpentinite, which likewise contains no chemically resistant minerals and which is not systematically jointed or foliated, forms no saprolite. This absence of saprolite formation from serpentinite also was noted by Cleaves and others (1974).

MASSIVE SUBSOIL

The diabase and serpentinite profiles exhibit very thin massive subsoils. This subsoil thinness is due to the lack of abundant resistant minerals in the parent rocks that can form a mechanically stable skeleton. Because little or no saprolite is produced from the parent rocks, no transition zone exists between saprolite and soil. The lack of resistant minerals also precludes the development of a B horizon that is denser and stronger than a subjacent massive zone, as in the quartzofeldspathic rocks. In mafic rocks, the alteration of rock to soil is progressive; mechanical and chemical processes are more difficult to separate than in the quartzofeldspathic rocks.

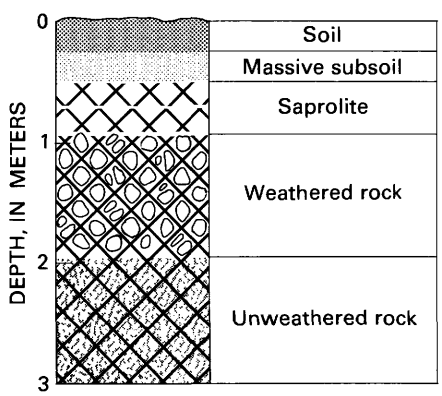

FIGURE 22.—Generalized weathering profile developed on diabase.

SOIL

The significance of dehydration in the soils derived from quartzofeldspathic rocks (cores F2, F3, and F11) is corroborated by weathering of the ultramafic rocks. In core F14, most of the vermiculite soil clay is dehydrated relative to the parent serpentine minerals (for example, clinochrysotile). The soils on both mafic and ultramafic rocks are mineralogically and chemically relatively simple residues of the parent rocks.

GEOLOGIC AND GEOMORPHIC INTERPRETATIONS

CONTROL OF REGOLITH THICKNESS BY BEDROCK LITHOLOGY AND STRUCTURE

The upper boundary (the geomorphic surface) and the lower boundary (the unweathered rock) of the Piedmont upland regolith are commonly widely separated; saprolite constitutes most of the weathering profile. The upland regolith, however, is not as thick and does not have the same characteristics everywhere as shown by the data presented for the five cores of this study.

Differences in regolith thickness in the mid-Atlantic Piedmont are related principally to parent rock type, with a secondary correspondence to local topography. The average thickness of regolith developed from quartzofeldspathic rock is three times the thickness of the average regolith developed on mafic rocks. Regolith on ultramafic rocks is very thin or absent. The thickest regolith developed on the crystalline quartzofeldspathic rocks of the upland occurs beneath hilltops. The regolith thins toward valley side slopes where fresh bedrock locally crops out (Froelich and Heironimus, 1977, pl. 2). These same consistent, first-order relations between regolith thickness and bedrock lithology and the second-order correspondence between regolith thickness and topography have been shown also in Montgomery County, Md., by Froelich (1975) and in Baltimore County, Md., by Cleaves (1973).

Basic data of regolith thickness estimates include either measured thicknesses from outcrops or records of lengths of water-well casings, both of which generally indicate the depth to fresh bedrock (Froelich and Heironimus, 1977). The water-well-casing data points from the Fairfax County and Vienna, Va., area (A.J. Froelich, 1977, unpublished data), are presented in figure 23. The graph shows that most of the casing lengths are between 6 and 30 m and that a mean depth is at about 15 m. Regolith thickness rarely exceeds 28 m but is known to exceed 50 m locally.

In addition to a primary correspondence to rock type, regolith thickness also corresponds consistently to topography. Figure 24 shows cross-section profiles of regolith over various rock types and topographic settings in Fairfax County. Although the relief on the top of fresh bedrock is subdued relative to the relief on the topographic surface, the base of the saprolite generally follows the shape of the topographic surface. The important aspects of the relation of regolith thickness to topography are that thickness is related to relief and is independent of absolute elevation and that thickness is consistent for a given rock type. The well-casing data, the outcrop observations, the geologic map (pl. 1), and the contoured isopach map (pl. 2) show that the quartzofeldspathic metamorphic rocks have an average regolith thickness of 18 m and a maximum thickness of about 50 m, that the thickness of regolith in the crystalline uplands is greatest beneath topographic highs and decreases markedly on valley side slopes, and that the regolith profiles of ultramafic and mafic rocks are commonly less than 2 m thick and 6 m thick, respectively.

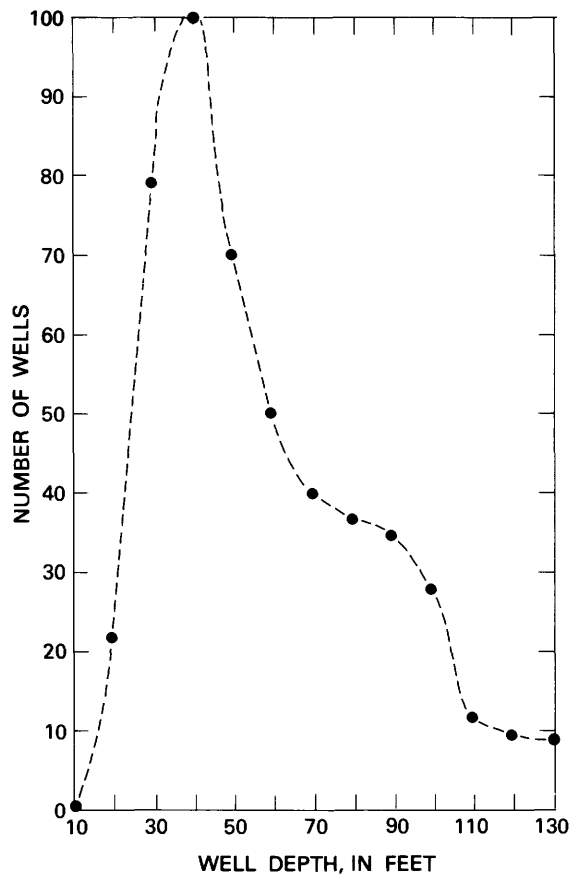

FIGURE 23.—Regolith thickness distribution as indicated by well-casing depths. Data points are from the Fairfax County and Vienna, Va., area; data points are not differentiated as to bedrock type (A.J. Froelich, 1977, unpublished data). Depth <20 ft means all wells are between 10 and 19 ft.

The consistency of the relations among regolith thickness, bedrock lithology, and local topography suggests some fundamental dynamic control over regolith thickness. The control is exercised by a combination of factors including rock composition, rock structures, regolith hydrology, and erosion rates.

Bedrock lithology (relative abundance of minerals and their chemical compositions) and rock fabric (grain-to-grain contacts of resistant minerals) affect the overall thickness of regolith chiefly by affecting the thickness of saprolite developed on that rock type. The representative weathering profiles shown in figures 17 and 22 not only summarize the detailed zonation of regolith but also show the proportional thicknesses of zones and subzones within the profiles.

The thickness of saprolite can be compared among rock types on the basis of the mass of material that is removed in saprolite production from a unit volume of rock versus the percentage of resistant minerals that survive weathering. Representative petrographic sections, drawn schematically from sections of metasedimentary, mafic, and ultramafic rock types, are shown in figure 25.

Comparison of the rock types indicates that only about one-third of the quartzofeldspathic metasedimentary rock mass, chiefly feldspar, is removed in saprolite production. In the diabase and serpentinite, however, resistant minerals that could form a skeletal framework to support the original volume are lacking. Comparison of the thickness of regolith of quartzofeldspathic rocks with the thickness of regolith of mafic rocks shows that the regolith thickness, which is directly related to the saprolite thickness, is inversely related to the abundance of reactive minerals. This general observation is supported by the details of rock structure and composition.

QUARTZOFELDSPATHIC ROCKS

The strength of saprolite developed on foliated metasedimentary and granitic rock derives from the orien-

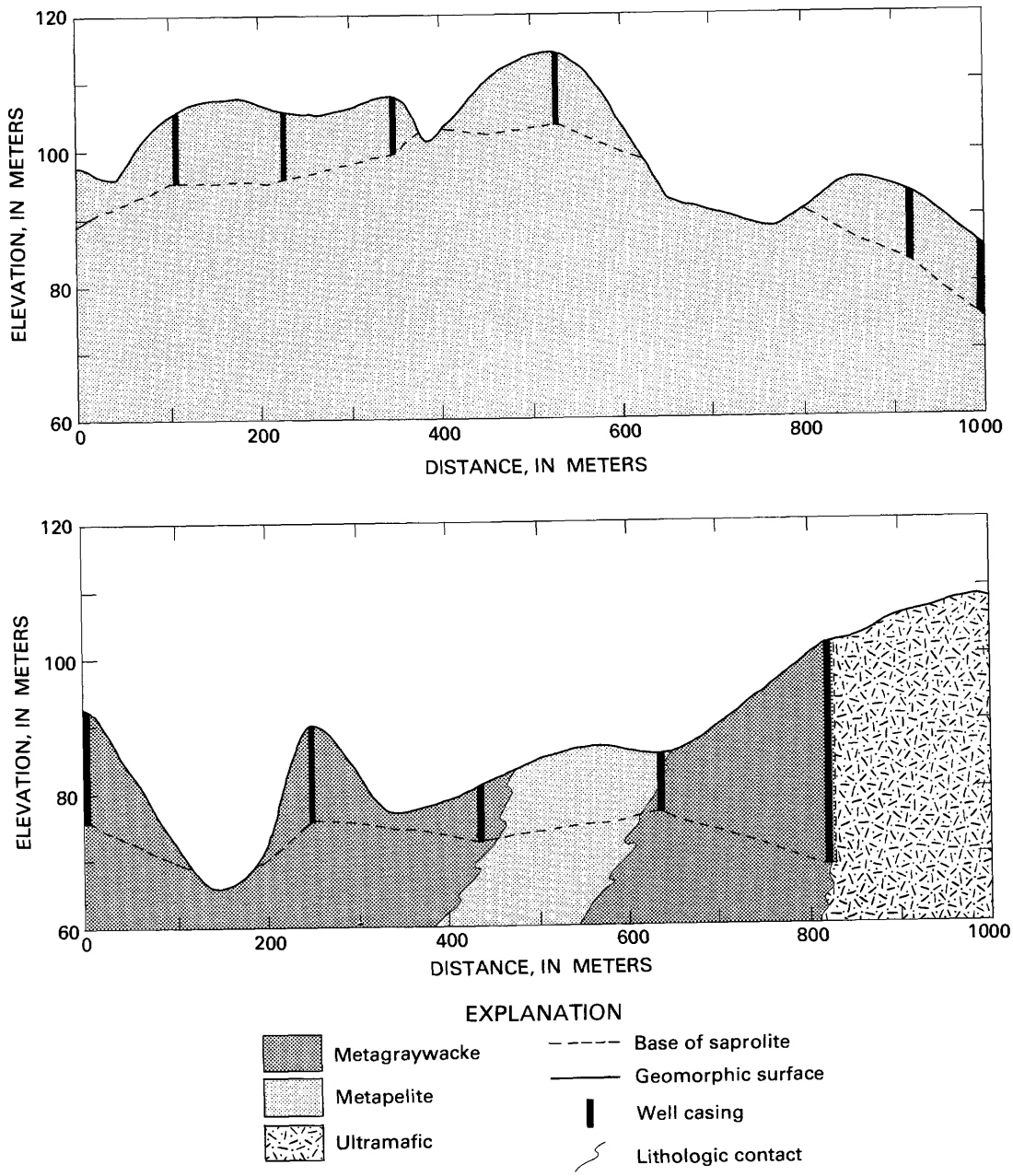

FIGURE 24.—Generalized cross sections of typical Piedmont regolith.

tation of and the large percentage of quartz and muscovite grains that are resistant to weathering. The original metamorphic fabric of these rocks, which consists of foliation planes defined by intergrowths of muscovite crystals and polycrystalline quartz aggregates, resists disintegration and deformation during chemical weathering. The fabric, therefore, acts as a stable framework in which the dissolution of less resistant minerals occurs. Comparison of mechanical strengths of the regolith profiles developed in metasedimentary and granitic rock types suggests that an important condition in the genesis of saprolite is the maintenance of mechanical strength during weathering.

The fabric of this stable quartz and mica framework is also important with respect to water movement through the saprolite. The foliation planes and interlocking quartz-mica foliation framework maintain the original volume of the rock. Mass removal provides for increasing porosity and directional permeability. Without a chemically and physically stable framework, access of solutions to unweathered minerals would be

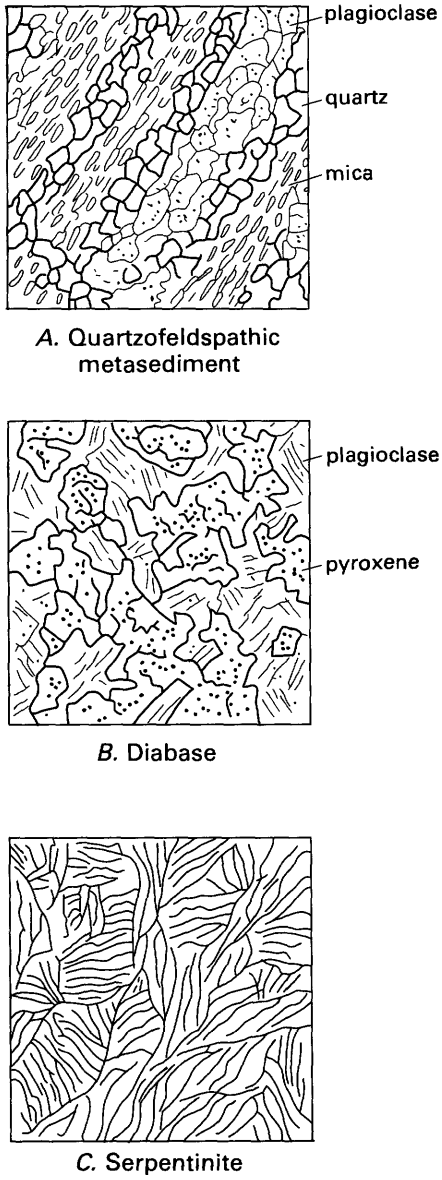

FIGURE 25.—Petrographic sketches of typical *A*, metasedimentary; *B*, mafic; and *C*, ultramafic Piedmont rocks (modified from Williams and others, 1954).

greatly restricted. Unlike the massive mafic and ultramafic rocks, the foliated quartzofeldspathic rocks form a skeletal framework that readily transmits water to the site of weatherable minerals.

On the basis of his study of regolith and landforms on the Piedmont of part of Baltimore County, Md., Cleaves (1973) concluded that the thickness of saprolite is related directly to total clay and total quartz content. He further concluded that the amount of authigenic clay in saprolite is a function of the amount of aluminum in the parent rock. Both of these conclusions are open to question. Aluminum-deficient ultramafic serpentinite produces little clay or saprolite; nevertheless, it cannot be concluded that clays are necessary for saprolite formation. For example, in the profiles on quartzofeldspathic rocks of Fairfax County, total clay content is generally less than 5 percent in the saprolite, and the clay appears to have minimal effect on the saprolite properties.

The chemical resistance or physical support afforded by quartz alone is probably not significant in determining the regolith thickness. Chemically resistant minerals such as quartz and muscovite are common in most of the metasedimentary rocks, and within these lithologies no obvious relation exists between variability of quartz content and regolith thickness. Rather, the saprolite thickness, over a variety of quartzofeldspathic rock types (pls. 1 and 2), is more likely a function of total quartz and muscovite content.

In foliated rocks of Fairfax County, quartz alone probably does not provide as much mechanical support of saprolite as had been suggested by Cleaves (1973). Photomicrographs of all quartzofeldspathic rock profiles (figs. 5, 8, and 11) show that the polycrystalline quartz grains are dissaggregated and, therefore, do not maintain a compacted grain-to-grain framework. The photomicrographs and macroscopic observations suggest that the mechanical support of the rock structure during weathering is due to the strength and fabric of the muscovite and quartz that form the bulk of the rock folia.

The metasedimentary rocks underlying most of the Fairfax County Piedmont are mineralogically and structurally ideal for isovolumetric weathering. Their generally steeply dipping foliation is maintained by resistant minerals (muscovite and quartz), while labile minerals (such as plagioclase and biotite) are removed by groundwater solutions that flow in relatively porous and permeable conduits such as joints and cleavage and then ultimately in smaller interconnected channels within the residual framework.

The isovolumetric weathering of these quartzofeldspathic rocks produces weathering profiles having the following characteristics:

(1) The strength of the saprolite, determined on the basis of blow counts, increases from a minimum at the top to a maximum near the base of the profile.
(2) Mass loss, determined on the basis of bulk density, decreases from the top to the bottom of the profile.
(3) Despite the mass loss due to dissolution of less resistant minerals (such as plagioclase and biotite), the quartz and muscovite remain relatively unaltered, and grain-to-grain contacts of muscovite retain structural integrity.

Joints and large fractures cause discontinuities in mechanical strength and can provide planes of weakness that easily fail under low stress (Obermeier, 1979). In its natural, undisturbed setting, however, the entire upland regolith has lateral support and little vertical overburden stress. It is, therefore, stable if undisturbed.

MAFIC AND ULTRAMAFIC ROCKS

Bedrock lithologic control of the regolith thickness is most clearly shown by characteristics of the weathering profile developed on serpentinite. The thinness or absence of the regolith on the serpentinite in upland position is due chiefly to the lack of resistant minerals such as quartz or muscovite to form a skeletal framework for saprolite.

Furthermore, either bare bedrock surfaces or clay-rich soil having low permeability causes a high amount of surface runoff and restricts infiltration of rainwater. As pointed out by Cleaves (1974), serpentinites contain few minerals that do not dissolve readily and congruently, and therefore, little material remains after chemical weathering to form a residual profile. The evidence presented here, however, suggests that a trioctahedral vermiculitic clay does form from the serpentinite.

Outcrop topography in Fairfax County suggests that most residual material after weathering of serpentinite is probably quickly eroded because of surface runoff on bare rock surfaces after storms. Larger ultramafic bodies commonly form slight topographic highs; the formation of these highs suggests that the combination of weathering and erosion of the regolith on quartzofeldspathic rocks has been more effective in lowering the landscape than has the predominantly chemical mass loss acting on the serpentinite.

The mafic diabase produces a relatively thin, irregular regolith commonly containing abundant, large, floating core-stones (Froelich and Heironimus, 1977). Although the fresh diabase contains a much higher proportion of weatherable minerals than the quartzofeldspathic metasedimentary or granitic rocks contain, weathering of diabase core-stones is not facilitated by rock structure. The thin regolith on diabase is related to the net balance of weathering rate and mechanical erosion rate.

Because the diabase lacks resistant minerals such as quartz and muscovite, no framework supports the saprolite structure. The conduits for ground-water flow in the diabase are limited to joints and fractures. Joint blocks weather from the outside, and the high permeability of the joints may preclude the movement of much water to carry on weathering reactions in the massive cores of joint blocks. In addition, the weathering of the major primary minerals of the diabase produces a weak mass of clayey soil that has no structural elements to support the matrix. The clay-rich soil probably also restricts infiltration of water into the saprolite and bedrock and, therefore, further restricts the amount of solution available for weathering reactions in joint blocks.

The expandable clay that is produced in the diabase saprolite is much more prone to volume changes due to wetting and drying cycles than is the kaolinite and nonexpandable vermiculite clay of the quartzofeldspathic regolith. Volume changes destroy most of the weak saprolite that is produced. The smectite-rich soil is also more plastic and, therefore, more prone to creep or slump (Obermeier, 1979) on low-angle slopes than is the kaolinite and vermiculite-rich soil of the quartzofeldspathic profiles.

The diabase regolith apparently is eroded more quickly than is the regolith on adjacent Piedmont rocks, as topographic comparisons demonstrate. The upland surface of the diabase, from which core F18 was taken, is at or below 91-m altitude (pl. 1). The adjacent metamorphic rock uplands, which exhibit an average 18 m of regolith, are as high as 137 m. The lower surface elevation of the weathering profile on the diabase strongly suggests that the regolith is being eroded more rapidly than is the thick regolith on the adjacent quartzofeldspathic rocks. Thus, the thinness of the diabase regolith probably is related to a relatively high erosion rate and to a lack of resistant minerals that would structurally support saprolite. Furthermore, the low topographic position of the early Mesozoic Culpeper basin suggests that thin regolith on both the diabase and the surrounding sandstones and shales is being eroded more rapidly than is the regolith on the adjacent metamorphic upland.

Thus, the ultramafic and mafic rocks occupy different local topographic and physiographic positions determined by relative erosion rates. The bedrock outcrops of serpentinite commonly form topographic highs. Bare serpentinite rock is resistant to erosion relative to regolith developed from quartzofeldspathic rocks. The diabase, by contrast, commonly occurs in topographic lows that are surrounded by uplands composed of crystalline schists.

SUMMARY

Despite significant differences in regolith thickness, the principal reactions responsible for the initiation of rock weathering and of saprolite formation are oxidation of ferromagnesian minerals and hydrolysis of plagioclase. The production of saprolite, however, is dependent upon rock type, particularly the presence of

resistant minerals and steeply dipping foliation as the dominant rock structure. Variation in saprolite thickness beneath uplands, and therefore, total regolith thickness, is determined by the distribution of the minerals in the rock, by the grain contact relations, and by the structural fabric of the rocks.

RESIDENCE TIME OF UPLAND REGOLITH

The weathering profiles described in this study are representative of only one part, the most stable upland, of the Piedmont landscape. Within the upland regolith, both the weathering front and the transition zone between saprolite and soil descend in altitude through time. In addition, the overall profile is zoned progressively with respect to time by irreversible chemical and mechanical processes. The Piedmont regolith, particularly saprolite, has been interpreted previously (Davis, 1899; Cleaves, 1973) as representing a weathering profile of extremely long residence time, perhaps greater than 10 m.y., having developed under tectonically stable conditions prior to the late Miocene. Consideration of kinetics of silicate mineral dissolution, however, indicates that saprolite formation from quartzofeldspathic rocks is controlled by relatively rapid geochemical reactions at the base of the profile in topographic settings that favor ground-water movement and that saprolite is being altered mechanically to soil by volume reduction near the top of the profile.

When considering the saprolite alone, the age difference between its bottom and top can be demonstrated by a simple argument about rates of processes. The uppermost saprolite (A) can be related in age to the lowermost saprolite (B) in one of three ways: (1) A<B; (2) A=B; or (3) A>B.

The first case is absurd. If A were younger than B, then the upper saprolite would have to undergo more chemical alteration than zone B in less time. Although it can be argued that the intensity of alteration is greater nearer the geomorphic surface than at the base, intensity of weathering in the upper half of the saprolite is not significant, as is shown by the lack of alteration of quartz and muscovite in the upper saprolite. Alteration as measured by mineralogical and chemical changes is most active at the base of the saprolite and in the soil.

The second case is highly implausible. For the two zones to be of the same age, the thickness of the regolith would have to have been established by some "event," such as a different climate. Since that event, weathering would have been confined within these boundaries, and no erosion could have occurred. The complexity of the chemical and mineral alterations and the gradients of density and chemistry, however, argue against a single causal factor forming the saprolite quickly during a previous geologic period.

The third case is the most plausible. The following observations support the likelihood of the third case:

(1) Ground-water solutions initiate the weathering reactions.
(2) Ground-water solutions descend to a local base level through time in response to hydraulic gradients that are related to the discharge elevation of local surface streams.
(3) Kinetically rapid chemical reactions occur first in the weathering process and remove the least stable minerals. Reactions involving residual minerals are kinetically slower.
(4) Stream-water composition can be related to the kinetically rapid reactions (Garrels and Mackenzie, 1967; Bricker and others, 1968; Pavich, 1986). Those reactions at or near the weathering front contribute most of the dissolved solids draining from the weathering terrain and determine the maximum rate at which the saprolite can develop.

Overall, therefore, the saprolite developed on the foliated quartzofeldspathic rocks apparently represents a weathering system having a finite residence time in which the most recent and active processes are occurring both at the base and at the top of the profile. Mechanical forces, as well as chemical processes, are responsible for the alteration of saprolite to massive subsoil, which in turn is altered to soil. Mechanical disturbance of near-surface material is effected by wetting and drying cycles, freezing and thawing cycles, and bioturbation. These forces did not penetrate to greater than 2 m in the cases investigated here. The contrast of process mechanisms of saprolite formation and soil genesis is schematically presented in figure 26.

The overall thickness of the regolith beneath a uniform surface area is determined by the differences among the rates of weathering front descent (r_1), compaction (r_2), and erosion of chemical mass loss from the soil (r_3). For example, in a 1-cm^2 column from the surface to the base of the profile, r_1 and r_3 can be converted from mass per time to centimeter per time by dividing loss of mass per time by bulk density. Compaction in the column also results in a change of centimeters per time. These rates vary among rock types and probably also vary through time as functions of the hydrologic mass balance (for example, due to variation in rainfall and evapotranspiration), bioturbation, and so on. The uniformity of regolith thickness on quartzofeldspathic rocks, however, strongly suggests long-term uniformity in these rates. Pavich (1986) presented evidence for a minimum rate of 4 m/Ma for the descent of the weathering front and upland surface. This mechanistic

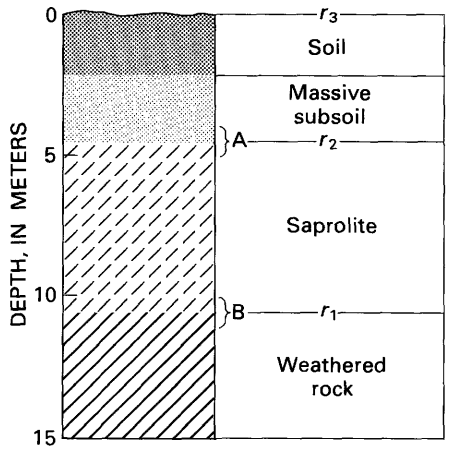

FIGURE 26.—Generalized regolith profile developed on quartzofeldspathic rocks showing rate-controlling steps that affect upland lowering. A, the uppermost saprolite; B, the lowermost saprolite. Rate of weathering front descent, r_1; compaction, r_2; erosion of and chemical mass loss from the soil, r_3.

model fits Hack's (1960) concept of dynamic equilibrium.

This model emphasizes that rock fabric and structure, rather than the resistance of minerals to alteration alone, play a primary role in determining the total regolith thickness. The foliation planes in quartzofeldspathic rocks of the Fairfax County Piedmont serve a critically important function in providing a generally steeply dipping path of preferential permeability and in providing strength to the weathered saprolite.

Despite arguments that invoke a more tropical climate or entire epochs for formation, the data obtained in this study indicate that the formation of saprolite can be accomplished by the alteration of chemically nonresistant minerals. Because the Piedmont is an active hydrologic system, the observed mineral alterations support the interpretation that the present widespread, thick saprolite mantle of the Piedmont is a comparatively recent geologic phenomenon. Davis (1899) and Cleaves (1973) suggested that the upland regolith is an erosional remnant of a former peneplained upland of less relief than presently observed. It is highly unlikely, however, that parts of a paleoregolith were selectively eroded from certain rock types (such as mafic and ultramafic) and were not eroded from others. The conclusion, therefore, is that the continuing rate of saprolite genesis is an important factor in determining regolith thickness.

In addition, postulating a noncontinuous origin of Piedmont regolith (Davis, 1899; Cleaves, 1973) implies that the weathering process began at the present geomorphic surface at some previous time and that no lowering of that surface has taken place since the weathering began. To presume that no surface lowering has taken place, erosion and chemical mass loss from the soil would have to be disregarded.

The recognition of erosion and surface lowering raises the question of the age of the top of the saprolite and of the residual soil overlying the saprolite. Estimates of the age of the soil may be improved by direct comparison of soils formed on the saprolite with soils forming on adjacent radiometrically dated Coastal Plain sediments. When compared, the soils on the Piedmont show relatively the same amount of development as the post-Miocene soils studied by Markewich and others (1987) and Owens and others (1983). For example, the quartz dissolution and the transformation of illite to vermiculite occur in soils that are greater than 100,000 years old, and sola exceed 1 m thickness in sediments that are perhaps 1 Ma to 2 Ma (Markewich and others, 1987). This qualitative comparison with Coastal Plain soils suggests that the uppermost part of the Piedmont regolith (soil and uppermost saprolite) is no older than Pliocene (5 Ma) and probably no older than Pleistocene (2 Ma).

If the 15 to 20 m of saprolite on the Piedmont upland were formed in the last 2 m.y., the average rate of saprolite formation is on the order of 1 m/100,000 yr. This suggested rate is the same order of magnitude as:

(1) the rate of post-Miocene saprolitization of crystalline bedrock beneath a cover of Coastal Plain sediment in Washington, D.C., that has been determined to be 1 m/500,000 yr (Pavich and Obermeier, 1985) and
(2) the rate measured by Moreira-Nordemann (1980) of rock weathering in South America by the uranium disequilibrium method.

Thus, evidence concerning the maximum residence time of the oldest part of the regolith, the soil, also indicates that the thickness of regolith is determined by the net balance of rates of weathering and erosion rather than by a strict absolute rate of either. This theory is corroborated by evidence from the Absaroka Mountains of Wyoming. There, erosion rates are eight times the North American average (much higher than the erosion rate of the Piedmont), and yet a 20-m-thick isovolumetric regolith has been observed (Miller and Drever, 1977).

The probability that regolith thickness is controlled by a steady state balance of weathering and erosion raises the question of what can be deduced about erosion rates and tectonics from observations of regolith thickness alone. Despite the postulated relation of

saprolite to a tectonically stable peneplain, as suggested by Davis (1899), a more logical hypothesis is that saprolite formation is actually facilitated by slow tectonic uplift and (or) lowering of stream base levels (for example, Pleistocene sea-level lowering). Thus, saprolite thickness is probably not indicative of tectonic stasis or of a particular uplift rate.

Mineral dissolution in the quartzofeldspathic weathering profiles indicates that saprolitization probably is most rapid under conditions of active ground-water-solution exchange; thus, up to some limit of mechanical stability of soil and saprolite, higher relief and higher hydraulic gradients will favor saprolitization. We observe in this study that the rate of saprolitization is controlled by the rate of alteration of the most reactive major mineral phase present and that the characteristics of saprolite developed from quartzofeldspathic schist can be achieved by chemical removal of only the plagioclase feldspar. Thickening of saprolite might by self-limiting due to recharge of ground water into the saprolite, dependent upon the hydrologic mass balance of precipitation and evapotranspiration determined in the soil.

The facilitation of both erosion and saprolitization by stream downcutting and by increase of relief in the drainage basin is more than a chance occurrence. All factors being equal (for example, rock mineralogy, rock structure, and climate), areas of more rapid (even if only moderately rapid) uplift should have more rapid saprolite formation than areas of little or no uplift. Thick saprolite does not logically imply tectonic stability in the 10^6- to 10^7-year time frame.

From various lines of evidence, therefore, we can draw the conclusion that thick saprolite (that is $\geq$ 10 m) can coexist with rates of tectonic uplift that may range from a few meters to tens of meters per million years. The rate or variation of rate of uplift of the Piedmont is not adequately known, but several lines of evidence show that the Piedmont is not tectonically static:

(1) The bases of Tertiary marine formations now lie well above sea level all along the Atlantic Coastal Plain. For example, the base of the Miocene Calvert Formation in the vicinity of Washington, D.C., is as high as 150 m above present sea level (Darton, 1951). From this evidence, an average uplift rate of about 20 m/Ma can be deduced.

(2) The Fall Line Zone of the mid-Atlantic States exposes numerous high-angle compressional faults that have thrust crystalline rocks over younger sedimentary rocks (Mixon and Newell, 1977; Prowell, 1977). These faults have been shown to have been active during the Cenozoic.

These observations cast doubt on the interpretation postulated by Davis (1899) and Cleaves and Costa (1979) that the upland regolith of the Piedmont is a remnant of a pre-Pliocene peneplain. The regolith observed in this study more likely represents a Pliocene and Quaternary weathering system that is the product of the interaction of bedrock and ground water in an actively eroding landscape.

SELECTED REFERENCES

Becker, G.F., 1895, A reconnaissance of the gold fields of the southern Appalachians: U.S. Geological Survey, 16th Annual Report, p. 289–290.

Bricker, O.P., Godfrey, A.E., and Cleaves, E.T., 1968, Mineral-water interaction during the chemical weathering of silicates, *in* Gould, R.F., ed., Trace inorganics in water: American Chemical Society, Advances in Chemistry Series 73, p. 128–142.

Busenberg, Euripedes, and Clemency, C.V., 1976, Dissolution kinetics of feldspar at 25 °C and CO_2: Geochimica et Cosmochimica Acta, v. 40, p. 41–49.

Cady, J.G., 1950, Rock weathering and soil formation in the North Carolina Piedmont region: Soil Science Society of America Proceedings, v. 15, p. 337–342.

Carroll, Dorothy, 1970, Clay minerals: A guide to their X-ray identification: Geological Society of America Special Paper 126, 80 p.

Clearly, W.J., and Connolly, J.R., 1971, Distribution and genesis of quartz in a Piedmont-Coastal Plain environment: Geological Society of America Bulletin, v. 82, p. 2755–2766.

Cleaves, E.T., 1968, Piedmont and Coastal Plain geology along the Susquehanna aqueduct, Baltimore to Aberdeen, Maryland: Maryland Geological Survey Report of Investigations no. 8, 45 p.

——— 1973, Chemical weathering and landforms in a portion of Baltimore County, Md.: Unpublished Ph.D. dissertation, The Johns Hopkins University, Baltimore, Md., 104 p.

——— 1974, Petrologic and chemical investigation of chemical weathering in mafic rocks, eastern Piedmont of Maryland: Maryland Geological Survey Report of Investigations no. 25, 28 p.

Cleaves, E.T., and Costa, J.E., 1979, Equilibrium, cyclicity and problems of scale—Maryland's Piedmont landscape, Maryland Geological Survey Information Circular 29, 32 p.

Cleaves, E.T., Fisher, D.W., and Bricker, O.P., 1974, Chemical weathering of serpentinite in the eastern Piedmont of Maryland: Geological Society of America Bulletin 85, p. 437–444.

Cleaves, E.T., Godfrey, A.E., and Bricker, O.P., 1970, Geochemical balance of a small watershed and its geomorphic implications, Geological Society of America Bulletin 81, p. 3015–3032.

Colman, S.M., 1977, Development of weathering rinds on basalt and andesite and their use as a Quaternary dating method: Unpublished Ph.D. dissertation, University of Colorado, Boulder, Colo., p. 89.

Crooks, J.W., O'Bryan, Deric, Longwill, S.M., Wilson, J.R., Jr., and McAvoy, R.L., 1967, Water resources of the Patuxent River basin, Maryland: U.S. Geological Survey Hydrologic Investigations Atlas HA-244, scale 1:250,000, 5 sheets.

Darton, N.H., 1951, Structural relations of Cretaceous and Tertiary formations in parts of Maryland and Virginia: Geological Society of America Bulletin 82, p. 745–780.

Davis, W.M., 1899, The Peneplain, *in* Johnson, D.W., ed., 1954, Geographical Essays: New York, Dover Publications, Inc., p. 350–380.

Deere, D.U., Hendron, A.J., Patton, F.D., and Cording, E.J., 1967, Design of surface and near-surface construction in rock, Chapter

II, *in* Fairhart, Charles, ed., Failure and breakage of rock—Proceedings of the Eighth Symposium on Rock Mechanics held at the University of Minnesota, Sept. 15-17, 1966, New York, American Institute of Mining, Metallurgical, and Petroleum Engineers, Inc., p. 237-302.

Deere, D.U., and Patton, F.D., 1971, Slope stability in residual soils: 4th Panamerican Conference on Soil Mechanics and Foundation Engineering, p. 87.

Denny, C.S., and Owens, J.P., 1979, Sand dunes on the Central Delmarva Peninsula, Maryland and Delaware, U.S. Geological Survey Professional Paper 1067-C, 15 p.

Drake, A.A., Jr., and Froelich, A.J., 1977, Bedrock map of Fairfax County, Va.: U.S. Geological Survey Open-File Report 77-523, scale 1:48,000.

Fisher, D.W., 1968, Annual variations in chemical composition of atmospheric precipitation, eastern North Carolina and southeastern Virginia: U.S. Geological Survey Water Supply Paper 1535-M, 21 p.

Froelich, A.J., 1975, Thickness of overburden map of Montgomery County, Maryland: U.S. Geological Survey Miscellaneous Investigations Map I-920-B, scale 1:62,500.

Froelich, A.J., and Heironimus, T.L., 1977, Thickness of overburden map of Fairfax County, Virginia: U.S. Geological Survey Open-File Report 77-797, scale 1:48,000.

Gardner, L.R., 1980, Mobilization of Al and Ti during weathering—Isovolumetric geochemical evidence: Chemical Geology, v. 30, p. 151-165.

Gardner, L.R., Kheorueromne, I., and Chen, H.S., 1978, Isovolumetric geochemical investigation of a buried granite saprolite near Columbia, S.C.: Geochimica et Cosmochimica Acta, v. 42, p. 417-424.

Garrels, R.M., and Howard, Peter, 1957, Reactions of feldspars and mica with water at low temperature and pressure: National Conference of Clays and Clay Minerals, 6th, Proceedings, p. 68-88.

Garrels, R.M., and Mackenzie, F.T., 1967, Origin of the chemical compositions of some springs and lakes: Advances in Chemistry Series 67, p. 222-242.

Goldich, S.S., 1938, A study of rock weathering: Journal of Geology, v. 46, p. 17-58.

Hack, J.T., 1960, Interpretation of erosional topography in humid temperature regions: American Journal of Science 258-A, p. 80-97.

Jackson, M.L., 1968, Weathering of primary and secondary minerals in soils: International Congress of Soil Science, 9th, Transaction 4, p. 281-291.

Johnson, W.M., Likens, G.E., Borman, F.H., and Pierce, R.S., 1968, Rate of chemical weathering of silicate minerals in New Hampshire: Geochimica et Cosmochimica Acta, v. 32, p. 531-545.

Johnston, P.M., 1962, Geology and ground-water resources of the Fairfax quadrangle, Virginia: U.S. Geological Survey Water-Supply Paper 1539-L, 61 p.

Lambe, T.W., 1951, Soil testing for engineers: New York, John Wiley, 165 p.

Lambe, T.W., and Whitman, R.V., 1969, Soil mechanics: New York, John Wiley, 553 p.

Langer, W.H., 1978, Surface materials map of Fairfax County, Virginia: U.S. Geological Survey Open-File Report 78-78, 9 p.

Langer, W.H., and Obermeier, S.F., 1978, Relationships of landslides to fractures in Potomac Group deposits, Fairfax County, Virginia, *in* Annual Highway Geology Symposium, 29th, May 3-5, Proceedings, p. 45-80.

Leo, G.W., Onder, Ercan, Kilic, Mehmet, and Avci, Murat, 1978, Geology and mineral resources of the Kuluncak-Sofular area, Malatya K39-a1 and K39-a2 quadrangles, Turkey: U.S. Geological Survey Bulletin 1429, 58 p.

Leo, G.W., Pavich, M.J., and Obermeier, S.F., 1977, Mineralogical, chemical, and physical properties of the regolith overlying crystalline rocks, Fairfax County, Virginia—A preliminary report: U.S. Geological Survey Open-File Report 77-644, 14 p.

Loughnan, F.C., 1969, Chemical weathering of the silicate minerals: New York, Elsevier, 154 p.

Luce, R.W., Bartlett, R.W., and Parks, G.A., 1972, Dissolution kinetics of magnesium silicates: Geochimica et Cosmochimica Acta, v. 36, p. 35-50.

Markewich, H.W., Pavich, M.J., Mausbach, M.J., Hall, R.L., Johnson, R.G., and Hearn, P.P., 1987, Age relations between soils and geology in the Coastal Plain of Maryland and Virginia: U.S. Geological Survey Bulletin, 1589-A, 34 p.

Meuser, Rutledge, Wentworth, and Johnston, (General Soil Consultants), 1967, Final Report—Subsurface Investigations, Vol. III, B & O Route, Washington Metropolitan Area Transit Authority: U.S. Department of Commerce, National Technical Information Service no. PB 179-655.

——— 1970, Final Report—Subsurface Investigation, I-66 Route (K001 to K004), Washington Metropolitan Area Transit Authority: U.S. Department of Commerce, National Technical Information Service no. PB 197-087.

——— 1973, Final Report—Subsurface Investigation, Branch Route (F004 to F08), Washington Metropolitan Area Transit Authority: U.S. Department of Commerce, National Technical Information Service no. PB 249-773.

Miller, W.R., and Drever, J.I., 1977, Chemical weathering and related controls on surface water chemistry in the Absaroka Mountains, Wyoming: Geochimica et Cosmochimica Acta, v. 41, p. 1693-1702.

Mixon, R.B., and Newell, W.L., 1977, Stafford fault system: Structures documenting Cretaceous and Tertiary deformation along the Fall Line in northeastern Virginia: Geology, v. 5, p. 437-440.

Moreira-Nordemann, L.M., 1980, Use of $^{234}U/^{238}U$ disequilibrium in measuring chemical weathering rate of rocks: Geochimica et Cosmochimica Acta, v. 44, p. 103-108.

Obermeier, S.F., 1979, Engineering geology of soils and weathered rocks of Fairfax County, Virginia: U.S. Geological Survey Open-File Report 79-1221, 59 p., 4 oversize sheets.

Owens, J.P., and Denny, C.S., 1979 [1980], Upper Cenozoic deposits of the central Delmarva Peninsula, Maryland and Delaware, U.S. Geological Survey Professional Paper 1067-A, 28 p.

Owens, J.P., Hess, M.M., Denny, C.S., and Dwornik, E.J., 1983, Postdepositional alteration and near-surface minerals in selected Coastal Plain formations of the Middle Atlantic States: U.S. Geological Survey Professional Paper 1067-F, p. F1-F45.

Pavich, M.J., 1974, A study of saprolite buried beneath the Atlantic Coastal Plain in South Carolina: Unpublished Ph.D. dissertation, The Johns Hopkins University, Baltimore, Md., 133 p.

——— 1986, Processes and rates of saprolite production and erosion on a foliated granitic rock of the Virginia Piedmont, *in* Colman, S.M., and Dethier, D.P., eds., Rates of chemical weathering of rocks and minerals: Orlando, Academic Press, p. 552-590.

Pavich, M.J., and Obermeier, S.F., 1985, Saprolite formation beneath Coastal Plain sediments near Washington, D.C.: Geological Society of America Bulletin, v. 96, p. 886-900.

Petrovic, Radomir, 1976, Rate control in dissolution of alkali feldspar: Geochimica et Cosmochimica Acta, v. 40, p. 537-548.

Pettijohn, F.J., 1941, Persistence of heavy minerals and geologic age: Journal of Geology, v. 49, p. 610-625.

Plaster, R.W., and Sherwood, W.C., 1971, Bedrock weathering and residual soil formation in central Virginia: Geological Society of America Bulletin 82, p. 2813-2826.

Porter, H.C., Derting, J.F., Elder, J.H., Henry, E.F., and Pendleton, R.F., 1963, Soil survey of Fairfax County, Va.: U.S. Department of Agriculture, 103 p.

Prowell, D.C., 1976, Implications of Cretaceous and post-Cretaceous faults in the Eastern United States [abs.]: Geological Society of America Bulletin, v. 8, no. 2, p. 249–250.

Rich, C.I., and Obenshain, S.S., 1954, Chemical and clay mineral properties of a red-yellow podzolic soil derived from muscovite schist: Soil Science Society of America, 19th, Proceedings, p. 334–339.

Richardson, C.A., 1976, Approximate depth to the water table, Montgomery County, Md.: U.S. Geological Survey Open-File Report 76–881, 4 p., scale 1:62,500.

Seiders, V.M., Mixon, R.B., Stern, T.W., Newell, W.F., and Thomas, C.B., Jr., 1975, Age of plutonism and tectonism and a new minimum age limit on the Glenarm Series in northeast Virginia Piedmont near Occoquan: American Journal of Science, v. 275, p. 481–511.

Shapiro, Leonard, 1975, Rapid analysis of silicate, carbonate, and phosphate rocks (rev. ed.): U.S. Geological Survey Bulletin 1401, 76 p.

Siever, Raymond, and Woodford, Norma, 1979, Dissolution kinetics and the weathering of mafic minerals: Geochimica et Cosmochimica Acta, v. 43, p. 717–724.

Siffert, Bernard, 1962, Some reactions of silica in solution—Formation of clay: Reports of the Geological Map Service of Alsace-Lorraine, no. 21, 100 p. [translated from French, Israel Program for Scientific Translation, Jerusalem, 1967].

Sirkin, L.A., Denny, C.S., and Rubin, Meyer, 1977, Late Pleistocene environment of central Delmarva Peninsula, Delaware-Maryland: Geological Society of America Bulletin, v. 88, no. 1, p. 139–142.

Sowers, G.F., 1954, Soil problems in the southern Piedmont region: American Society of Civil Engineers, Proceedings, v. 80, Separate 416.

——— 1963, Engineering properties of residual soils derived from igneous and metamorphic rocks: Panamerican Conference on Soil Mechanics and Foundations Engineering, 2d, Brazil, p. 39–62.

Stumm, Werner, and Morgan, J.J., 1970, Aquatic chemistry: New York, Wiley-Interscience, 582 p.

Terzaghi, Karl, and Peck, R.P., 1948, Soil mechanics in engineering practice: New York, John Wiley, 729 p.

Thornbury, W.D., 1965, Regional geomorphology of the United States: New York, John Wiley, p. 88–99.

Williams, Howell, Turner, F.J., and Gilbert, C.M., 1954, Petrography—An introduction to the study of rocks in thin section: San Francisco, W.H. Freeman and Co., 406 p.

Wollast, Roland, 1967, Kinetics of alteration of K-feldspar in buffered solutions at low temperature: Geochimica et Cosmochimica Acta, v. 31, p. 635–648.

APPENDIX TABLES A1–A4

TABLE A1.—*Major elements of metapelite and metagraywacke of the Peters Creek Schist and corresponding regolith*

[—, not detected]

	Metapelite							
Sample no.	F2-1	F2-2B	F2-2E	F2-4D	F2-6A	F2-14	F2-16	F2-17
Analysis no.	1	2	3	4	5	6	7	8
SiO_2	51.0	49.4	59.2	55.9	69.0	67.6	68.5	73.8
Al_2O_3	25.8	26.0	18.4	19.4	14.4	15.8	14.7	11.8
Fe_2O_3	8.4	9.7	7.6	9.1	5.3	4.4	3.8	2.0
FeO	.76	.64	.80	.92	.96	.84	1.2	2.2
MgO	1.1	1.1	1.2	1.2	1.2	1.1	1.8	1.0
CaO	.13	.04	.06	.01	.01	1.7	1.9	1.7
Na_2O	.21	.08	.05	.13	.03	1.6	2.9	2.5
K_2O	3.9	3.3	2.9	3.9	2.1	1.7	2.1	1.6
H_2O	6.6	7.6	6.6	5.7	4.6	3.2	1.7	.73
TiO_2	1.4	1.3	1.1	1.3	.97	1.2	.90	.85
MnO	.09	.11	.09	.10	.07	.11	.09	.07
CO_2	.02	.02	.04	.02	.04	.27	.08	.02
Total	99.	99.	98.	98.	99.	100.	100.	98.
Depth (m)	.5	.9	1.2	2.4	3.2	10.	13.4	15.6
Bulk density (g/cc)	1.82	2.07	1.77	1.95	1.72	2.17	2.46	2.46

	Metagraywacke						
Sample no.	F3-1C	F3-2E	F3-7B	F3-10D	F3-13	F3-31	F3-31
Analysis no.	9	10	11	12	13	14	15
SiO_2	65.4	70.8	75.2	64.2	66.8	49.6	62.0
Al_2O_3	16.0	15.6	13.3	17.5	15.7	15.4	17.7
Fe_2O_3	6.5	4.9	4.6	6.7	6.7	16.3	7.4
FeO	.32	.32	.20	.32	.44	1.6	.40
MgO	.35	.23	.13	.67	.89	2.1	.76
CaO	.13	.02	.01	—	.02	.05	.07
Na_2O	.04	—	—	.01	.05	—	.02
K_2O	2.3	2.3	1.6	3.5	3.8	1.5	2.8
H_2O	5.4	4.0	3.9	4.9	3.4	7.2	6.1
TiO_2	1.0	.90	.77	.90	.86	3.8	1.2
MnO	.06	.03	.02	.03	.03	.19	.06
CO_2	.02	.02	.04	.02	.04	.02	.02
Total	98.	99.	100.	99.	99.	98.	99.
Depth (m)	.6	1.2	4.0	5.8	7.0	18.0	22.0
Bulk density (g/cc)	1.96	1.86	1.80	2.01	1.81	1.68	2.05

	Metagraywacke				
Sample no.	F3-42	F3-46A	F3-46B	F3-47A	F3-47B
Analysis no.	16	17	18	19	20
SiO_2	71.5	70.2	69.0	74.9	71.5
Al_2O_3	13.3	14.2	13.8	11.0	13.2
Fe_2O_3	4.4	4.0	3.0	2.0	1.4
FeO	.80	1.2	1.7	3.5	3.2
MgO	1.0	1.1	1.1	1.4	1.3
CaO	.11	.23	.91	0.5	1.4
Na_2O	.10	.94	2.1	1.3	2.6
K_2O	3.1	3.3	3.3	2.1	2.0
H_2O	2.7	2.3	1.8	2.1	2.6
TiO_2	.83	.75	.89	.58	.73
MnO	.03	.04	.04	.09	.08
CO_2	.02	.02	.32	.27	.21
Total	98.	98.	98.	100.	100.
Depth (m)	23.0	28.0	28.3	33.5	33.9
Bulk density (g/cc)	2.52	2.54	2.57	2.66	2.58

TABLE A1.—Continued

	Metapelite							
Sample no.	F4-1C	F4-2A	F4-2C	F4-8A	F4-16A	F4-16C	F4-25A	F4-25B
Analysis no.	21	22	23	24	25	26	27	28
SiO_2	60.5	51.7	55.0	56.1	47.7	44.3	58.4	70.9
Al_2O_3	17.5	25.2	24.0	23.4	15.7	23.4	17.0	13.4
Fe_2O_3	7.9	9.0	8.6	7.6	16.6	13.0	6.7	3.0
FeO	.56	.80	.76	.75	1.8	1.5	1.3	1.1
MgO	.77	.91	.94	1.1	2.0	3.2	2.0	.85
CaO	.03	.01	.03	.03	3.6	.39	1.6	1.1
Na_2O	.10	0.2	.18	.23	—	.18	4.8	4.5
K_2O	3.4	5.7	5.2	5.9	1.2	3.6	2.2	1.1
H_2O	.42	5.0	4.3	3.8	5.5	7.1	2.9	1.3
TiO_2	1.1	1.4	1.2	1.0	4.2	2.7	1.3	.70
MnO	.07	.10	.08	.08	.35	.20	.09	.70
CO_2	8.0	.02	.12	.32	.04	.02	.02	—
Total	100.	100.	100.	100.	99.	100.	98.	98.
Depth (m)	.5	.8	1.1	4.0	8.4	8.5	14.8	14.9
Bulk density (g/cc)	1.67	2.13	2.22	2.21	1.49	1.47	2.31	2.06

	Metagraywacke					
Sample no.	F5-2C	F5-6B	F5-6D	F5-10	F5-18	F5-20
Analysis no.	29	30	31	32	33	34
SiO_2	71.7	66.9	69.0	64.0	52.8	62.1
Al_2O_3	17.1	15.0	18.8	17.8	23.4	16.2
Fe_2O_3	1.6	7.7	1.1	7.0	7.1	5.8
FeO	0.2		.16	.80	2.9	1.8
MgO	.19	.36	.16	.66	2.4	2.2
CaO	.06	.03	.02	.01	.07	.50
Na_2O			.92	.06	.65	1.8
K_2O	2.3	2.7	2.4	5.4	5.8	3.6
H_2O	5.3	4.5	6.6	3.5	3.2	2.9
TiO_2	.15	.71	.06	1.1	1.2	.98
MnO	.02	.57	.03	.08	.10	.14
CO_2	.04	1.30	.73	.04	.06	.06
Total	99.	99.	100.	100.	100.	98.
Depth (m)	10.8	2.9	3.1	14.9	17.4	20.4
Bulk density (g/cc)	1.43	1.76	1.72	2.21	2.21	2.62

TABLE A2.—*Major elements of Occoquan Granite and corresponding regolith*

Sample no.	F10-A	F10-B	F10-C	F10-D	F10-E	F10-F		F11-A
Analysis no.	35	36	37	38	39	40		41
SiO_2	78.7	73.9	73.1	75.0	76.3	74.4		67.0
Al_2O_3	12.9	13.8	15.1	14.1	13.4	15.0		16.5
Fe_2O_3	1.4	1.3	1.7	1.8	1.5	1.4		4.2
FeO	.20	.16	.20	.48	.52	.56		.40
MgO	.49	.61	.76	.57	.57	.65		.50
CaO	.95	1.0	2.3	2.5	2.0	.98		.08
Na_2O	4.0	5.6	4.9	3.2	3.0	4.6		.30
K_2O	1.1	.81	1.1	2.4	2.8	2.1		1.9
H_2O	1.2	.84	.98	.76	.58	1.0		5.8
TiO_2	.21	.23	.32	.33	.30	.34		1.1
MnO	.03	.02	.01	.04	.03	.03		.02
CO_2	.02	.05	.02	.04	.01	.01		.03
Total	101.	98.	100.	101.	101.	101.		98.
Depth (m)	1.2	3.3	3.4	4.3	5.5	6.7		0.6
Bulk density (g/cc)	2.29	2.38	2.44	2.60	2.61	2.61		1.54
Sample no.	**F11-B**	**F11-C**	**F11-D**	**F11-E**	**F11-F**	**F11-G**	**F11-H**	**F11-I**
Analysis no.	**42**	**43**	**44**	**45**	**46**	**47**	**48**	**49**
SiO_2	73.4	78.3	70.9	72.6	79.3	75.6	74.7	74.4
Al_2O_3	14.3	13.3	17.3	16.0	12.7	14.7	15.2	13.5
Fe_2O_3	3.9	1.8	1.7	1.8	1.3	1.5	1.5	.33
FeO	.56	.36	.36	.32	.20	.24	.36	1.3
MgO	.49	.47	.49	.47	.37	.39	.40	.37
CaO	.07	.20	.03	.02	.36	1.8	2.2	2.2
Na_2O	.30	.15	.07	.06	.84	2.7	2.8	2.7
K_2O	1.7	1.6	2.5	3.2	2.6	2.9	3.2	3.0
H_2O	4.5	4.0	5.2	4.6	2.4	1.2	.56	.69
TiO_2	.79	.33	.34	.33	.21	.24	.25	.23
MnO	.01	.02	.07	.07	.06	.03	.02	.03
CO_2	.02	.01	.06	.02	.05	.04	.01	.07
Total	100.	101.	99.	99.	100.	101.	101.	99.
Depth (m)	1.5	4.3	6.7	11.0	15.0	20.0	21.0	22.0
Bulk density (g/cc)	1.69	1.61	1.51	1.69	1.6	2.37	2.52	2.69

TABLE A3.—*Major elements in diabase and diabase regolith*

[—, not detected]

Sample no.	F18-1A	F18-1C	F18-1D	F18-2B	F18-3	F19-1C	F19-2A	F19-2C	F19-3	F19-4
Analysis no.	58	59	60	61	62	63	64	65	66	67
SiO_2	73.8	51.8	55.3	52.4	52.3	70.7	56.3	51.1	52.9	52.1
Al_2O_3	9.1	10.8	16.5	16.7	15.5	10.1	15. 5	16.9	16.0	14.2
Fe_2O_3	5.7	24.0	11.1	3.0	2.3	7.2	11.4	5.9	2.4	1.5
FeO	1.5	—	.92	5.9	7.8	1.7	1.2	4.3	7.2	9.4
MgO	.35	.37	.99	5.4	6.8	.53	1.1	5.1	6.3	7.9
CaO	.16	.07	.33	8.5	10.6	.11	.58	7.4	10.8	10.9
Na_2O	.32	.10	.20	2.0	2.1	.48	.38	1.5	2.1	1.9
K_2O	1.1	.62	.50	.52	.52	1.3	.81	.56	.52	.49
H_2O	1.8	5.9	7.8	1.8	.51	3.4	6.9	2.7	.74	.60
TiO_2	2.9	2.4	1.5	.85	.94	2.9	1.9	.83	.92	.89
MnO	.29	1.4	.07	.12	.14	.07	.11	.12	.13	.16
CO_2	.02	.06	.04	.04	.02	.02	.06	.06	.02	.02
Total	97.	98.	96.	97.	100.	99.	96.	96.	100.	100.
Depth (cm)	12	25	50	90	100	35	75	90.	100.	190.
Bulk density (g/cc)	1.76	2.04	2.03	2.03	2.98	1.84	1.89	2.04	2.92	3.01

TABLE A4.—*Major elements in serpentinite and serpentinite regolith*

[—, not detected]

Sample no.	F14-1B	F14-1D	F14-21	F14-22	F15-1B	F15-1C	F15-22	F15-23
Analysis no.	50	51	52	53	54	55	56	57
SiO_2	64.1	43.5	42.8	41.2	65.5	62.0	40.4	41.3
Al_2O_3	11.9	9.4	1.6	.91	12.4	11.0	1.1	1.0
Fe_2O_3	10.1	23.3	4.9	6.7	6.9	10.8	7.8	6.3
FeO	.36	.24	.96	1.4	.40	.48	1.8	1.6
MgO	3.9	8.5	38.5	39.0	4.7	5.7	37.1	38.9
CaO	.28	.15	.01	.02	.24	.27	.01	.02
Na_2O	.52	.09	—	—	.49	.41	—	—
K_2O	1.5	.70	.03	.02	1.5	1.2	.02	.02
H_2O	5.0	7.8	11.9	11.6	5.5	5.8	11.3	11.7
TiO_2	.94	.61	—	—	.89	.81	—	—
MnO	.17	.45	.06	.07	.08	.10	.10	.08
CO_2	.02	.02	.02	.02	.02	.02	.02	.02
Total	99.	98.	101.	101.	99.	99.	100.	101.
Depth (cm)	25	50	65	450	25	35	45	125
Bulk density (g/cc)	1.84	1.79	2.38	2.60	1.76	1.92	2.32	2.58